AGGREGATION STUDIES ON SPHALERITE SYSTEMS

Mitra Mirnezami

Department of Mining, Metals and Material Engineering
McGill University
Montreal, Quebec

A thesis submitted to the Faculty of Graduate Studies and Research in partial fulfillment of the requirements for the degree of Doctor of Philosophy

December, 2002

Your file Votre référence
ISBN: 0-612-88531-3
Our file Notre référence
ISBN: 0-612-88531-3

In the name of God

To my parents, my dear husband, and my children

ABSTRACT

The aggregation behaviour of sphalerite suspension and the role of zinc and magnesium ions are investigated. Aggregation is monitored by suspension analysis (turbidity) and optical microscopy and, in particular, a conductivity-settling technique. To probe the mechanisms, electrophoretic mobility (zeta potential) measurements and field emission scanning electron microscopy (FE-SEM) imaging are used.

In the case of sphalerite alone, for samples from a variety of sources, aggregation occurred at pH 8-10, well above the range in iso-electric point (pH 2-6). The aggregation is attributed to the presence of $Zn(OH)_2$, the dominant species over this pH range. To test whether zinc hydrolysis products promote aggregation silica and chalcopyrite suspensions were doped with Zn^{2+} ions; aggregation over the same pH range was found. This observation is similar to that of Healy and Jellet (1967) for zinc oxide, ZnO. They suggested aggregation was due to release of Zn^{2+} ions to form $Zn(OH)_2$ which polymerizes and flocculates the particles. The same mechanism is proposed for sphalerite.

Aggregation due to magnesium ions was determined using the settling rate of sphalerite and silica suspensions (individually) as a function of Mg^{2+} concentration, pH and suspension density (%v/v solids). Aggregation at pH >10 was found for both minerals corresponding to magnesium hydroxide. However, the mineral's response to the three variables suggests the mechanism for each is different. The proposed mechanism of aggregation by $Mg(OH)_2$ for sphalerite is chemical bridging and for silica, electrostatic bridging. Electrostatic bridging is revealed by aggregation passing through a maximum as a function of both coagulant concentration and pH. For sphalerite, while there is a maximum with $[Mg^{2+}]$ (Mg^{2+} concentration) there is none with pH (after allowing for the self-aggregation of sphalerite). Further, electrostatic bridging requires surface patches of the bridging material ($Mg(OH)_2$) and the FE-SEM images showed no such evidence. The interpretation for silica aggregating with Mg^{2+} follows that proposed by Krishnan and Iwasaki (1986). The pH, $[Mg^{2+}]$ and solid concentration effects are compatible with

electrostatic bridging, as is the morphology as hydroxide patches were identified by FE-SEM.

In certain cases the conductivity-settling data suggested the particles were more conductive than the liquid. The conductivity-settling technique was adapted to measure the electrical conductivity of particles dispersed in water. The conductivity was estimated at the iso-conductivity point where the solution and the particles have the same conductivity. The technique was tested on chalcocite, chalcopyrite, galena, pyrite and sphalerite. The order of mineral conductivity followed that of their electrochemical rest potential, as expected. It is observed that the adsorption of xanthate significantly reduced the conductivity of chalcopyrite and copper activation increased the conductivity of sphalerite but treatment with lead had no effect.

RÉSUMÉ

Le processus d'agrégation de la sphalérite en suspension ainsi que l'effet des ions Zn^{2+} et Mg^{2+} sur agrégation sont étudiés. L'agrégation est évaluée par l'analyse des matériaux en suspension (turbidité), par microscopie optique et plus particulièrement à l'aide d'une technique de conductivité-sédimentation. Afin de vérifier les mécanismes, des lectures de mobilité électrophorétique (potentiel zeta) et l'imagerie au microscope à émission des champs électroniques à balayage (FE-SEM) sont utilisées.

Dans le cas de la sphalérite seule, l'agrégation fut observée à un pH de 8 à 10 pour des échantillons provenant de sources différentes. Ce pH est bien au-dessus du point iso-électrique (pH 2-6). L'agrégation est alors attribuée à la présence du $Zn(OH)_2$, l'espèce dominante à ce pH. Afin de vérifier le potentiel des produits de l'hydrolyse du Zn^{2+} à promouvoir l'agrégation, des ions Zn^{2+} furent ajoutés à des suspensions de silice et de chalcopyrite; l'agrégation fut observée pour le même écart de pH. Ces résultats sont en accord avec les observations de Healy et Jellet (1967) pour l'oxide de zinc, ZnO. Ces derniers suggérent que l'agrégation est due à la libération d'ions Zn^{2+} formant du $Zn(OH)_2$ qui se polymérisent et floculent les particules. Ce même mécanisme est proposé pour l'agrégation de la sphalérite.

Le rôle des ions Mg^{2+} dans l'agrégation fut déterminé à l'aide du taux de sédimentation des suspensions de sphalérite et de silice (individuellement) en fonction de la concentration de Mg^{2+}, du pH et de la densité de la suspension (% v/v solides). L'agrégation fut observée à un pH de 10 et plus pour les deux minéraux, correspondant à la formation de l'hydroxyde de magnésium. Par contre, l'effet des trois variables sur les minéraux suggère que le mécanisme pour chacun est différent. Les mécanismes d'agrégation par du $Mg(OH)_2$ proposés sont le pont chimique pour la sphalérite et le pont électrostatique pour la silice. Le pont électrostatique est identifiable par le fait que l'agrégation passe par un maximum en fonction de la concentration de coagulant et du pH. Dans le cas de la sphalérite, il y a un maximum en fonction du coagulant mais pas en fonction du pH (en tenant compte de l'agrégation naturelle de la sphalérite). Aussi, les

ponts électrostatiques nécessitent la précipitation, à la surface du minerai, de particules permettant la formation des ponts (hydroxyde de magnésium). Ces précipités ne furent pas détecté par imagerie FE-SEM. L'interprétation de l'agrégation de la silice par du Mg^{2+} est en accord avec les observations de Krishnan et Iwasaki (1986). Les effets du pH, de la concentration du Mg^{2+} et de la densité des solides sont compatibles avec la formation de ponts électrostatiques. La morphologie des précipités d'hydroxydes observés par imagerie FE-SEM est elle aussi en accord avec la théorie électrostatique.

Dans certains cas, les courbes de conductivité-sédimentation suggéraient que les particules étaient plus conductrices que le liquide. La technique de conductivité-sédimentation a donc été adaptée afin de mesurer la conductivité électrique de particules dispersées dans l'eau. La conductivité est déterminée comme étant le point d'iso-conductivité où la solution et les particules ont la même conductivité. Cette technique fut utilisée pour la chalcocite, la chalcopyrite, la galène, la pyrite et la sphalérite. L'ordre de conductivité observé pour les minéraux a suivi l'ordre de leur potentiel électrochimique, tel que prévu. Il fut aussi observé que l'adsorption du xanthate réduit de façon significative la conductivité de la chalcopyrite alors que l'activation de la sphalérite par le cuivre augmente sa conductivité et que l'activation par le plomb n'a aucun effet.

CONTRIBUTION OF AUTHORS

This thesis was prepared in accordance with article C of the guidelines Concerning Thesis Preparation of McGill University. This article reads as follows:

1. Candidates have the option of including, as part of the thesis, the text of one or more papers submitted, or to be submitted, for publication, or the clearly-duplicated text (not the reprints) of one or more published papers. These texts must conform to the "Guidelines for Thesis Preparation" with respect to font size, line spacing and margin sizes and must be bound together as an integral part of the thesis. (Reprints of published papers can be included in the appendices at the end of the thesis.)

2. The thesis must be more than a collection of manuscripts. All components must be integrated into a cohesive unit with a logical progression from one chapter to the next. In order to ensure that the thesis has continuity, connecting texts that provide logical bridges proceeding and following each manuscript are mandatory.

3. The thesis must conform to all other requirements of the "Guidelines for Thesis Preparation" in addition to the manuscripts. The thesis must include the following: a table of contents; a brief abstract in both English and French; an introduction which clearly states the rational and objectives of the research; a comprehensive review of the literature (in addition to that covered in the introduction to each paper); a final conclusion and summary; a thorough bibliography; Appendix containing an ethics certificate in the case of research involving human or animal subjects, microorganisms, living cells, other biohazards and/or radioactive material.

4. As manuscripts for publication are frequently very concise documents, where appropriate, additional material must be provided (e.g., in appendices) in sufficient detail to allow a clear and precise judgement to be made of the importance and originality of the research reported in the thesis.

5. In general, when co-authored papers are included in a thesis the candidate must have made a substantial contribution to all papers included in the thesis. In addition, the candidate is required to make an explicit statement in the thesis as to who contributed to such work and to what extent. This statement should appear in a single section entitled "Contributions of Authors" as a preface to the thesis. The supervisor must attest to the accuracy of this statement at the doctoral oral defense. Since the task of the examiners is made more difficult in these cases, it is in the candidate's interest to clearly specify the responsibilities of all the authors of the co-authored papers.

The following are manuscripts written by the author and were used in preparation of this thesis. All the experiments are also conducted under the author's directions. Manuscript 1 comprises Chapter 4, and manuscript 2 and manuscript 3 make Chapters 5 and 6 respectively.

1. M. Mirnezami, M.S. Hashemi A., and J. A. Finch, "Measurement of Conductivity of Sulphide Particles Dispersed in Water", has been accepted for publication by *Canadian Metallurgical Quarterly.*

2. M. Mirnezami, L. Restrepo, and J. A. Finch, "Aggregation of Sphalerite: Role of Zinc Ions" accepted for publication by *Journal of Colloid and Interface Science*.

3. M. Mirnezami, K. Robertson, J. A. Finch, "Aggregation by Magnesium Ions" to be submitted to the *International Journal of Mineral Processing.*

4. E. El-Ammouri, M. Mirnezami, D. Lascelles, and J.A. Finch, "Aggregation Index (AI) and a Methodology to Study the Role of Magnesium in Aggregation of Sulphide Slurries" accepted for publication in *CIM Bulletin.*

5. M. Mirnezami. M.S. Hashemi A., J.A. Finch, "Aggregation Effect of Zn^{2+} and Mg^{2+} Ions in Sulphide Mineral Pulps" submitted for presentation at XXII International Mineral Processing Congress, Cape Town, 2003.

All of the manuscripts presented above are co-authored by Prof. James A. Finch in his capacity as research supervisor. All the experiments were done under the author's direction. Manuscript 1 includes M.S. Hashemi A. (Student at Department of Chemical Engineering, McGill University) recognizing her contribution into the measuring the conductivity of some sulphide minerals. Manuscript 2 includes L. Restrepo, (Student at Department of Mining, Metals and Materials Engineering, McGill University) recognizing her contribution into measuring the settling velocity of silica treated with Zn ion. Manuscript 3 includes K. Robertson, (Master's student at Department of Mining, Metals and Materials Engineering, McGill University) for his contribution into FE-SEM image acquisition. The author was a co-writer of the Manuscript 4; the contribution of the author was the basic study using a turbidity technique. Manuscript 5 includes M.S. Hahsemi A. for her contribution into the performing part of the experiments (Response of silica to Zn and Mg). Beyond the contributions of the co-authors mentioned here, all of the work presented in this dissertation was performed by the author.

ACKNOWLEDGEMENTS

First and foremost I would like to thank my advisor, Professor Finch, for his guidance, suggestions, criticism and financial support that he has provided throughout the course of my research and studies.

I would like to express my sincere appreciation to my parents and my beloved family for their years of patience, affection and encouragement.

I would like to acknowledge the financial support of the Canadian Mining Industry Research Organization–Metallurgical Processing Division, CAMIRO-MPD (representing Noranda, Boliden-Westmin, Hudson Bay Mining and Smelting, Les mines Selbaie, Louvicourt, Breakwater Resources and Agnico-Eagle) and the Natural Sciences and Engineering Research Council of Canada (NSERC).

Last, but not the least, special thanks go to my friends over mineral processing group for giving me memories that I will cherish for the rest of my life.

TABLE OF CONTENTS

CHAPTER 3

Experimental Techniques

CHAPTER 4

Measurement of Conductivity of Particles Dispersed in Water

CHAPTER 5

Aggregation of Sphalerite: Role of Zinc Ions

CHAPTER 6

Aggregation by Magnesium Ions

CHAPTER 7

Conclusions, Contributions, and Future Work

APPENDIX A

Aggregation Index (AI) and a Methodology to Study the Role of Magnesium in Aggregation of Sulphide Slurries

APPENDIX B

Aggregation Effect of Zn^{2+} and Mg^{2+} ions in Sulphide Mineral Pulps Slurries

LIST OF FIGURES

LIST OF TABLES

CHAPTER 1

Introduction

1.1 Problem of Aggregation

Sphalerite is usually the source of zinc. The associated sulphide minerals are typically of lead (galena), copper (usually chalcopyrite), and iron (pyrite; pyrrhotite and occasionally (marcasite)) with non sulphide gangue ranging from silicates to carbonates. The common approach is to float Cu/Pb minerals followed by sphalerite after activation with Cu ions. Any sphalerite, which reports to the Cu/Pb concentrate(s) lowers the grade and represents a loss in zinc units. There are four general routes by which sphalerite may enter a concentrate: 1- as locked particles, i.e., recovery of composites such as chalcopyrite/sphalerite; 2- entrainment, i.e., recovery in the water carried by the bubbles into the froth product; 3- true flotation, i.e., sphalerite directly attaches to the bubble; and 4- recovery in aggregates of another mineral which itself attaches to the bubble. Aggregation as a possible cause of misplacement of minerals in flotation has long been suspected (Gaudin and Sun, 1946). Aggregation is generally counter productive for all physical separations (Rushton et al, 1996), unless selective aggregation can be achieved.

Aggregation may occur by various mechanisms. Aggregation processes based on reducing inter-particle repulsion (i.e., by compression of the electrical double layer thickness or by charge neutralization) are classified as coagulation (La Mer, 1964). When aggregation results from the action of an immiscible bridging liquid, it is known as agglomeration (Laskowski, 1992). If aggregation is induced by polymer bridging, the process is called flocculation (La Mer, 1964). Bridging forces of a different type also arise between charged surfaces that are "bridged" or cross-linked by multivalent counterions (Israelachvili, 1992). In water treatment the addition of certain metal ions is commonly used to promote aggregation. The mechanisms include both coagulation and bridging flocculation either by polymeric species (O'Melia, 1986) or by the precipitating metal hydroxide, which is known as sweep flocculation (Gregory, 1986). Differentiation between the mechanisms is often difficult; in this study, aggregation is used as a generic term.

There are two forms of aggregation, homo- and hetero-aggregation. Homo-aggregation usually applies to particles of one particle (mineral) type, while hetero-aggregation refers to when two different minerals aggregate. A familiar case of hetero-aggregation is the coating of fines of one mineral on larger particles of another (called slime coating). With homo-aggregation, an aggregate of particles of one mineral type may entrap particles of another mineral.

The literature on the aggregation of sulphide minerals is limited and even more so on sphalerite alone. Muster and Prestidge (1995) investigated the rheological behaviour (as an indication of inter-particle interaction) of sphalerite over pH range 4 to 10, including the effect of copper activation and xanthate treatment. They found that the presence of copper ions at pH 4 induced strong aggregation, which was not explicable by electrostatic considerations. They attributed the aggregation to hydrophobic interactions. Xanthate treatment at pH 5.5 caused dispersion rather than aggregation as indicated by the decreasing yield value. At pH 10 an increase in yield value at low xanthate concentration was observed, but at higher concentrations the yield value was decreased. They

concluded that the aggregation of sphalerite was subtly controlled by both electrostatic and hydrophobic interactions.

Muster et al. (1995) performed a rheological study and surface force measurements (using atomic force microscopy) on synthetic sphalerite. They found that under alkaline conditions in the presence or absence of copper ions, DLVO (Van der Waals plus electrostatic force) forces predominated and low yield values and pull off forces were observed. Under acidic conditions an attractive hydrophobic force was found predominant even when the ZnS surface was strongly charged. It was concluded that hydrophobic interactions were increased in the presence of copper (II) ions.

Lange et al. (1997) tried to correlate flotation and aggregation of fine (< 20 μm) and coarse (38-75 μm) sphalerite, the aggregation being determined using particle size measurements and optical microscopy. It was shown that fine sphalerite particles aggregated during conditioning at pH 5.5, both before any reagents were added and after the copper and xanthate conditioning. They found that at pH 8.5 aggregation was slow and continual, attributed to hydroxide formation on the surface causing electrostatic repulsion.

Toikka et al. (1998) investigated the interaction between zinc sulphide and silica in aqueous electrolyte by using colloid probe atomic force microscopy. They found that the sign of ZnS potential, which was positive at pH 5.8 on the basis of zeta potential measurements, to be negative under the condition of surface force measurement. They concluded that the iso-electric point observed at pH 7.2 in electrokinetic studies is due to adsorption of zinc hydrolysis products rather than the properties of ZnS surface. They attributed the discrepancy to the different solid/liquid ratio used in two measurements.

Vergouw et al. (1998a,b), using zeta potential measurements and a settling technique, studied the aggregation of three sulphide minerals and their paired combinations. They also studied the role of some metal ions of interest in mineral processing. Generally, they

showed aggregation of single minerals occurred near the iso-electric point (iep). The exception was sphalerite where the maximum aggregation did not correspond to the iep (ca. pH 3) but was shifted to higher pH (ca. pH 8-11). An attractive hydrophobic force was suggested (i.e., similar to Muster et al., 1995). With paired minerals, the iep of each shifted due to cross-contamination. The maximum aggregation corresponded to the pH region where the zeta potential of both minerals approached zero.

DiFeo et al. (2001) focused on the aggregation of sphalerite and its behaviour in the presence of silica and Ca ions. Similar to Vergouw et al. (1998 a,b), they found some aggregation of sphalerite over the pH range 2 to 8 and strong aggregation at pH 8.5, again a pH much higher than the iep. They also attributed the phenomenon to hydrophobic interactions. For sphalerite with silica, hetero-aggregation was observed from pH 3 to 7.5, homo-aggregation of sphalerite and dispersion of silica at ca. pH 2 and 8.5, and dispersion at pH 9.5. In the sphalerite/silica/calcium system, homo-aggregation of sphalerite and dispersion of silica was observed from ca pH 2 to 7, while hetero-aggregation occurred above pH 7.

The literature shows a range of behaviour and quite complex interactions. As a start to understanding the possible role of entrapment in the misreporting of sphalerite in flotation, the study commenced with a detailed examination of the aggregation behaviour of sphalerite alone and explored the governing mechanism(s). Subsequently, interactions with some metal ions, notably Mg^{2+}, were examined.

1.2 Objectives of Thesis

The overall objective is to delineate and interpret the aggregation behaviour of sphalerite.

The specific objectives are:

- To investigate the aggregation behaviour of sphalerite.
- To examine the effect of metal ions on aggregation, paying specific attention to Zn and Mg ions.

- To propose the mechanism of aggregation by Zn and Mg ions.

1.3 Methodology

To achieve the objectives the following methodology was used. Sphalerite samples from various sources were obtained. The effect of metal ions was investigated by adding as the chloride. To help study the mechanism, comparison with the behaviour of silica was used. Aggregation was measured using a combination of techniques: settling velocity, suspension analysis (turbidity), field emission scanning electron microscopy and optical microscopy. Electrophoretic mobility (zeta potential) measurements were used to correlate against the aggregation results.

1.4 Structure of Thesis

The thesis consists of the eight chapters. Some are in the style of a manuscript for publication so inevitably some repetition with other chapters occurs.

The objectives of the project and the methodology are given in chapter 1 together with the structure of thesis.

In chapter 2 background material is discussed, especially fundamental aspects of aggregation.

Chapter 3 reviews the experimental procedure used including the conductivity-settling technique, field emission scanning electron microscopy (FE-SEM), suspension analysis, optical microscopy, EDTA (ethylendiamine tetraacetate, $Na_2C_{10}H_{14}O_8N_22{\cdot}H_2O$) extraction and electrophoretic mobility measurements.

Chapter 4 presents the conductivity-settling technique as a method for measuring the electrical conductivity of particles dispersed in water. The technique is tested on chalcocite, chalcopyrite, galena, pyrite and sphalerite. This chapter entitled "Measurement of Conductivity of Sulphide Particles Dispersed in Water", by M.

Mirnezami, M.S. Hashemi A., and J. A. Finch, has been accepted for publication by *Canadian Metallurgical Quarterly.*

Chapter 5 details the mechanism of aggregation of sphalerite. The aggregation behaviour of sphalerite from six sources is investigated using the conductivity-settling technique, suspension analysis, optical microscopy, zeta potential measurement and EDTA extraction. This chapter entitled "Aggregation of Sphalerite: Role of Zinc Ions" by M. Mirnezami, L. Restrepo, and J. A. Finch has been accepted for publication by *Journal of Colloid and Interface Science.*

Chapter 6 demonstrates the aggregating effect of Mg ions. In this study sphalerite and silica are used to probe the extent and mechanism of aggregation. This chapter is entitled "Aggregation by Magnesium Ions" by M. Mirnezami, K. Robertson, J.A. Finch, to be submitted to the *International Journal of Mineral Processing.*

Chapter 7 contains the overall conclusions and recommendations for future work.

Appendix A demonstrates the impact of various ions, present in plant process water, on aggregation. An aggregation index is introduced. The contribution of the author was the basic study using a turbidity technique. This section is entitled "Aggregation Index (AI) and a Methodology to Study the Role of Magnesium in Aggregation of Sulphide Slurries" by E. El-Ammouri, M. Mirnezami, D. Lascelles, and J.A. Finch, accepted for publication in *CIM Bulletin.*

Appendix B investigates two aggregation maxima, at pH 8-10 and 10-12, occasionally seen in settling studies on slurries from Cu/Zn flotation plants. From measurements on sphalerite and silica suspensions the double maxima were replicated by Zn ions (pH 8-10) and Mg ions (pH 10-12). Mechanism of aggregation is studied. This section is entitled "Aggregation Effect of Zn and Mg Ions in Sulphide Mineral Pulps Slurries" by M. Mirnezami. M.S. Hashemi A., J.A. Finch, submitted for presentation at XXII International Mineral Processing Congress, Cape Town, 2003.

1.5 References

DiFeo, A., Finch, J.A., Xu, Z., Sphalerite – silica interactions: effect of pH and calcium ions. *Int. J. Miner. Process.*, **61**, pp. 57-71 (2001).

Gaudin, A.M. & Sun, S.C., Correlation between mineral behaviour in cataphoresis and in flotation. *Trans, AIME*, **169**, p. 347 (1946).

Gregory, J., The action of polymeric flocculants. In: B.M. Moudgil and P. Somasundaran (Eds.), *Flocculation, sedimentation and consolidation,* Engineering Foundation, New York, N.Y., pp. 125-138 (1986).

Israelachivili, J.N., Adhesion forces between surfaces in liquids and condensable vapours. *Surface Science Report, A review journal*, **14**, 3, pp. 109-159 (1992).

Lange, A.G., Skinner, W.M. & Smart, R. St. C., Fine: coarse particle interactions and aggregation in sphalerite flotation. *Minerals Engineering*, **10**, (7), pp. 681-693 (1997).

La Mer, V.K., Coagulation symposium introduction. *J. Colloid Science,* **19**, pp. 291-293 (1964).

Laskowski, J.S., Oil assisted fine particle processing, In Laskowski, J.S. and Ralston, J. *Colloid chemistry in mineral processing,* Developments in Mineral Processing Series, Vol. 12, Elsvier Science Publishers B. V., Netherlands, p. 387 (1992).

Muster, T.H. & Prestidge, C.A., Rheological investigations of sulphide mineral slurries. *Minerals Engineering*, **8** (9), pp. 1541-1555 (1995).

Muster, T.H., Toikka, G Hayes, R.A., Prestidge, C.A., Ralston, J., Interactions between zinc sulphide particles under flotation-related conditions. *Colloids and Surfaces*, **106**, pp. 203-211 (1995).

O'Melia, C.R., Polymeric inorganic flocculants. In: B.M. Moudgil and P. Somasundaran (Eds.), *Flocculation, sedimentation and consolidation*, Engineering Foundation, New York, N.Y., pp. 159-169 (1986).

Rushton, A., Ward, A.S., Holdich, R.G., Solid-liquid filtration and separation technology, VCH, Weinheim, pp. 1-31 and 221-226 (1996).

Toikka, G., Hays, R. A., Ralston, J., Surface forces between zinc sulfide and silica in aqueous electrolyte, *Colloids and Surfaces*, **141**, pp. 3-8 (1998).

Vergouw, J.M., DiFeo, A., Xu, Z., Finch, J.A., An agglomeration study of sulphide minerals using zeta potential and settling rate: Part I: Pyrite and galena. *Minerals Engineering*, **11**, (2), pp. 159-169 (1998).

Vergouw, J.M., DiFeo, A., Xu, Z., Finch, J.A., An agglomeration study of sulphide minerals using zeta potential and settling rate: Part II: Sphalerite/Pyrite and sphalerite/galena. *Minerals Engineering*, **11**, (7), pp. 605-614 (1998).

CHAPTER 2

Background

2.1 Introduction

The common method of processing Pb-Cu-Zn sulphide ores is flotation. Typically first Cu sulphides and galena are recovered as a bulk concentrate, then sphalerite is activated with copper sulphate and floated with xanthate. This process does not always yield satisfactory performance (recovery and grade). There are four possible factors involved in lowering grade and recovery: locking, entrainment, accidental activation and aggregation.

The problem of locking or inadequate liberation can be solved by increasing the level of comminution. Entrainment is directly related to water recovery. Counter-measures include cleaning stages, pulp dilution and froth washing. Accidental activation is related to metal ions present in the pulp, which affect the surface properties of a mineral. For example, lead ions can activate and cause sphalerite to float along with copper sulphides and galena (Rashchi et al., 2002; Lascelles et al., 2002; Wong et al., 2002). Aggregation can cause misplacement of one mineral to the concentrate of another mineral in two ways: Different minerals can hetero-aggregate or aggregates of one mineral can

physically entrap particles of another mineral. This thesis focuses on the aggregation mechanism.

2.2 Forces Involved in Aggregation/Dispersion

Most early attempts to explain the stability of a suspension considered only the surface charge of the particles. The existence of a charge was recognized as the primary cause of stability, thus neutralization of the charge would lead to aggregation. Until recently it was believed that only two forces operated between surfaces in a liquid such as water – the attractive Van der Waals force and the electrostatic "double layer" force which could be attractive or repulsive. These two forces together form the basis of the well known Derjaguin - Landau - Verwey - Overbeek, or DLVO theory (Israelachivili 1992).

2.2.1 Van der Waals forces

Van der Waals forces are weakly attractive between electrically neutral molecules, or parts of molecules. These attractions involve the synchronization of the orbital of the valence electrons in interacting molecules. At a certain point, the mutually repulsive force of the electrons is lessened and weak bonds can be made. These are Van der Waals interactions.

Although calculation of the Van der Waals forces between spherical particles is mathematically complex the resulting equation for equal-sized spheres is simple and has the form:

$$v_A = - A_{121} \frac{r}{12d} \qquad (r >> d) \qquad (2\text{-}1)$$

where V_A is the interaction energy between spheres of radius r, d is the distance of closest approach between the spheres and A_{121} is the Hamaker constant. The complex part of the equation involves determining the Hamaker constant. Tables of values for some systems are available (Hough and White, 1980).

2.2.2 Electrostatic forces

Coagulation is the adhesion of particles by forces of molecular and atomic origin. One force, the electrostatic force, results from the interaction of the double layer, which surrounds all particles in water. Particles are subjected to a random movement due to Brownian motion and mixing effects. This brings some particles into close enough proximity to allow the attractive surface forces to bind them into aggregates. If the surface of the particles is charged the resulting repulsive force may be sufficient to prevent aggregation. Added chemicals can alter the surface charge to either promote or prevent aggregation.

There are two forms of aggregation (coagulation) related to electrical effects: If the surface charge is brought to near zero the force of repulsion is lost and particles aggregate. This is referred to as homo-coagulation as generally the particles are of the same type. When different minerals have opposite charge there is a positive force of attraction inducing aggregation, this is called hetero-coagulation.

2.2.2.1 Surface charge

Electrical charge can be generated on a solid surface by a number of mechanisms. These include specific chemical interactions, preferential dissolution of surface ions, and lattice substitution.

Specific Chemical Interactions

Specific chemical interaction between the surface species and solute or solvent (H_2O) is termed chemisorption. These interactions include reactions with the aqueous phase, which lead to the formation of different compounds or species (Fuerstenau et al., 1984).

Preferential Dissolution of Ions

In the absence of specific chemical interactions, solids can acquire a surface charge by preferential dissolution of ions (deBruyn and Agar, 1962). The premise is that for simple uni-valent ionic solids, which must have equal surface distribution of cations and anions on a cleavage plane, the sign of the surface potential developed in a saturated solution is

determined by the relative magnitude of the free energies of hydration of the ions which constitute the crystal lattice. The ion with the greater negative hydration energy tends to hydrate to a greater extent and leave the surface with an excess of the opposite ion, whereby the sign of the surface charge is established.

Lattice Substitution

A third mechanism whereby a solid surface may acquire a potential is by lattice substitution. The replacement of aluminum for silicon in clays, for example, is responsible for the difference in electrical characteristics observed between the faces and edges of these minerals.

2.2.2.2 Development of electrical double layer

In the development of surface charge, whether by specific chemical interaction, preferential dissolution of surface ions, or lattice substitution, the solid surface acquires a potential with respect to the solution. The surface charge is compensated by an equal charge distribution in the aqueous phase. The charge in solution together with the charge on the solid surface is referred to as the *electrical double layer.* A schematic representation of the potential drop across the double layer is presented in Figure 2.1.

Various models have been developed to describe the structure and properties of this double layer. Some models require several experimentally-derived parameters. A compromise is to describe the double layer with the Gouy-Chapman model for a diffuse double layer.

Experimental work has shown that the Gouy-Chapman model is only applicable when the concentration of indifferent ions and the surface potential (Ψ_0) are low. One reason is, that in the model, the ions are considered as point charges and the size of the ions is neglected.

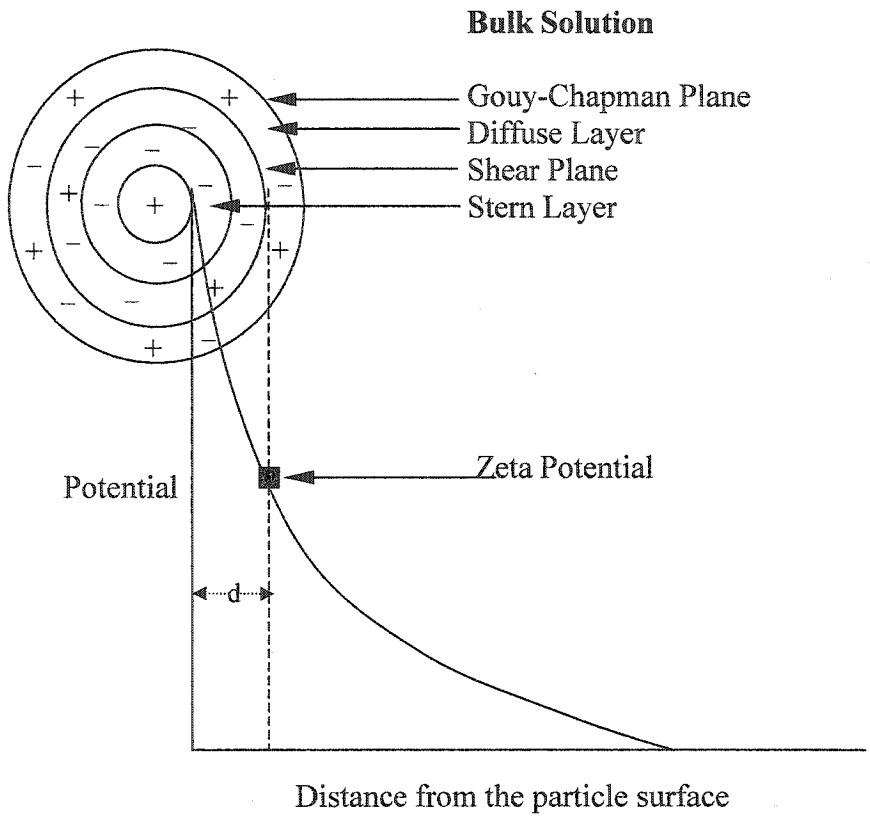

Figure 2.1: Gouy-Chapman model with Stern modification.

In 1924 Stern introduced a modification to the Gouy-Chapman model. He took into account the size of the indifferent ions and introduced the Stern layer (thickness *d*) as the size of the hydrated ionic radius (but with some deformation due to the electrostatic interaction with the surface). The value of *d* is therefore the nearest distance that an ion can approach the surface without specific adsorption.

An important parameter measuring the surface charge, is the zeta-potential. The zeta-potential is defined as the potential at the shear plane between the adsorbed ions near the surface and the surroundings diffuse layer (Fig. 2.1).

2.2.3 Structural forces

The DLVO theory was developed from two types of interactions – electrical double layer and Van der Waals. More recently, discrepancies in DLVO theory have been explained by additional forces, which are thought to arise from the re-arrangement of water

molecules near the interface, hence the term "structural" forces. The structural forces are known to be important at short range and produce either repulsion in a liquid that is able to wet the substrate (the substrate is hydrophilic), or attraction when the solid is poorly wetted by the liquid (the solid is hydrophobic) (Churaev and Derjaguin, 1985). The hydrophobic structural forces can cause attraction (Israelachivili and Pashly, 1982), whereas the hydration forces can have an important contribution to repulsion.

2.2.3.1 Attractive hydrophobic forces

A hydrophobic surface is one that is inert to water in the sense that it can not bind to water molecules via ionic or hydrogen bonds. Hydrocarbons and fluorocarbons are hydrophobic, as is air. The attractive hydrophobic force has many important manifestations and consequences. The hydrophobic force can be far stronger than the Van der Waals attraction. The aggregates formed in this way can be very stable as they are able to withstand disruptive turbulent energies at high shear rates (Warren, 1975). The magnitude of the hydrophobic interaction falls with decreasing hydrophobicity of the surfaces.

In the case of sulphide minerals there is disagreement on their hydrophobicity. For instance, chalcopyrite was found to be floatable by Fuerstenau and Raghavan (1976), and non-floatable by Yoon (1981). No bubble-particle attachment for galena was shown by Sutherland and Wark (1955), some flotation by Finkelstein et al. (1975), and either flotation or lack of flotation for two different galena samples by Lekki and Drzymala (1990).

The controversy regarding natural flotation of sulphide minerals results from the complexity of the sulphide-water interactions. From the thermodynamic point of view, sulphides are unstable and in the presence of water and oxygen tend to form a variety of metal oxy and sulfur oxy compounds. The oxidation provides both hydrophilic products (metal oxides and hydroxides) and hydrophobic species (elemental sulfur or sulfur-excess sites). Therefore, oxidation renders the common sulphides, depending on the environment, either hydrophobic or hydrophilic.

2.2.3.2 Repulsive hydration forces

The hydration force is not of simple character. Clearly, the unusual properties of water related to its strong polarity are implicated, but the nature of the surfaces is more important in the sense that solid/water interactions change with the solid, while obviously water is common to all. Some particle surfaces can have their hydration forces regulated, for example by ion exchange, while others remain hydrophilic despite changing ionic conditions. Usually, such surfaces can be rendered hydrophobic by chemically modifying the surface groups.

2.3 Other Mechanisms

Matijević (1973) demonstrated that there are various processes such as ion exchange, condensation, coordination, and polymerization, which play a role in aggregation.

Polyvalent cations such as Mg^{2+} are known to promote aggregation, notably when present as hydrolysis products. The hydrolysis reactions are sensitive to pH and the products ("complexes") influence aggregation via different mechanisms. They can induce aggregation due to charge neutralization by adsorption of positively charged precipitates, or sweep flocculation, due to aggregation (growth) of the hydroxide itself. Sweep flocculation describes domains where abundant precipitation of hydrolyzable metal ion occurs that enmeshes the suspended particulates. In that case, the optimal conditions (pH, coagulant concentration) for aggregation are reported to be independent of the nature of suspended particles being those which maximize the aggregation of precipitates (Packham, 1965). Surface hydroxide species can cause bridging. The bridging mechanism has two sub-categories: electrostatic (Krishnan and Iwasaki, 1986) and chemical (Healy and Jellet, 1976). In electrostatic bridging, positively charged hydroxide precipitates bridge between negatively charged particles. If the particles become fully coated, the resultant positive (negative) charge causes re-dispersion. Electrostatic bridging can be distinguished from aggregation due to charge neutralization, as the pH of maximum aggregation does not occur at the pH of charge reversal. The conditions causing re-dispersion are high pH and/or high salt concentration, which promote more

complete coverage. In the case of chemical bridging one form is H-bonding via the hydration layers on the hydroxide species (Attia, 1992). In this mechanism surface charge does not play a significant role and increasing the amount of hydroxide either by raising the pH or by increasing the salt concentration should not cause re-dispersion unlike the case of electrostatic bridging.

2.4 Selective Aggregation

Selective aggregation can occur in an initially dispersed mixed system, when differences in the rate of aggregation of the various species are sufficient that one component may separate out, leaving the other in suspension. The separation process can be controlled by, for example, careful adjustment of the surface potential, so that homo-aggregation of one component begins yet hetero-aggregation or mutual aggregation is avoided. To achieve selective aggregation, it is desirable that the two components have a narrow particle size range. Conditions must be chosen where the two particle types have a large difference in surface potential (Pugh, 1971). Pugh (1974) experimentally tested the procedure with binary mixtures of quartz/rutile. A similar series of experiments with quartz and finely ground natural hematite (Pugh, 1974), latex/mineral mixtures (Visca et al. 1988), clay mixtures (Frey and Langay 1979), and natural water systems (clay minerals) (Thomas and Murray, 1989) have also been reported.

It has been shown that selective aggregation may be achieved in hetero-dispersed colloidal systems based on a difference in particle size (Iler, 1975). Iler showed that larger particles of colloidal silica could be selectively aggregated from the smaller fraction by careful control of the aggregation condition using calcium ions.

Particles may also be separated using hydrophobic/hydrophilic interactions. Xu and Yoon (1989) showed that although zeta potentials were similar fresh (hydrophobic) suspensions were shown to be unstable over a much wider range of pH values than oxidized (hydrophilic) coal. In this system it would be feasible to selectively aggregate fresh coal from oxidized coal by careful adjustment of pH.

2.5 References

Attia, Y. A., In *Colloid Chemistry in Mineral Processing*, (J.S. Laskowski, and J. Ralston, Eds.) Developments in Mineral Processing Series, Vol. 12, Elsvier Science Publishers B. V., Netherlands, 295 (1992).

Churaev, N.V. & Derjaguin, B. V., Inclusion of structural forces in the theory of stability of colloids and films, *J. Colloids Interface Sci.* **103** (2) pp: 542, (1985).

DeBruyn, P.L. and Agar, G.E., Froth flotation, Fuerstenau, D.W., ed. AIME, New York. P. 91 (1962).

Finkelstein, N.P., Allison, S.A., Lovell, V.M. and Stewart, B.V., Natural and induced hydrophobicity in sulphide mineral systems. In: P Somasundaran and R.G. Grieves (Eds.), Advances in interfacial Phenomena of particulate/ solution/ Gas systems, Am. *Inst. Chem. Eng., Symp.* Ser. No. 150, 71, pp. 165-175 (1975).

Fuerstenau, D.W. and Raghavan S., Some aspects of the thermodynamics of flotation. In: M.C. Fuertenau (Ed.), A.M. Gaudin Memorial Volume. AIME, NewYork, **3**, 21-6 (1976).

Fuerstenau, M.D., Miller, J.D., Kuhn, M.C., Chemistry of flotation, American Institute of Mining, Metallurgical and Petroleum Engineers, Inc., New York, pp. 5-7 (1985).

Hough, D. B. & White, L. R., The calculation of Hamaker constant from Lifshitz theory with application to wetting phenomena, *Adv. Colloid Interf. Sci.*, **14**: 3 (1980).

Iler, R., J. Coagulation of colloidal silica by calcium ions, mechanism, and effect of particle size, *Colloid Interface Sci.*, 53: 476 (1975).

Israelachivili, J.N.and Adams, G.E., Measurement of forces between two mica surfaces in aqueous electrolyte solutions in the range 0-100 nm, *J. Chem.Soc. Faraday Trans.* **1**,74, 975 (1978).

Israelachivili, J.N., Adhesion forces between surface in liquid and condensable vapours, *Surface Science Report, A review journal*, V14, No. 3, (1992).

Israelachivili, J.N.& Pashly, R., The hydrophobic interaction is long range, decaying exponentially with distance, *Nature*, 300, pp: 341(1982).

Lascelles, D. and Finch, J.A., "Quantifying accidental activation. Part I. Cu ion production". *Minerals Engineering*, **15**, pp. 567-571 (2002).

Lekki J. and Drzymala J., Flometric analysis of the collectorless floatation of sulphide materials. *Colloids Surfaces*, **40,** pp.179-190 (1990).

Matijević, E. Colloid stability and complex chemistry, *J. Colloid and Interface Science*, **43**, (2), pp. 217-245 (1973).

Rashchi, F, Sui, C., Finch, J.A., "Sphalerite activation and surface Pb ion concentration", International Journal of Mineral Processing, **67**, pp. 43-58 (2002).

Sutherland, K.L. and Wark, I.W., Principles of flotation, Australian Institute of Mining and Metallurgy, Melbourne (1955).

Warren, L. J., Slime coating and shear flocculation in the sheelite- sodium oleate system, Trans. Ins. Min. Metall.,Sect., *Min. Proc. Metall.*, 84 :c 99-104 (1975).

Wong, G., Lascelles, D., and Finch, J. A., "Quantifying accidental activation. Part II. Cu activation of pyrite", *Minerals Engineering*, **15**, pp. 573-576 (2002).

Xu, Z. and Yoon, R-H., A study of hydrophobic coagulation, *J. Colloid Interf. Sci.* **17**, 29, 427-434 (1989).

Yoon R.H., Collectorless flotation of chalcopyrite and sphalerite ores by using sodium sulphide. *Int. J. Miner. Process.* **18**, V. 192, p 653 (1981).

CHAPTER 3

Experimental Techniques

3.1 Introduction

The state of aggregation of a suspension can be investigated in various ways, but there is no agreed method of quantifying aggregation. Measures such as settling rate (Vergouw et al., 1997), viscosity (Muster and Prestidge, 1995), optical microscopy (Adler, 1987), particle size distribution (Lange et al., 1997), atomic force microscopy (AFM) (Muster et al., 1995), and turbidity (Maroto and de las Nieves, 1998) have been used.

In this study a combination of techniques, settling, suspension analysis and optical microscopy, were used to define the state of aggregation. To investigate the mechanism, zeta potential measurements, EDTA extraction and scanning electron microscopy (SEM) were utilized.

3.2 Settling

3.2.1 Theory

The extent of aggregation can be judged by settling rate. Very fine particles, of only a few micrometers diameter, settle slowly by gravity alone. If the particles under certain conditions aggregate, the settling rate is higher. For an aggregating suspension, a sharp interface with a clear supernatant can often be seen. The measurement of the rate of descent of the interface can be informative. Settling tests are usually carried out manually, but work by the McGill Mineral Processing group has automated the data collection (Uribe-Salas et al., 1993; Vergouw et al., 1997).

The original theory describing the movement of a particle in an infinite fluid was derived by Stokes (1891). The terminal velocity of a spherical particle in the laminar flow regime is given by:

$$V_S = \frac{2g}{9\eta}(\rho_s - \rho_l)a^2 \qquad (3\text{-}1)$$

where η is the viscosity of the liquid, ρ_s and ρ_l are the densities of the solid and liquid respectively, g is the acceleration due to gravity and a is the radius of the particle.

In reality many factors other than those included in the equation influence the flow behaviour and hence the terminal velocity of particles. They divide into those depending on the particle properties and those depending on the flow system. Accordingly, many refinements have been made to the Stokes equation. Still there remains a common shortcoming, the assumption that a particle settles without interference from other particles.

Aggregation increases the size of the sedimenting unit but decreases the effective particle density due to the immobilization of the liquid within the aggregate. For small aggregates in a dilute system the size effect is dominant, increasing both the sedimentation rate and the volume of the settled bed. With more extensive aggregation in a concentrated system, the lower aggregate density and decreased effective void volume become dominant, thus

increasing suspension stability. On the other hand, when interparticle repulsion is high, stability of a relatively coarse system toward settling will be poor with no mass subsidence, but with individual particles sedimenting at rates depending upon their size resulting in a compact bed. Sadowski and Laskowski (1980) measured hindered settling rates of several mineral slurries and related the results to the stability of the systems.

In this research work a conductivity-settling technique (Uribe-Salas et al., 1993,1994; Vergouw et al., 1997) is used to define the state of aggregation. The technique measures conductance as a function of time. There have been a number of studies over the last century on the conductivity of dispersions (e.g. Maxwell, 1882; Fricke, 1924, Meredith and Tobias, 1962; Turner, 1976; Banisi et al., 1993).

Measurement of electrical conductivity of dispersions has been used in mineral processing systems, to estimate level in thickeners (Gomez et al., 1998), gas and solids holdup in flotation (Uribe-Salas et al, 1993) and as a substitute for pH measurement for pH ≥ 12 (Agar et al., 1996).

The theory of the conductivity of dispersions was first developed by Maxwell who derived:

$$\frac{\kappa_m}{\kappa_c} = \frac{\frac{\kappa_d}{\kappa_c} + 2 - 2\varepsilon(1 - \frac{\kappa_d}{\kappa_c})}{\frac{\kappa_d}{\kappa_c} + 2 + \varepsilon(1 - \frac{\kappa_d}{\kappa_c})} \qquad (3\text{-}2)$$

where:

κ_m = conductivity of the dispersion

κ_c = conductivity continuous phase (or clear liquid)

κ_d = the conductivity of the dispersed phase (or particles)

ε = volumetric fraction of dispersed phase

In the case of a non-conductive dispersed phase ($\kappa_d = 0$) Maxwell's model reduces to:

$$\frac{\kappa_m}{\kappa_c} = \frac{1-\varepsilon}{1+0.5\varepsilon} \tag{3-3}$$

The volume fraction of dispersed phase for non-conductive particles has been determined on several occasions using equation (3-3) (Turner, 1976; Uribe-Salas et al., 1993 and Banisi et al., 1994).

For the case of interest here knowing the conductivity of dispersion and of the liquid enables the solids concentration (or holdup) (ε_s) to be calculated.

In the study generally a fixed volume fraction of 2% solids was used. Figure 3.1 shows a typical conductance/time response on settling. For this case the ratio κ_m/κ_c is 0.96, which on substitution in equation (3-3) predicts a solids concentration (holdup) of 2%, i.e. as expected.

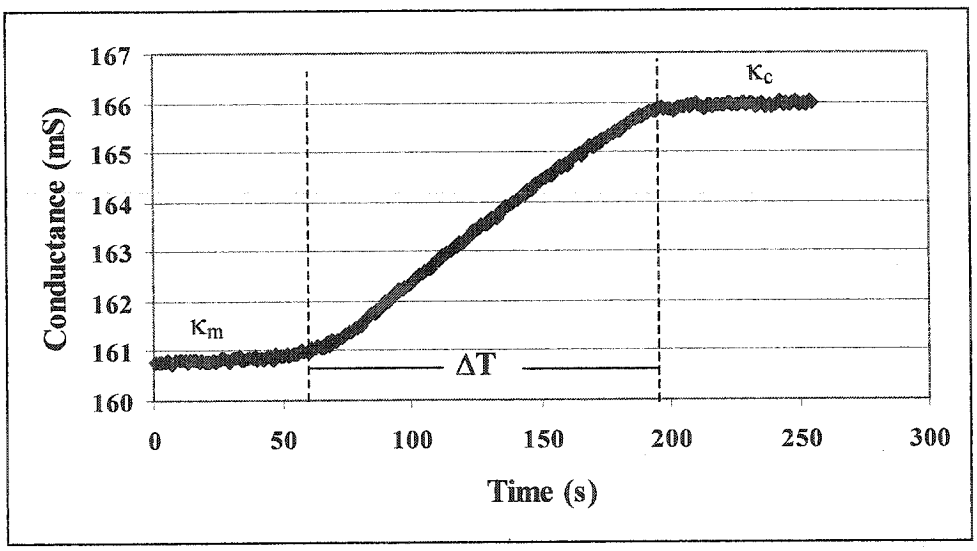

Figure 3.1: Conductance versus time response: 2% v/v non conductive solids

This result is strictly for non conducting particles. As will be shown some sulphide minerals exhibit a degree of conductivity. To avoid this complication in aggregation studies the work was performed in the presence of background electrolyte. By adding electrolyte the conductivity of the continuous phase is increased and the conductivity of the particles becomes negligible by comparison.

Alternatively, the technique opens a way of estimating the conductivity of the dispersed phase as described in Chapter 4 (Mirnezami et al., 2001), and also the shape of the particles (Furunchi et al., 1988).

3.2.2 Instrumentation

A cylinder was modified to collect settling data automatically by monitoring electrical conductivity (Fig.3.2). The cylinder was made from Plexiglas (non-conductive) and was 3.8 cm in diameter and 29 cm high. The cylinder stands on a plastic base and the top is covered with a rubber stopper after filling with suspension. Two identical ring electrodes, separated L=8.3 cm, are mounted internally flush to the walls and connected to a conductivity meter (Taccusel model CD 810) interfaced with a computer (data acquisition board, DAS-8PGA). A computer program was developed in Visual BASIC to record the conductance as a function of time (every 0.5 s).

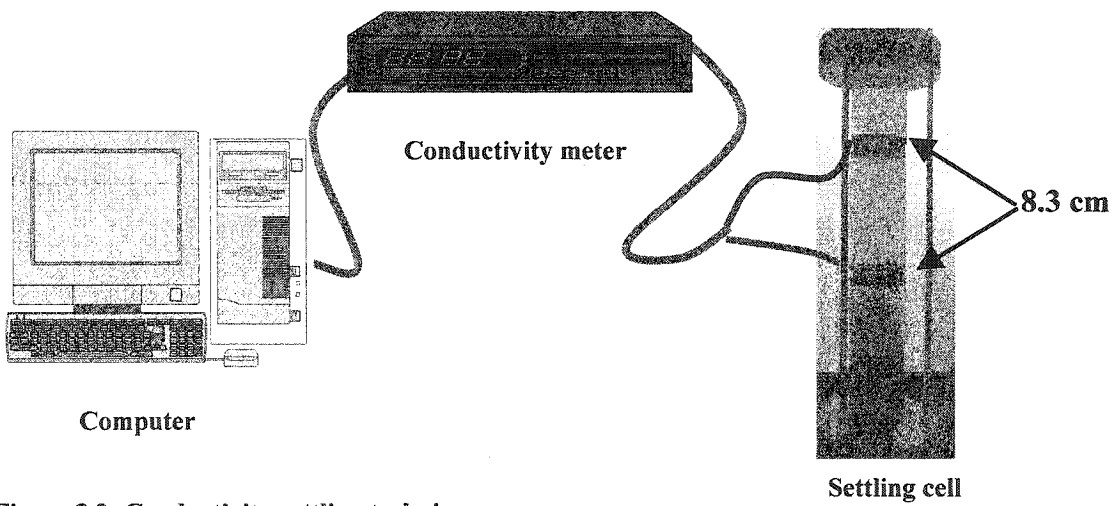

Figure 3.2: Conductivity-settling technique

To start, the suspension was mixed by end-over-end rotation of the cylinder. Data collection was initiated once the cylinder was stood vertically. The conductivity vs. time (Fig. 3.1) was plotted on the monitor to give a visual check on the process. Measuring the time to pass between the electrodes, ΔT, gives the settling velocity, $8.3/\Delta T$. The data were processed using Excel. The relative standard deviation on the settling rate from repeat experiments is ca. 1%.

3.3 Suspension Analysis (Pipet Method)

Direct sampling methods have the advantages of requiring relatively simple, inexpensive apparatus and allowing straightforward interpretation of results. Sampling is accomplished either by withdrawing samples from the suspension using a pipet or collecting a sediment sample at the base of a sedimentation column. The former was used.

The sampling height is usually kept constant and samples of known volume withdrawn at predetermined time intervals. Pipet methods are divided in two categories, the fixed pipet and free pipet (Allen, 1990). The fixed pipet method leaves the pipet in the dispersion at a fixed depth and withdraws samples at a predetermined time. In this method, particles moving downward under the pipet are not replaced by particles from above. Hence the concentration below the pipet is lower than the actual concentration elsewhere at the same depth. The free pipet methods involve insertion of the pipet to a specific depth at a time specified for sampling. The free pipet method has the advantage of eliminating the shadow effect in fixed pipet measurements. In this study, the free pipet method was used and the concentration of particles was determined by drying. Suspension conditioning was performed in a beaker. After conditioning the suspension was poured into a graduated cylinder. The slurry was allowed to settle for 2 minutes. One ml of suspension was taken from a specific height, filtered, dried and weighed.

3.4 Optical Microscopy

3.4.1 Theory

Direct observation would help confirm the presence of aggregates inferred from settling and turbidity experiments and give some insight into the size and structure. Relatively large aggregates (20-1000μm) have been examined with a low-powered optical microscope, either after the aggregates have settled or after removing individual aggregates from suspension. To illustrate, Camp (1968) measured the size of the aggregates produced by the coagulation of ferric oxide by alum. A 1 cm^2 glass tube was used to withdraw a 15 cm^3 sub-sample from a 2 liter suspension containing about 0.0013

wt % solids. The tube was then placed horizontally on the base of a low-powered (40×) microscope and left for 5-10 minutes to ensure that all aggregates had settled to the bottom glass face of the tube. The aggregate size determined ranged from 15 to 156 μm. Withdrawal of a suspension sample instead of individual aggregates provides a more representative sample (Lagavanker and Gemmel, 1969). However, as the suspension sediments within the sampling tube onto the microscope mount there is a possibility of aggregates settling onto one another, which would be difficult to distinguish from a single, large aggregate. This source of error can be reduced using dilute suspensions (as done by Camp) but not eliminated.

Moudgil and Vasudevan (1989) measured the size of aggregates of montmorillonite and kaolinite flocculated with a high molecular weight polyethylene oxide. Individual aggregates were removed from the suspension using a spatula and placed on a glass slide. Water surrounding the aggregate was then removed with absorbent paper and the slide placed under a microscope and the particle size measured. Although it was claimed that there was no change in the aggregate dimensions after the water had been removed, this will generally only be the case with strong, dense aggregates.

Recently, Lange et al. (1997) used an optical microscope to observe aggregate structures during copper activation and xanthate addition to sphalerite. In their study, two drops of the sample pulp were pipetted onto a shallow pitted slide and sealed with a coverslip. Samples were viewed immediately with a metallurgical microscope, equipped with a camera connected to an image analyzer. Since the concentration of slurry in Lange et al.'s study was much higher in comparison with that of Camp (1968) and Lagavanker and Gemmel (1969) the problem of overlapping particles existed. In addition, there is another source of uncertainity associated with their technique arising from possible distortion caused by the shear during removal from the suspension.

3.4.2 Method applied

The procedure was akin to that of Lagavanker and Gemmel (1969). Aggregates were selected with a spatula and placed onto a shallow pit slide, sealed with a coverslip and viewed under a stereomicroscope (Olympus), equipped with a Polaroid camera.

3.5 Zeta Potential

3.5.1 Theory

Almost all particulates or macroscopic materials in contact with a liquid acquire an electronic charge on their surfaces. Zeta potential is an important and useful indicator of this charge which can be used to predict and control the stability of suspensions or emulsions. The zeta potential (ξ) is the potential drop across the mobile part of the double layer that surrounds a particle and is responsible for the electrokinetic behaviour of the particle under an electric field. From double layer theory, the ξ-potential may be equated to the Stern layer potential ψ_δ and the sign and magnitude reflect the type of ions and species, which form the double layer. Surface charge is important with regard to suspension stability, rheology, sedimentation characteristics, and other surface-driven phenomena.

Instruments to measure zeta potential are based on one of the following principles: a) *electrophoresis*- the movement of the charged particles under an applied field relative to the surrounding liquid; b) *electro-osmosis* the movement of the liquid relative to a charged surface; c) *streaming potential*- the electric field created when a liquid flows along a stationary charged surface; and d) *sedimentation potential*- the electric field created when charged particles move relative to a stationary liquid (Hunter, 1981). Most ξ-potential measurements today are carried out on small particles in dilute suspensions using the electrophoresis technique. For concentrated suspensions, instruments have been developed to use electric and ultrasonic impulses to determine zeta potential values (Marlow, 1988).

If an electric field is applied across a suspension of small particles, the particles will tend to move toward either the anode or the cathode depending on whether the solid surface carries a positive or negative charge. The migration speed U (electrophoretic velocity or mobility) of the particles is directly proportional to the magnitude of the zeta potential. An equation proposed by Smoluchowski relates the mobility to the zeta potential:

$$U = \frac{\xi . \varepsilon}{\eta} \qquad (3\text{-}4)$$

where η is the viscosity of the water and ε is the dielectric constant. It has become traditional to use the approximate formula to arrive at a nominal zeta potential, which is adequate for most purposes. If electrophoretic velocity is expressed in μm/s / V/cm, zeta potential in mV is given by $\zeta \approx 12.8\ U$ (at 25°), assuming the dielectric constant and viscosity of water in the diffuse double layer have the same values as for bulk water.

For oxide systems the zeta potential versus pH curves are fairly reproducible with a well-defined iso-electric point (condition under which the ξ-potential is zero). For minerals such as sulphides, a wide range of values have been reported associated with the oxidation kinetics of the surface (Pugh, 1988).

Despite reservations attached to zeta potential in the case of sulphides, their experimental values provide useful information about their surface chemistry in water. Somasundaran (1980) pointed out that one reason why predictions of coagulation based on zeta potential measurements sometimes fail is that surface charge measurements and coagulation experiments are not carried out under the same condition, e.g. solids concentration. This may be particularly troublesome in the case of sulphides due to their high reactivity compared to oxides.

3.5.2 Instrumentation

Zeta potential measurements were performed by a Laser-Zee meter (Model 501, Pen Kem, Inc.) and the micro-electrophoretic apparatus Zeta Plus (Brookhaven Instruments

Corporation, USA). These instruments determine the electrophoretic mobility and convert to zeta potential using the model of Smoluchowski.

3.5.2.1 Laser-Zee meter

The suspension to be measured is placed in a chamber that consisted of: a) measurement compartment, b) two electrodes in the compartment, a molybdenum anode and a palladium cathode, and c) a rugged support base, on which the chamber is positioned.

Inside the instrument a prism receives an image, rotates a few degrees, flips back and repeats the cycle. The image causes the microscope inside the instrument to scan in one direction and then reset. The rate and direction of the prism motion is adjusted so that the apparent motion caused by the prism exactly matches the particle velocity caused by the electric field. This makes the particles appear stationary and the zeta potential is then displayed on the readout. The claimed accuracy is ± 1 mV.

3.5.2.2 Zeta Plus

The technique employs laser light scattering and comparison to a reference beam. The laser beam passes through the sample in a cell, which holds two electrodes. Light is scattered by the particles moving due the electric field. The frequency of light scattered into the detector is Doppler shifted by an amount proportional to the velocity of the particles.

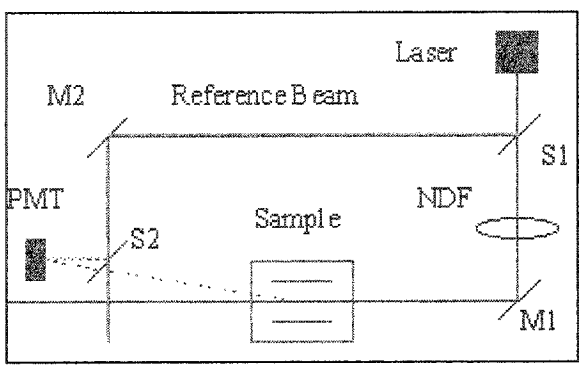

Figure 3.3: Zeta Plus optics

This scattered beam is mixed with the reference beam at the detector (photo-multiplier tube (PMT)). The reference beam is modulated and a frequency shift gives a signal from which both sign and magnitude of the electrophoretic mobility is calculated from:

$$\omega = q.v \tag{3-5}$$

$$\omega = \frac{4\pi \sin(\frac{\theta}{2})}{\lambda} \mu E \, Cos(\Phi)$$

ω = *frequency shift*

n = *liquid refraction index*

θ = *scattering angle*

λ = *laser wave length*

E = *electric field strength*

μ = *electrophoretic mobility*

ϕ = *angle between the scattering vector (q) and particle velocity (v)*

3.6 EDTA Extraction

In studying the action of metal ions in flotation, various methods have been adopted to determine the type and concentration of metal ions on a mineral surface. One method is extraction by use of a chelant followed by solution analysis. EDTA is a well-known chelating agent for many metals, forming soluble EDTA-metal complexes. Trahar and co-workers (Senior and Trahar, 1991; Shanon and Trahar, 1986) used this chelant extensively to study surface metal ions and others have followed this lead.

In this study the EDTA extraction method is used to estimate the amount of metal ions present on the surface of the particles.

3.7 Scanning Electron Microscopy (SEM)

The Scanning Electron Microscope (SEM) uses electrons to form an image. There are many advantages over a light microscope. The SEM has a large depth of field and produces images of high resolution, which means that closely spaced features can be examined at high magnification. Preparation of the samples is relatively easy since most SEMs only require the sample to be conductive. These advantages make the SEM one of the most frequently used instruments in research today.

3.7.1 Theory

The conventional SEM uses a beam of electrons focused by electromagnets onto a spot on the specimen surface. The electron beam originates from a filament made of various materials. The most common filament is the tungsten hairpin. A voltage is applied to the filament, causing it to heat up and shed electrons i.e., to function as cathode. The anode attracts these electrons causing them to accelerate rapidly. Some accelerate past the anode and on down the column, to the sample. Other examples of filaments are Lanthanum Hexaboride and field emission guns. The field emission gun offers considerably improved performance. The field emission cathode is usually a single-crystal tungsten fashioned into a sharp point and spot-welded to a tungsten hairpin. The significance of the small tip radius, about 100 nm or less, is that an electric field can be focussed to a high degree. A current density up to 10^5 A/cm^2 may be obtained from a field emitter comparing with about 10^3 A/cm^2 from a tungsten hairpin filament.

The three main signals emitted by the electron beam-sample interaction are:

1- Secondary electrons: These ejected electrons are low energy, weakly bound electrons. Due to their low energy, they can not travel far before they are recaptured; therefore, they can only be detected if they have escaped from or near the surface of the sample. Because of this, the secondary electron signal only carries topographic information about the sample.

2- Backscattered electrons. If a primary electron (an electron from the source beam) strikes the nucleus of a sample atom, an elastic collision may occur. The rebounding electron is termed a back-scattered electron. Back-scattered electrons have more energy than secondary electrons and can escape from deeper within the sample. Because materials with high atomic number back scatter more electrons than materials with low atomic number, the back-scattered signal provides compositional information.

3- Characteristic X-rays. When a beam electron ejects an inner shell atomic electron from its orbital, outer shell electrons jump in to fill the vacancy. The energy associated with this jump is emitted as an X-ray, whose energy is characteristic of the atom from which it came. This type of signal provides elemental information about the sample.

Images from secondary electrons were used in this study.

3.7.2 Instrumentation

The secondary electron images were taken at up to 10^5 times magnification on a Hitachi S-4700 FE-SEM. The samples imaged were 25-30 μm silica and 25-38 μm sphalerite at different pH in the presence of Mg. The conditioning regime was the same as in the aggregation tests with 2% v/v solids.

3.8 References

Agar, G.E., Khan, F., Markovich, B., Mukherjee, A., Shea, B., and Kelly, C. Laboratory Flotation Separation of INCO Bulk Matte, *Minerals Engineering*, **9**, (12), pp 1215-1226 (1996).

Allen, T., Particle size measurement, 4th ed., Chapman and Hall, London (1990).

Banisi, S., Finch, J.A., and Laplante, A.R., on-line gas and solids holdup estimation in solid-liquid-gas systems, *Minerals Engineering*, **7**, (9), pp 1099-1113 (1994).

Banisi, S., Finch, J.A. and Laplante, A.R., Electrical conductivity of dispersions: A review, *Minerals Engineering*, **6**, (4), pp 369-385 (1993).

Camp, J.I., Floc Volume concentration, *J. Am. Water works assoc.* **60** (6): 656-673 (1968).

Gomez, C. O., Probst, A., and Finch, J.A. Monitoring thickener operation using a conductivity probe. *Minerals and Metallurgical Processing,* **15**, (4), pp. 9-16 1998.

Hunter, R.J., Zeta Potential in colloid science, principles and applications, Academic Press, London, (1981).

Lagavanker, A. L., and Gemmel,R. S., A size-density relationship for flocs, *J. Am. Water Works assoc.* **60** 9, 19-40 (1969).

Marlow, b.J., Fairhurst, D. and Pendse, H. P. Colloid vibration potential and the electrokinetic characterization of concentrated colloids, *Langmuir*, **4**, pp:611 (1988).

Maxwell, J.C., *A Treatise on Electricity and Magnetism*, 2nd. Edn. Vol.I, Clarendon Press, Oxford, (1881).

Meredith, R.E. and Tobias, C. W., *Advances in Electrochemistry and Electrochemical Engineering,* Vol. 2, Interscience Publishers, New York, pp 15 (1962).

Mirnezami, M., Hashemi,M.S., and Finch, J.A. Measurement of conductivity of particles dispersed in water, accepted for publication by *Canadian Metallurgical Quarterly*, (2002).

Moudgi, B. M., and Vasudevan, T.V., Evaluation of floc properties for dewatering fine particle suspensions, *Min. Metall. Process.* **6** (3): 142-145 (1989).

Pugh, R.J., in: Forssberg, E. (Editor), Proc.XVI Int. Miner. Process. Congr., Elsvier, pp:751-62 (1988).

Sadowski, Z. & Laskwski, Hindered settling – A new method of the i.e.p. determination of minerals, *J. Colloids Surf.* , **1**, pp:151-159 (1980).

Somasundaran, P., Principles of flocculation, dispersion and selective flocculation. In:P. Somasundaran (Editor), Fine Particles Processing. SME, **2**, 947-976 (1980).

Stokes, G.G. *Mathematical and physical papers*, Vol. 3, Cambridge UniversityPress, Cambridge, (1891).

Turner, J.C.R., Two-phase conductivity. The electrical conductance of liquid-fluidized beds of spheres, *Chem. Eng. Sci.* **31,** pp 487-492 (1976).

Uribe-Salas, A., Vermet, F., & Finch, J.A., Apparatus and technique to measure settling velocity and holdup of solids in water slurries. *Chemical Engineering Science*, **48** (4), pp 815-819 (1993).

Vergouw, J.M. Anson, J., Dahlke, R., Xu, Z., Gomez, C. and Finch, J.A., A new automated data acquisition technique for settling tests. *Minerals Engineering,* **10** (10), pp 1095-1105 (1997).

CHAPTER 4

Measurement of Conductivity of Particles Dispersed in Water

4.1 Abstract

A method for measuring the electrical conductivity of particles dispersed in water is tested on common sulphide mineral samples (chalcocite, chalcopyrite, galena, pyrite and sphalerite). Using the automated conductivity-settling technique, aqueous solutions of KCl and $NaNO_3$ were used to change the conductivity of the medium. The particle conductivity was estimated at the iso-conductivity point where the solution and the particles have the same conductivity. The adsorption of xanthate significantly reduced the conductivity of chalcopyrite and copper activation increased the conductivity of sphalerite but not lead activation. These observations suggest that the measured conductivity is associated with the solid/water interface. The conductivity values are compared with rest potential values from literature.

4.2 Introduction

The physico-chemical properties of solid particle-aqueous solution dispersions control many processes in the chemical and metallurgical industries. The electrical conductivity of such dispersions is a function of solid type and concentration (% solids) and the nature of the solid-water interface. The complexity in modeling dispersion conductivity is apparent from the pioneering work of Maxwell (1881) to the more recent contributions (e.g. Meredith and Tobias, 1962; Turner, 1976; Banisi et al., 1993).

The models generally do not consider the properties of the solid-water interface. For solid particles, the interface between a particle and aqueous solution is characterized by an electric double layer. The double layer properties relevant to the present discussion include the potential, the capacitance (representing the charge required to change the double layer potential), and the impedance (representing the voltage change associated with the passage of current) (Shuey, 1975). In terms of conducting electric current through the dispersion, on the solid side of the interface this is accomplished by electrons while on the solution side it is accomplished by ions. Van Der Put and Bijsterbosch (1980) investigated the effect of charged particles on the dispersion conductivity and calculated a surface conductivity from the experimental data.

The interest here is sulphide minerals. These are semiconductors with a wide range of reported conductivity, which depends on their composition (Table 4.1). Electrical conductivity of a sulphide mineral can be affected by surface composition, which depends on the extent of oxidation and in the case of flotation, adsorption of various reagents. Sutherland and Wark (1955), describing the work of Buchanan and O'Connor, cited an increase in surface conductivity of sphalerite upon conditioning with copper sulphate. Bessier et al. (1990), using a high-frequency dielectric method, demonstrated that the conducting property of sphalerite is increased by treatment with Cu ions but not with Pb, Hg and Ag ions.

Table 4.1: Bulk Conductivity of Sulphide Minerals (after Shuey, 1975)

Mineral	Conductivity (S/m)
Pyrite	$0.3x10^2 - 10^3$
Chalcocite	$0.25 \times 10^2 - 8 \times 10^5$
Chalcopyrite	$10 - 10^4$
Galena	$0.5 - 0.3 \times 10^6$
Sphalerite	$10^{-12} - 10^{-9}$

Conditioning sphalerite with copper ions is used in flotation to promote (activate) reaction with the collecting agent xanthate. It is accepted that Cu exchanges with Zn in the sphalerite lattice (Finkelestein, 1997) and it is hypothesized this increases the conductivity of the solid, allowing adsorption of xanthate through an electron transfer (electrochemical) reaction. Panayotov (1995) showed the interaction with thiol collectors depended on the mineral displaying some electrical conductivity. The relatively weak interaction of xanthate with sphalerite has been ascribed by Dixon et al. (1975) to the high band gap (4 eV (Shuey, 1975)) compared to other sulphides (e.g., 0.77 eV for pyrite (Horita 1973)). Sphalerite's low conductivity makes it unable to sustain the electron transfer necessary for the adsorption of xanthate. It is likely that the band gap at the sphalerite surface is lowered in the presence of copper (Ralston and Healy, 1980).

Sulphide minerals being semiconductors assume a particular electrochemical potential in an aqueous medium. The electrification of the semiconductor-electrolyte interface results in a voltage or electric potential of the bulk semiconductor relative to bulk electrolyte, which is called Galvani potential (or rest potential at equilibrium). Electrification is a chemical reaction, which causes charge transfer across the interface. At equilibrium the Galvani potential ϕ is given by

$$me\ \phi = -\Delta G \qquad (4\text{-}1)$$

where me is the charge transferred and ΔG is the change of free energy in the electronation reaction. A positive potential corresponds to the release of free energy.

In the lowest state of total electronic energy, orbitals are occupied up to some energy value, the Fermi level (E_F) and are unoccupied above. Different types of solids may be distinguished by where the Fermi level lies relative to the energy band. In a metal the Fermi level is within a band, while for a semiconductor the Fermi level lies within a gap separating a full valence band from an empty conduction band (Fig. 4.1).

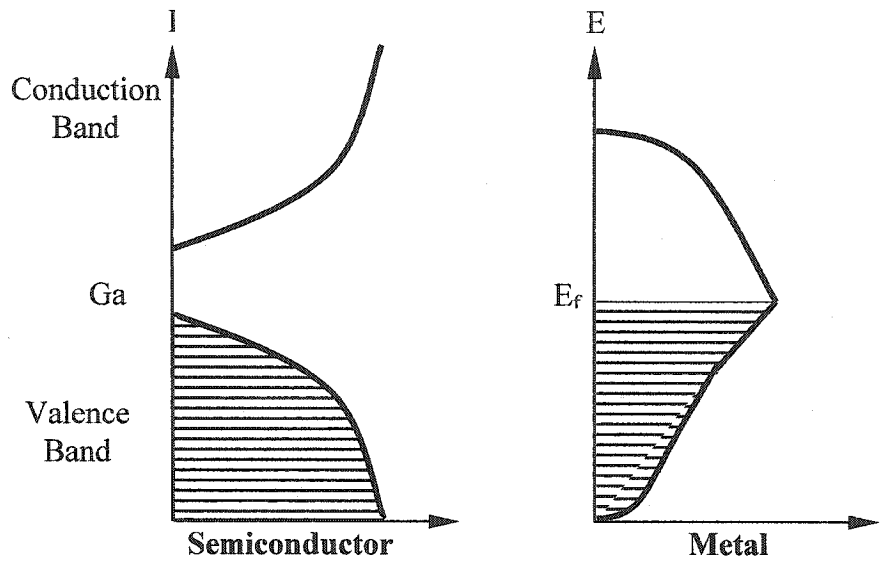

Figure 4.1: Density of carriers versus energy for semiconductors and metals.

As carrier (holes or electrons) concentration increases the Fermi level moves towards the conduction band increasing the conductivity. With this concept the change of potential is

$$\Delta\phi = \Delta E_F \qquad (4\text{-}2)$$

Thus raising the Fermi level towards the conduction band should increase the Galvani potential by the same magnitude. Details on the relationship between conductivity, rest potential and free energy are given in Shuey (1975).

The rest potential can be measured in a cell consisting of a mineral electrode and a reference electrode in open circuit (i.e., zero-current) (Prentice, 1991). Rand (1977) gave the order of rest potential of some sulphide minerals at pH 9 as

pyrite>pentlandite>chalcocite>chalcopyrite>covellite>
bornite>arsenopyrite>pyrrhotite>galena

and others have generally confirmed this (Sato, 1960; Yelloji Rao and Natarajan, 1989).

Measurements show pyrite has the highest rest potential among the sulphide minerals. For this reason it is sometimes referred to as the "most noble". While there is some controversy, sphalerite is generally placed below galena and treated as electrochemically inactive.

In this communication the conductivity-based settling technique (Uribe-Salas et al.,1993; Vergouw et al.,1997) is adopted to determine the conductivity of particles dispersed in water.

The measure is made by controlling the liquid conductivity till there is no change in the conductivity on settling; that is, the iso-conductivity point is reached where the particle conductivity equals the liquid conductivity. Dakshinamurti (1960) defined an iso-conductivity value as that at a concentration of electrolyte where the relative conductivity (conductivity of continuous phase to conductivity of dispersion) remains unity as the concentration of solids is varied. Using Dakshinamurti's data, Street (1963) calculated the surface conductivity of kaolin. Turner (1973) estimated the conductivity of ion exchange resin beads from experiments near the iso-conductivity point by varying the electrolyte concentration of the solution. Soulier et al. (1998) explored this principle to measure the conductance of ion-exchange textiles. Here it is shown that the iso-conductivity values reflect the properties of the sulphide mineral / water interface.

4.3 Sample and Solution Preparation

Chalcopyrite, chalcocite, sphalerite, pyrite and galena specimens were purchased from Ward's Scientific Establishment. A copper concentrate (chalcopyrite) was obtained from

Boliden Westmin (B.C. Canada). The Ward's samples were crushed in a jaw crusher, hand sorted, pulverized and wet sieved to obtain a -25 μm fraction. The concentrate was wet screened at 400 mesh and the +38 μm fraction was pulverized and wet sieved to -25 μm. This was done to minimize the effect of reagents added in the plant by creation of substantial fresh surface. All materials were kept under acetone to minimize subsequent oxidation. Chemical composition of the samples is shown in Table 4.2.

Table 4.2: Chemical Compositions of the Minerals

Samples	% Wt of Element			
	Zn	Fe	Cu	Pb
Chalcocite	-	2.00	72.00	-
Chalcopyrite	3.23	26.92	30.60	0.19
Galena	<0.04	<0.005	0.04	84.47
Pyrite	0.42	40.80	0.14	0.24
Sphalerite	65.0	0.3	0.1	0.0
Cu Concentrate*	4.29	32.55	28.56	4.45

* 0.91% was insoluble

De-ionized water, conductivity $< 0.54 \times 10^{-6}$ S/m, was the medium. The conductivity was varied using KCl and $NaNO_3$ (analytical grade) considered as indifferent electrolytes (in the sense that they should not contribute to particle conductivity). The solutions were allowed to reach room temperature prior to testing.

Sodium isopropyl xanthate (Cytec) was purified twice by dissolving in acetone and precipitated by petroleum ether (Rao, 1971). Fresh 5×10^{-3} M stock solution was prepared daily at ca. pH 9-9.5. The required amount of stock solution was added to the conditioning beaker to give a concentration of 5×10^{-5} M.

Cupric nitrate and lead nitrate, A.C.S. reagent grade from Fisher Scientific Co, were used for treatment (activation) of sphalerite.

Prior to the experiments the solid was removed from the acetone and dried in air. The experiments began with zero salt concentration. Fresh samples were conditioned for 10 minutes in water (at 2% v/v unless otherwise stated) and the natural pH recorded. In cases where chalcopyrite was treated with xanthate and sphalerite with Cu and Pb-salts, the suspension was filtered and the solids were transferred to de-ionized water for conductivity measurements. In the copper treatment of sphalerite it was observed for copper concentrations lower than 10^{-1} M that release of Cu ions to the solution occurred and interfered with measurements. To overcome this problem the filtered particles were washed thoroughly with 500 ml de-ionized water.

4.4 Procedure

The conductivity-settling technique measures conductance as a function of settling time in a conventional settling cylinder modified to include a conductivity cell. Figure 4.2 shows the result for chalcopyrite in de-ionized water (curve a). The conductivity decreases on settling from that of the well-mixed suspension (κ_m) to that of clear liquid (or continuous phase) (κ_c), indicating the chalcopyrite is more conducting than the water. The figure shows that the response changes as the conductivity of the medium is increased (curves b and c). Curve c represents the usual situation (most solids are non-conducting relative to the water in mineral processing). Curve b represents close to the iso-conductivity point; thus the conductivity of the chalcopyrite particles (κ_d) is around 0.58 S/m.

The estimation of κ_d was made by plotting $\frac{\kappa_c - \kappa_m}{\kappa_c}$ (reduced conductivity) against κ_c where $\kappa_d = \kappa_c$ when the reduced conductivity is zero. This point is determined by a polynomial fit to the data.

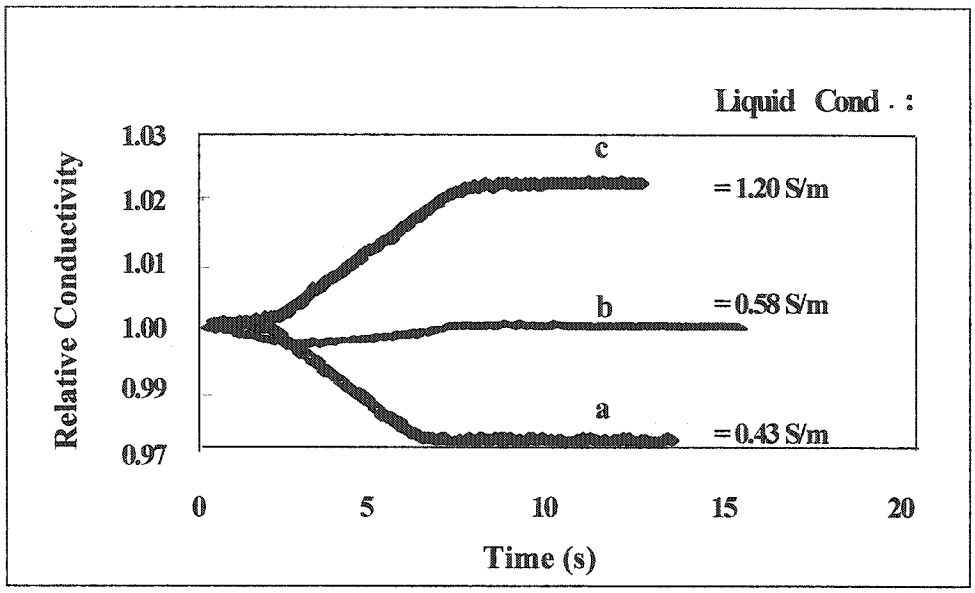

Figure 4.2: Conductivity settling curves for chalcopyrite particles in solutions with different conductivity.

4.5 Results and Discussion

4.5.1 Establishing the technique

The method of estimating the particle conductivity was tested using the two background electrolytes (KCl and $NaNO_3$ (Figure 4.3)) and by varying solids holdup (% solids) (Table 4.3). Neither should influence the value, and the figures support this.

Figure 4.3 shows the data follow the same relationship and yield the same κ_d, the mean and 95% confidence interval of seven tests being 0.60± 0.02 for KCl and 0.58 ± 0.05 for $NaNO_3$. For subsequent tests KCl was used.

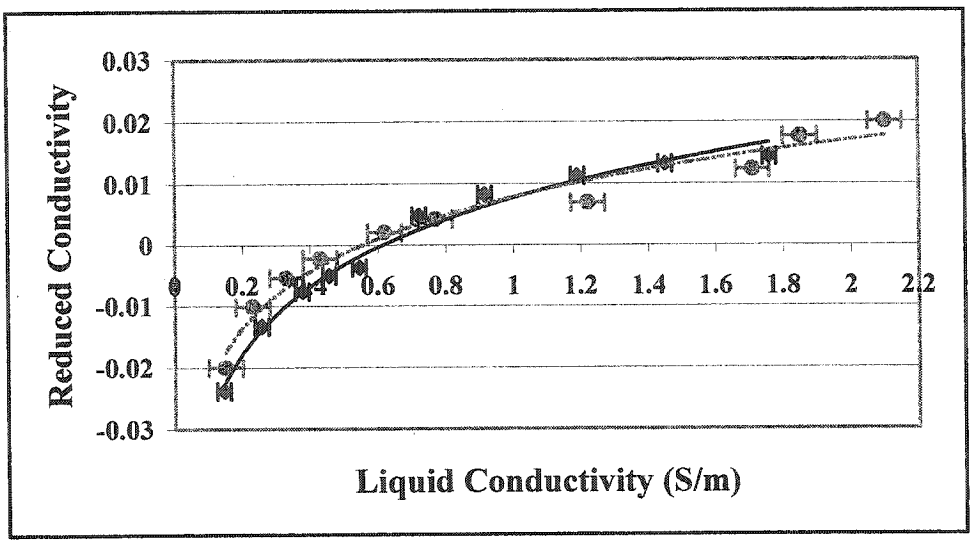

Figure 4.3: Estimating chalcopyrite conductivity by varying the liquid conductivity using two background electrolytes: KCl ♦$NaNO_3$ ⊛.

Table 4.3 shows κ_d was independent of % solids at least over the restricted solids holdup range imposed by the current design of settling apparatus (at > 3% v/v the settled bed interferes with the lower electrode). For these solids holdup measurements the copper concentrate was used. The difference in κ_d value, ~ 0.60 (Ward's) and 0.70 (Westmin concentrate), is well within the variation in natural materials.

Table 4.3: Effect of solids concentration on conductivity of chalcopyrite (Copper concentrate sample).

% Solids	κ_d (S/m)
1.5	7
2	7.2
3	6.9

4.5.2 Conductivity

The estimated conductivity for the four sulphide minerals is given in Figure 4.4. Except for sphalerite which is non-conducting (i.e., in agreement with Table 4.1) the conductivity of these sulphide particles dispersed in water is considerably below the bulk values. The two values appear to represent different properties; the present values probably indicate a surface conductivity.

The order shown in Figure 4.4, is the same as that of the rest potential. This follows from equation (4-2) where increasing conductivity increases the potential.

4.5.2 Effect of some flotation reagents

4.5.3.1 Xanthate

Chalcopyrite (Westmin) was conditioned (2% v/v) with $5x10^{-5}$ M xanthate. The result (Table 4.4) was a significant reduction in conductivity. Since adsorption alters the surface only, this change further suggests it is the surface conductivity that is being detected. A decrease in surface conductivity corresponds to the observed decrease in rest potential for xanthate treated chalcopyrite (Labonté and Finch, 1990).

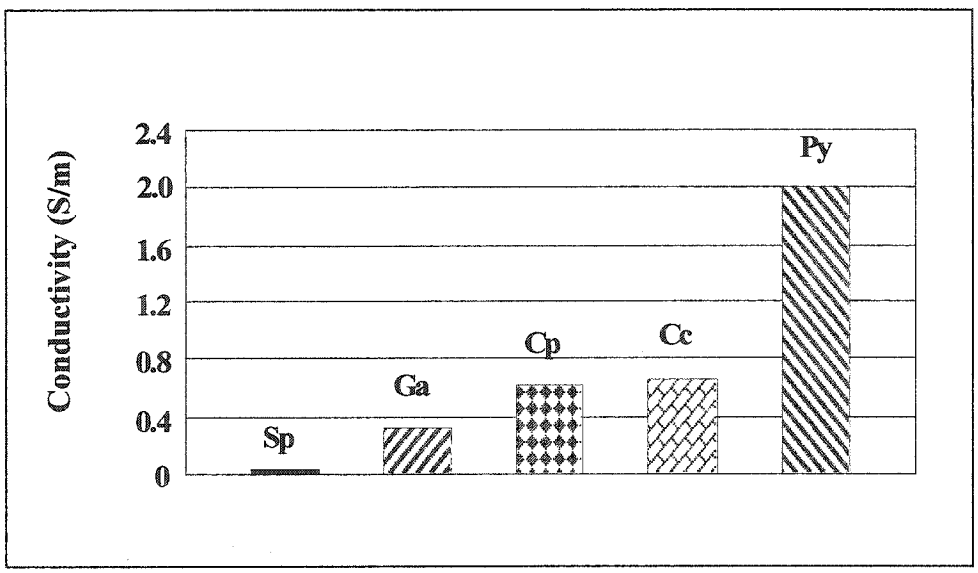

Figure 4.4: Conductivity of the sulphide minerals tested; sphalerite (Sp), galena (Ga), chalcopyrite (Cp), chalcocite (Cc) and pyrite (Py).

4.5.3.2 Copper/ lead treatment of sphalerite

Treatment with Cu ions is general practice to activate sphalerite for flotation with xanthate collector while accidental activation is often ascribed to lead ions (Finkelestein, 1997). For Cu ions exchange for lattice Zn ions is the widely accepted mechanism, although for Pb it is less clear (Finkelestein, 1997). Nevertheless a change in surface conductivity could be anticipated in both cases.

Table 4.4: Effect of flotation reagents on the conductivity (2% v/v and –25 μ).

Mineral	Conditions	κ_d (S/m)
Chalcopyrite	[Xn] = $5x10^{-5}$	0.37
Sphalerite	[Cu] < 10^{-1} M	0
Sphalerite	[Cu] =10^{-1}, 1 M	3.20, 3.25
Sphalerite	[Pb] = 10^{-4} to 1 M pH 4, 6 and 9.5	0

Table 4.4 shows this is the case for Cu. At low concentrations no effect was detected but at 10^{-1} M and above a sharp increase in conductivity occurred. The increase mirrors the increase in rest potential upon Cu activation (Chen and Yoon, 2000). The lack of response below 10^{-1} M (even $8x10^{-2}$ M showed no effect) is surprising when compared with the concentrations commonly used for activation (e.g., 10^{-4} M (Lange et al. 1997)). It is observed that Cu migrates several atomic layers deep into sphalerite (Prestidge et al., 1994). In terms of conductivity this may mean that a critical surface concentration and/or depth of penetration is required and this necessitates a high solution concentration to provide the driving force. Low concentrations also gave rise to re-release of adsorbed Cu ions, requiring the preparation procedure to be modified, as noted. This again suggests the Cu has not migrated into the surface sufficiently.

For Pb, under no conditions was an increase in conductivity observed. The pH was varied in these tests to explore the implication in the work of Trahar et al. (1997) that at pH 4 Pb exchanges with Zn in the sphalerite lattice analogous to Cu activation. No effect on

conductivity comparable to copper was detected. This is compatible with the observation that exchange is not energetically favoured and if it occurs, is restricted to the outer atomic layer only (Ralston and Healy, 1980). The result is consistent with the observation of Bessier et al. (1990). Recent voltammetry measurements (Morey et al., 2001) at pH 4.5 and 10 suggest adsorption of Pb^{II} onto sphalerite but not formation of PbS, in agreement with our findings.

4.6 Conclusions

The conductivity-settling technique has been adapted to measure the conductivity of sulphide particles dispersed in water by locating the iso-conductivity point. The effect of surface modification was detected: xanthate adsorption on chalcopyrite reduced the conductivity and Cu activation of sphalerite increased the conductivity but not lead activation. The conductivity measured appears to be associated with the solid-water interface and is much lower than the bulk value. The trend in conductivity correlated with the (electrochemical) rest potential, as expected.

4.7 References

Banisi, S., Finch, J.A., and Laplante, A.R., Electrical conductivity of dispersions: A review, *Minerals Engineering*, **6,** (4), pp 369-385 (1993).

Bessier,J. Chilihi, K., Thiebaut J.M., and Roussy, G. Dielectric study of the activation and deactivation of sphalerite by metallic ions. *International Journal of Mineral Processing*, **28**, pp1-13 (1990).

Chen, Z. and Yoon, R.H. Electrochemistry of sphalerite activation at pH 9.2. *International Journal of Mineral Processing*, **58**, pp 57-66 (2000).

Dakshinamurti, C. Studies on the conductivity of clay systems. *Soil Sci.* **90**, pp 302-305 (1960).

Finkelstein, N.P., The activation of sulphide minerals for flotation a review, *International Journal of Mineral Processing,* **52**, pp 81-120 (1997).

Horita, H., Some semiconducting properties of natural pyrite. *Japanese Journal of Applied Physics,* **12**, pp 617-618 (1973).

Labonté, G. and Finch, J.A. Behavour of redox electrodes during flotation and relationship to mineral floatabilities. *Minerals and metallurgical processing,* **7**, (2), pp106-109 (1990).

Lange, A.G., Skinner, W.M. and Smart, R.C., Fine: coarse particle interactions and aggregation in sphalerite flotation. *Minerals Engineering*, **10**, (7), pp 681-693 (1997).

Maxwell, J.C., *A Treatise on Electricity and Magnetism*, 2nd. Edn. Vol.I, Clarendon Press, Oxford, (1881).

Meredith, R.E. and Tobias, C. W., *Advances in Electrochemistry and Electrochemical Engineering,* Vol. 2, Interscience Publishers, New York, pp 15 (1962).

Morey, M.S., Grano, S.R., Ralston, J., and Prestidge, C.A. The electrochemistry of Pb^{II}activated sphalerite in relation to flotation, *Minerals Engineering*, **14**, (9) pp. 1009-1017 (2001).

Panayotov, V., *Energetical Basis of the Ore Dressing Processes,* University of Mining and Geology, UNIPLAN – Ltd. (1995).

Prentice, G., *Electrochemical Engineering Principles*, Prentice Hall, Englewood Cliffs, NJ., (1991).

Prestidge, C.A., Thiel, A.G., Ralston, J. and Smart, R.C., The interaction of ethyl xanthate with copper (II)-activated zinc sulphide: kinetic effects. *Colloids and Surfaces A: Physicochemical and Engineering Aspects*, **85**, pp 51-68 (1994).

Ralston, R. and Healy, T.W., Activation of zinc sulphide with Cu^{II}, Cd^{II}, and Pb^{II}, I. Activation in weakly acidic media. *International Journal of Mineral Processing*, **7**, (3), pp 175-201 (1980 a).

Rao, S.R., *Xanthates and Related Compounds*, Marcel Dekker, New York, pp 55-78 (1971).

Rand, D.A.J. Oxygen reduction on sulphide minerals. Part III., Comparison of activities of various copper, iron, lead, and nickel electrodes., *Journal of Electroanalytical Chemistry,* Vol.83, pp 19-33 (1977).

Sato, M., Oxidation of sulphide ore bodies, II. Oxidation mechanisms of sulphide minerals at 25° C. *Econ. Geol.* 55, pp 361-373 (1960).

Shuey R., *Semiconducting Ore Minerals*, Elsevier, Amsterdam, pp 145 and 251 (1975).

Soulier, S., Sistat, P., Dejean, E., Sandeaux, J., Sandeaux, R. and Gavach, C. Electrical conductance of ion-exchange textiles equilibrated with sodium chloride solutions. *J. Membrane Sci.*, **141**, pp 111-12 (1998).

Street, N., Iso-conductivity value of clays. *Soil Sci.* **95**, pp 367 (1963).

Sutherland, K.L., and Wark, I.W., *Principles of Flotation,* Australian Institute of Mining and Metallurgy (Inc.) pp 401-402 (1955).

Trahar,W.J., Senior, G.D., Heyes, G.W. and Creed, M.D., The activation of sphalerite by lead – A flotation perspective. *International Journal of Mineral Processing*, **49**, pp121-148 (1997).

Turner, J.C.R., Electrical conductivity of liquid-fluidized beds, *A. I. Ch. E. Symp. Series*, **69,** (128), pp 115-122, (1973).

Turner, J.C.R., Two-phase conductivity. The electrical conductance of liquid-fluidized beds of spheres, *Chem. Eng. Sci.* **31,** pp 487-492 (1976).

Uribe-Salas, A., Vermet, F., and Finch, J.A., Apparatus and technique to measure settling velocity and holdup of solids in water slurries. *Chemical Engineering Science*, **48** (4), pp 815-819 (1993).

Van Der Put, A.G. and Bijsterbosch, B.H., Electrical conductivity of dilute and concentrated aqueous dispersions of monodisperse polystyrene particles. Influence of surface conductance and double-layer polarization. *J. Colloid Interface Sci.*, **75,** (2), pp 512-524, (1980).

Vergouw, J.M. Anson, J., Dahlke, R., Xu, Z., Gomez, C. and Finch, J.A., A new automated data acquisition technique for settling tests. *Minerals Engineering,* **10** (10), pp 1095-1105 (1997).

Yelloji Rao, N.K. and Natarajan, K.A., Electrochemical effects of mineral-mineral interactions on the flotation of chalcopyrite and sphalerite, *International Journal of Mineral Processing*, **27**, pp 279-293 (1989).

CHAPTER 5

Aggregation of sphalerite: role of zinc ions

5.1 Abstract

Sphalerite from six sources is shown to aggregate at ca. pH 7-9, confirmed by different techniques (settling velocity, suspension analysis and optical microscopy). This does not correlate with the iso-electric point, which is consistently < pH 6. A similar observation was made by Healy and Jellet (1967) for ZnO (and reconfirmed here) who suggested Zn hydrolysis products were responsible. The hypothesis is tested using chalcopyrite and silica suspensions in the presence of Zn^{2+} ions. It is found that aggregation occurs over the same pH range, 7-9. Solution and surface analysis (extraction by EDTA) shows sphalerite released sufficient Zn^{2+} ions to promote aggregation. The pH range 7-9 corresponds to hydroxide precipitation suggesting this is the species responsible. Aggregation of sphalerite due to polymerization/ flocculation action of zinc hydroxide is proposed.

5.2 Introduction

In the processing of Pb-Cu-Zn sulphide ores, a common problem is sphalerite misreporting to the lead and copper concentrates. One mechanism by which minerals may misreport is through aggregation with a floatable mineral and recovery by entrapment. Aggregation as a possible cause of misplacement of minerals in flotation has long been suspected (Gaudin and Sun, 1946). The extent of the problem in plant practice, however, is largely unknown.

The state of aggregation of a suspension can be investigated several ways, but there is no agreed method of quantifying aggregation. Measures such as settling rate (Vergouw et al., 1997), viscosity (Muster and Prestidge, 1995), optical microscopy (Adler, 1987), particle size distribution (Lange et al., 1997), atomic force microscopy (AFM) (Muster et al., 1995), and turbidity (Maroto and de las Nieves, 1998) have been used.

Aggregation may occur by various mechanisms. Aggregation processes based on reducing inter-particle repulsion (i.e., by compression of the electrical double layer thickness or by charge neutralization) are classified as coagulation (La Mer, 1964; Subrahmanyan and Forssberg, 1990; Muhl, 1993). When aggregation results from the action of an immiscible bridging liquid, it is known as agglomeration (Laskowski, 1992). If aggregation is induced by polymer bridging action, the process is called flocculation (La Mer, 1964). Bridging forces of a different type also arise between charged surfaces that are "bridged" or cross-linked by multivalent counterions (Israelachvili, 1992). In water treatment the addition of certain metal ions is commonly used to promote aggregation. The mechanisms include both coagulation and bridging flocculation either by polymeric species (O'Melia, 1986) or by the precipitating metal hydroxide, which is known as sweep flocculation (Gregory, 1986). Differentiation between the mechanisms is often difficult; in this communication, aggregation is used as a generic term.

Many cases of aggregation follow the DLVO theory, which considers electrostatic and van der Waals interactions. These interactions, however, are confounded by other factors.

Hydrated surface species are hydrophilic and can induce a force of repulsion, while hydrophobic surface species can induce aggregation. An example of the former is silica, which remains dispersed at the iso-electric point (pH_{iep}) as the surface silanol (SiOH) groups are strongly hydrophilic (Ducker et al., 1992); an example of the latter is strongly hydrophobic coal, which aggregates despite large negative zeta potential (Leja, 1982).

Specific adsorption of ions can neutralize the charge on the particle and facilitate aggregation. The aggregation efficiency of salts follows the Schulze-Hardy rule (Hiemenz and Rajagopalan, 1997), but is often influenced by factors such as hydrolysis reactions. Hydrolysis is common to most cations. These reactions can lead to the formation of various hydrolyzed species and hydroxide precipitates. The hydrolysis products include monomers, such as $M(OH)_t^{(z-t)}$ (z=oxidation number, t=1,2,3,..) , and polynuclear species such as $M_2(OH)_t^{(z-t)+}$, $M_3(OH)_{2t}^{(3z-2t)+}$, etc. Sillen (1971) proposed a general mechanism of hydrolysis in which $M(OH)_t^{(z-t)+}$ groups are added stepwise to the cation:

$$M^{z+} \xrightarrow{M(OH)_t^{(z-t)+}} M_2(OH)^{(2z-t)+} \xrightarrow{M(OH)_t^{(z-t)+}} M_3(OH)_{2t}^{(3z-2t)+} .....$$

In many cases, soluble hydrolyzed species convert to colloidal particles (Baes and Mesmer, 1976) and precipitate as hydroxides, a process which can have a significant impact on aggregation.

As a start to understanding the possible role of entrapment in the misreporting of sphalerite in flotation, its aggregation behaviour was studied. The literature on sphalerite suspensions reveals a range of observations.

Vergouw et al. (1998) reported pH_{iep}=4 but maximum aggregation (settling rate) at pH 10, despite a zeta potential of ca. –40 mV. They suggested a hydrophobic force was induced sufficient to overcome the electrostatic repulsion although the species responsible was not suggested.

DiFeo et al. (2001) also found that aggregation did not correspond to the pH_{iep} of sphalerite; maximum settling rate was observed at ca. pH 8.5 where the corresponding zeta potential was ca. –27 mV. Based on Vergouw et al. (1998), they also attributed the effect to surface hydrophobicity. Referring to the work of Zhang et al. (1995), DiFeo et al. suggested the hydrophobic force was related to the dominant ZnS species over the range pH 6-9 being the one where Zn^{2+} is oriented into the solid phase with S exposed to the water, which makes the surface of sphalerite *appear* sulphur-rich (metal-deficient) inducing hydrophobicity. (Oxidation to induce metal deficiency is not plausible at alkaline pH (Healy and Moignard, 1976).)

Muster and Prestidge (1995) did observe that the maximum aggregation of sphalerite occurred at the iso-electric point, in this case pH 7. This high pH_{iep} suggests an oxidized surface.

Muster et al. (1995) performed a rheological study and surface force measurements (using atomic force microscopy) on synthetic sphalerite. At pH 4 the shear stress was lower relative to pH 6 to 8 indicating the suspension was dispersed. However, at pH 4 atomic force microscopy indicated attraction. They attributed this lack of correlation to the differences in solid/liquid ratio between the two experimental techniques inducing different levels of oxidation, as postulated by Somasundaran (1980).

Lange et al. (1997) tried to correlate flotation and aggregation of fine (< 20 μm) and coarse (38-75 μm) sphalerite determined using particle size measurements and optical microscopy. At acid pH aggregation occurred: small aggregates formed which increased in size with conditioning time. Aggregates were also observed at pH 8.5, but those larger than ca. 30 μm were weak and tended to break.

The present study aims to interpret the aggregation behaviour of sphalerite as a function of pH. Samples from various sources were used. Aggregation was studied using a combination of techniques: settling velocity, suspension analysis (turbidity) and optical

microscopy. Electrophoretic mobility (zeta potential) measurements were used to correlate against the aggregation results. Consistently, aggregation did not correlate with the pH_{iep}.

This observation is similar to that of Healy and Jellet (1967) for zinc oxide, ZnO. They suggested aggregation was due to release of Zn^{2+} ions to form $Zn(OH)_2$ which polymerizes and flocculates the particles. Their observation on ZnO is re-confirmed here. To test whether Zn hydrolysis products promote aggregation silica and chalcopyrite suspensions were doped with Zn^{2+} ions; aggregation over the same pH range as found for ZnO and sphalerite was found. The aggregation of sphalerite is, therefore, attributed to flocculation by hydrolyzed $Zn(OH)_2$.

5.3 Experimental

5.3.1 Minerals

Sphalerite was obtained from six sources, as zinc concentrate from five mineral processing plants and mineral specimens from Ward's Natural Science Establishment. The Ward's sample (Carthage, Tennessee, USA) was crushed by jaw crusher, hand picked, pulverized and wet sieved to separate the –25 μm fraction. The concentrates were wet screened at 400 mesh and the +38 μm fraction was pulverized and wet sieved to isolate the –25μm fraction. This was done to reduce the effect of reagents added in the plant.

Chemical composition of the samples along with a measure of the size distribution (%–20 and %–2 μm, determined by Sedi Graph) is shown in Table 5.1.

Table 5.1: Chemical compositions and size distribution of -25 μm sphalerite samples

Source	% Wt of Element				Size Distribution	
	Zn	Fe	Cu	Pb	%–20μm	%–5μm
Ward's	65.0	0.3	0.1	0.0	61	15
Boliden Westmin	40.0	17.5	0.4	0.04	40	10
Brunswick Mine	48.0	13.2	0.1	0.2	80	8
Hudson Bay M&S	48.0	12.4	1.2	0.1	75	10
Les mines Selbaie	51.0	8.2	1.3	0.1	51	8
Louvicourt	57.0	7.0	0.7	0.6	81	11

Microprobe analysis was performed on twenty sphalerite grains for each sample. The results (Table 5.2) revealed a range of composition, notably in iron content, which varied from 0.24 to 7.66 %Wt. The lead content in all the samples was less than 0.001 %Wt.

Table 5.2: Microprobe analysis on sphalerite grains

Source	% Wt of Element with 95% Confidence Interval			
	Zn	S	Fe	Cu
Ward's	67.58±0.083	32.68±0.019	0.241±0.010	0.063±0.007
Boliden Westmin	67.36±0.060	32.68±0.041	1.142±0.054	0.061±0.030
Brunswick Mine	60.50±0.136	33.12±0.032	7.036±0.098	0.005±0.001
Hudson Bay M&S	60.23±0.089	33.21±0.016	7.658±0.067	0.038±0.017
Les mines Selbaie	66.50±0.117	32.97±0.036	2.097±0.092	0.103±0.029
Louvicourt	60.54±0.127	33.28±0.027	6.602±0.116	0.026±0.011

Zinc oxide (80% -25 μm, 99.50% pure) was obtained from Fisher Scientific Co. The silica (100% -30 μm, 99.50% pure) was purchased from US Silica. Chalcopyrite specimens (Durango, Mexico) were purchased from Ward's Natural Science Establishment. The chalcopyrite was crushed in a jaw crusher, hand sorted, pulverized and wet sieved to obtain a -25 μm fraction

5.3.2 Reagents

The reagents used, all A.C.S. reagent grade from Fisher Scientific Co, were magnesium chloride, hydrochloric acid and sodium hydroxide.

5.4 Techniques

5.4.1 Settling

A cylinder was modified to collect settling data automatically by monitoring electrical conductivity (Uribe-Salas et al., 1993,1994; Vergouw et al., 1997). The cylinder was made from Plexiglas (non-conductive) and was 3.8 cm in diameter and 29 cm high. The cylinder stands on a plastic base and the top is covered with a rubber stopper after filling with suspension. Two identical ring electrodes, separated L=8.3 cm, are mounted internally flush to the walls and connected to a conductivity meter (Taccusel model CD 810) interfaced with a computer (data acquisition board, DAS-8PGA). A computer program was developed in Visual BASIC to record the conductance as a function of time (every 0.5 s).

To start, the suspension was mixed by end-over-end rotation of the cylinder. Data collection was initiated once the cylinder was stood vertically. The conductivity vs. time was plotted on the monitor to give a visual check on the process. Measuring the time to pass through the cell, T (s), gives the settling velocity, 8.3/T (cm/s). The data were processed using Excel. The relative standard deviation on the settling rate from repeat experiments was ca. 1%. Generally, settling tests were conducted without background electrolyte (e.g. KCl)

5.4.2 Suspension analysis

This analysis is a variety of turbidity measurement. After conditioning, the slurry was allowed to settle for 2 minutes in a 60 mL tube. One mL of suspension was taken from a specific height, filtered, dried and weighed. The weight of solid is a measure of turbidity.

For the settling and suspension analysis tests, slurries were prepared by adding the required mass of mineral to distilled water in a conditioning vessel to give 2% on a volume base (i.e., 2% v/v). The slurry was continuously agitated by a magnetic stirrer and conditioned for 20 minutes at the given pH to allow equilibrium (established by reaching a stable pH).

5.4.3 Optical microscopy

Direct observation helps confirm the indirect measurements (settling rate, suspension analysis). The conditioning regime was the same as for the settling/suspension analysis tests. After conditioning in a beaker, a $1cm^3$ glass tube was used to withdraw a sub-sample from the suspension. The sample was transferred to a second beaker and diluted several times with supernatant. Aggregates were selected with a spatula and placed onto a shallow pit slide, sealed with a coverslip and viewed under a stereomicroscope (Olympus), equipped with a Polaroid camera.

5.4.4 Zeta potential

Zeta potential measurements were performed on sphalerite using a Laser-Zee meter (Model 501, Pen Kem, Inc.) and on ZnO using the micro-electrophoretic apparatus Zeta Plus (Brookhaven Instruments Corporation, USA). These instruments determine the electrophoretic mobility and convert to zeta potential using the model of Smoluchowski.

The suspension for zeta potential measurement was made by adding 0.5 g of mineral to 500 mL 10^{-3} M KCl supporting electrolyte and conditioned in the same way as for the aggregation tests. For acidic and alkaline regions fresh samples were used.

Zeta potential measurements on two sphalerite samples were also performed on specimens extracted from the suspension after settling. This was done to test whether differing oxidation levels between the electrophoretic mobility and settling tests may contribute to discrepancies. In these cases, the settling test was done with background electrolyte (10^{-3} M KCl).

5.4.5 EDTA extraction

At pH 6 and 9, sphalerite from a settling test was vacuum filtered. The filtrate was analyzed by atomic absorption spectroscopy to determine the amount of Zn^{2+} in the solution. The filtered solids were then washed with 25 mL distilled water to remove entrained solution and treated with ethylenediaminetetraacetic acid (EDTA). This involved contacting 25 mL of 0.05 M EDTA per gram of sphalerite for half an hour (Sui et al., 1999). After, the suspension was vacuum filtered and the extract analyzed by atomic absorption spectroscopy to measure the amount of Zn extracted. This is taken as a measure of Zn ions present on the surface.

5.5 Results

5.5.1 Sphalerite

Figure 5.1 shows the settling velocity of sphalerite from the different sources as a function of pH is similar. With increasing pH, the settling velocity increased and reached a maximum at neutral to moderately alkaline pH (7-9) then decreased. Over the pH range giving the maximum settling velocity the supernatant was clear, otherwise the liquid retained some particles.

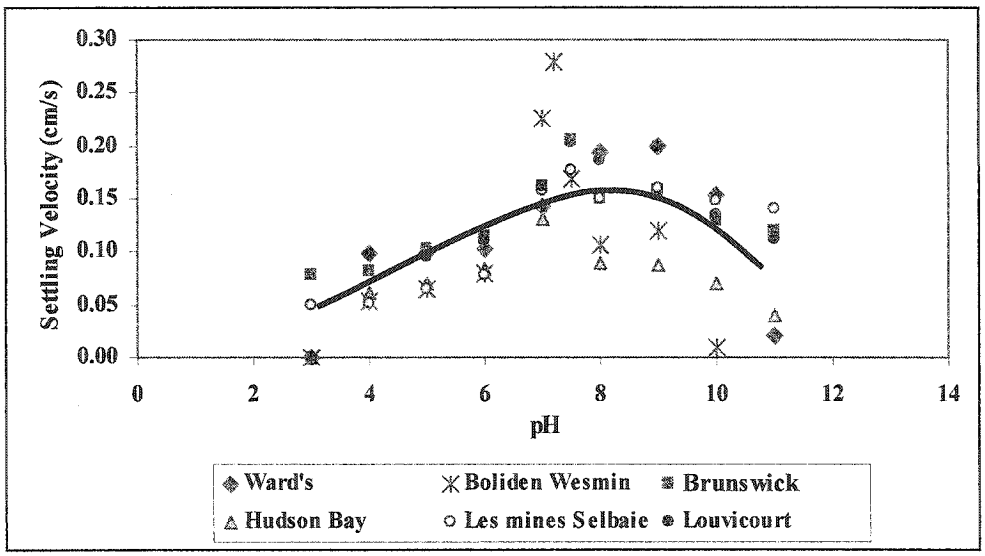

Figure 5.1: Settling velocity of sphalerite from different sources as a function of pH. Note: The sharp variation for the Boliden Wesmin sample was a repeatable phenomenon.

For suspension analysis, samples from two plants, Selbaie and Hudson Bay, to give a range of iron in composition (2.10-7.66%), as well as the Ward's sphalerite were used. The results (Fig. 5.2) were in good agreement with the settling data: Between pH 7 and 9 the amount of sphalerite remaining in suspension was low indicating the highest aggregation.

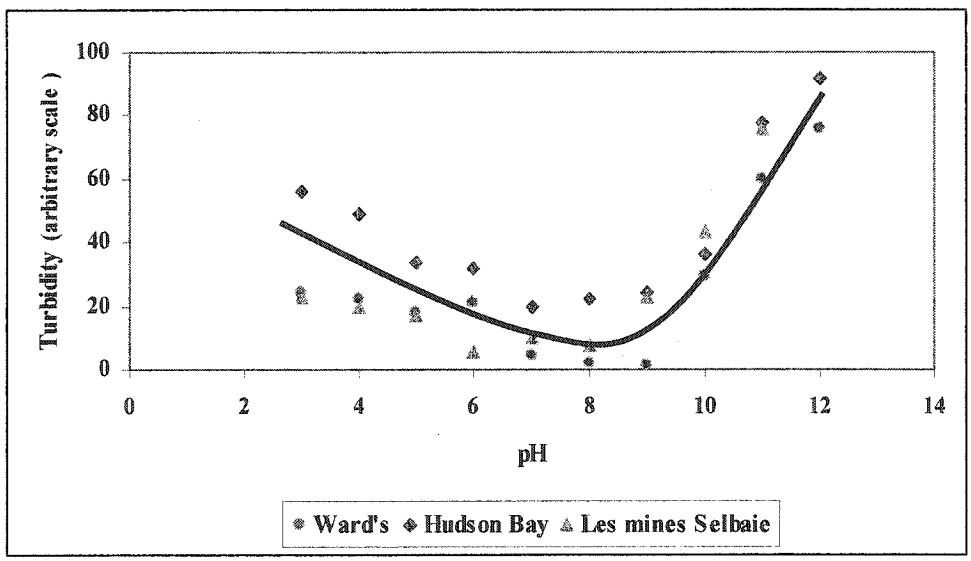

Figure 5.2: Turbidity measurements for three samples of sphalerite.

Visually, dispersed particles were evident at pH 4 (Fig. 5.3a). Increasing the pH induced aggregation, clearly observed at pH 8.5 where aggregates larger than 1mm are visible (Fig. 5.3b). By pH 11 (Fig. 5.3c), the sample was re-dispersed.

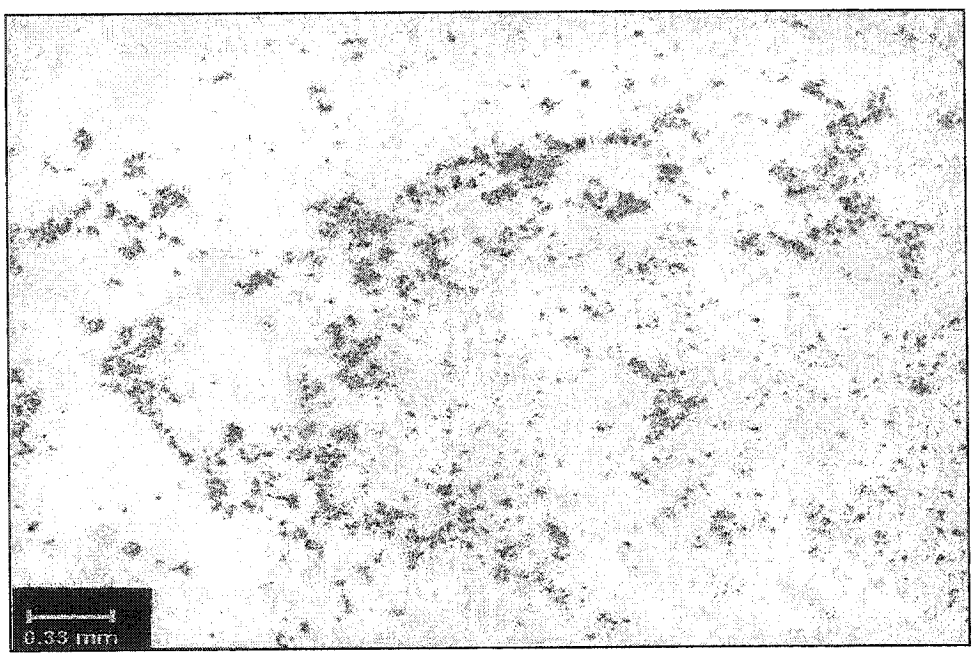

(a)

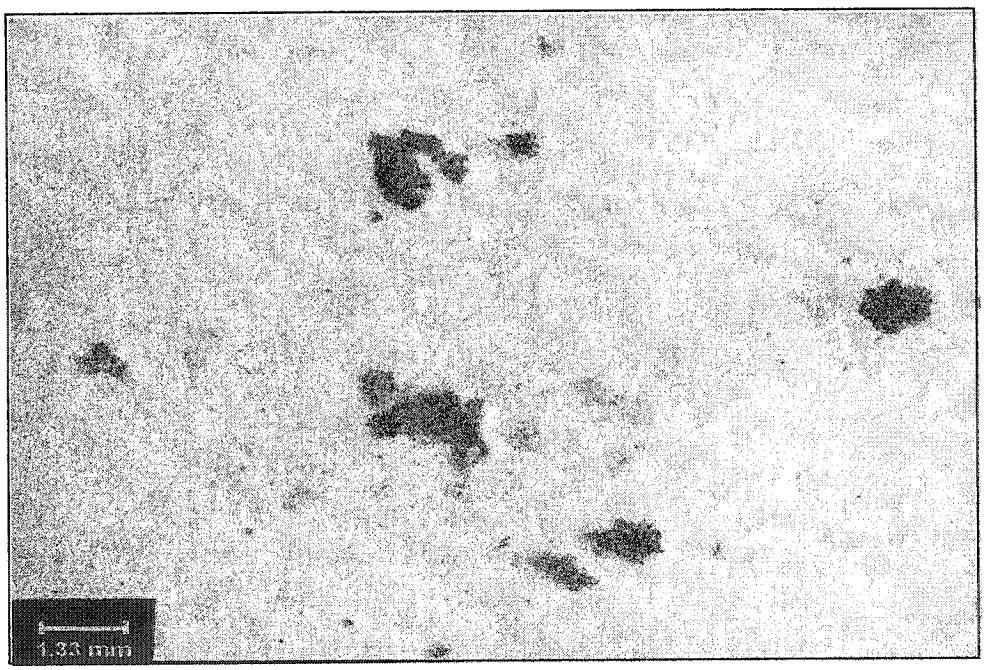

(b)

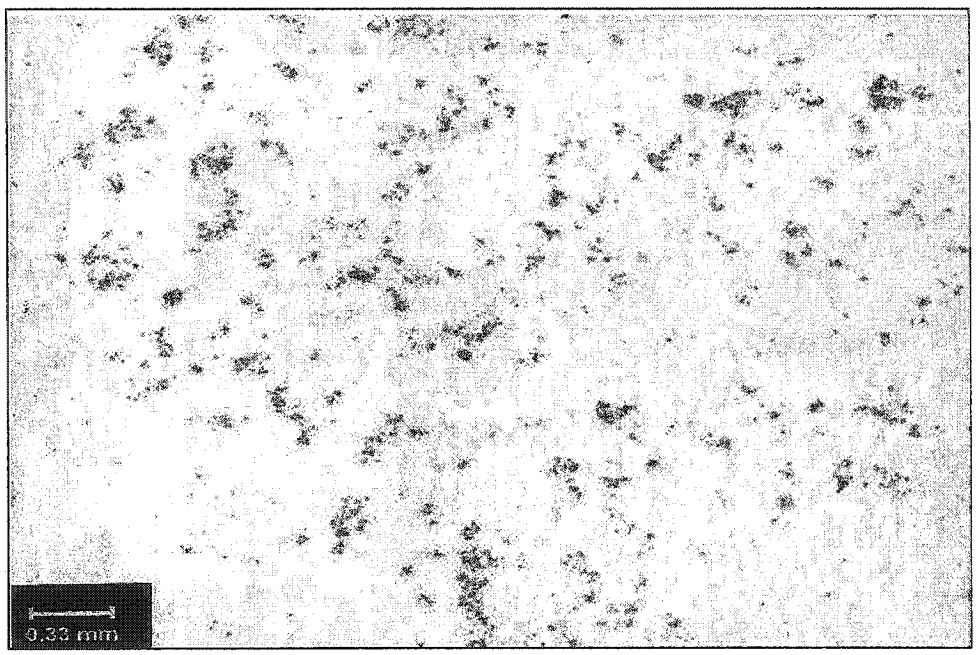

(c)

Figure 5.3: Optical microscopy images of sphalerite at: a) pH 4, b) pH 8.5, and c) pH 11.

Zeta potential as a function of pH for the three sphalerite samples (Ward's, Selbaie and Hudson Bay) is given in Figure 5.4. Previous workers have reported the iso-electric point (pH_{iep}) of non-oxidized sphalerite as ca. pH 2 while oxidized samples could range up to pH 8.5, close to the pH_{iep} of zinc hydroxide (Gaudin and Sun, 1946; Healy and Moignard, 1976; Muster and Prestidge, 1995; Zhang et al., 1995). The pH_{iep} of the sphalerite samples here varied from 3 to 6. The Ward's sphalerite had an iep at pH 3, suggesting an almost non-oxidized surface. For the plant samples the iep is shifted to higher pHs suggesting the presence of zinc oxidation products, or the influence of the Fe in the lattice. Figures. 5.4a and b indicate there is no significant discrepancy in zeta potential measured before and after settling. (Background electrolyte was used in these tests and it was also the case that the settling rate was not influenced by the electrolyte.)

From Figure 5.4, it is evident that the variation in aggregation is not related to the zeta potential. In two cases, Ward's and Selbaie (Figs. 5.4a and 5.4c), maximum aggregation occurs at a significantly higher pH than the pH_{iep}. The maximum in aggregation for both samples corresponds to a zeta potential <-15 mV where repulsion leading to dispersion would be expected. In the case of Hudson Bay (Fig. 5.4b), the variation in aggregation is less than the range in zeta potential, +10 to -40 mV would suggest. This lack of agreement between the pH_{iep} and maximum aggregation corresponds to observations of Vergouw et al. (1998) and DiFeo et al. (2001), but not to Muster and Prestidge(1995).

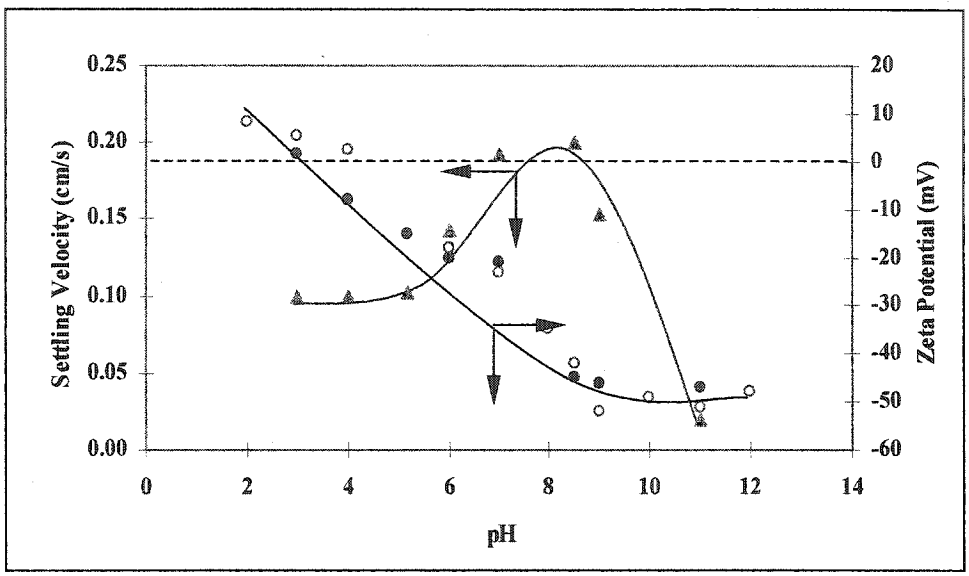

(a)

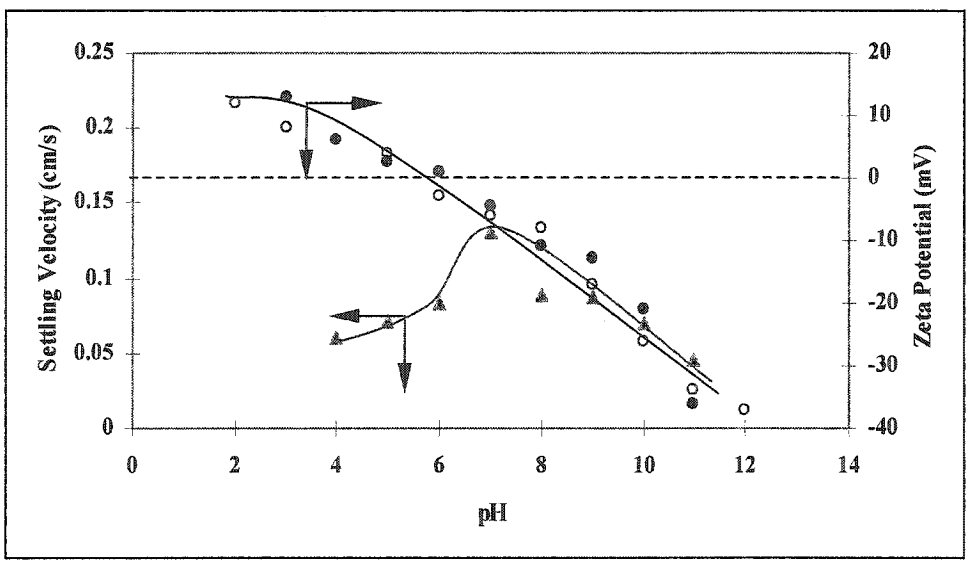

(b)

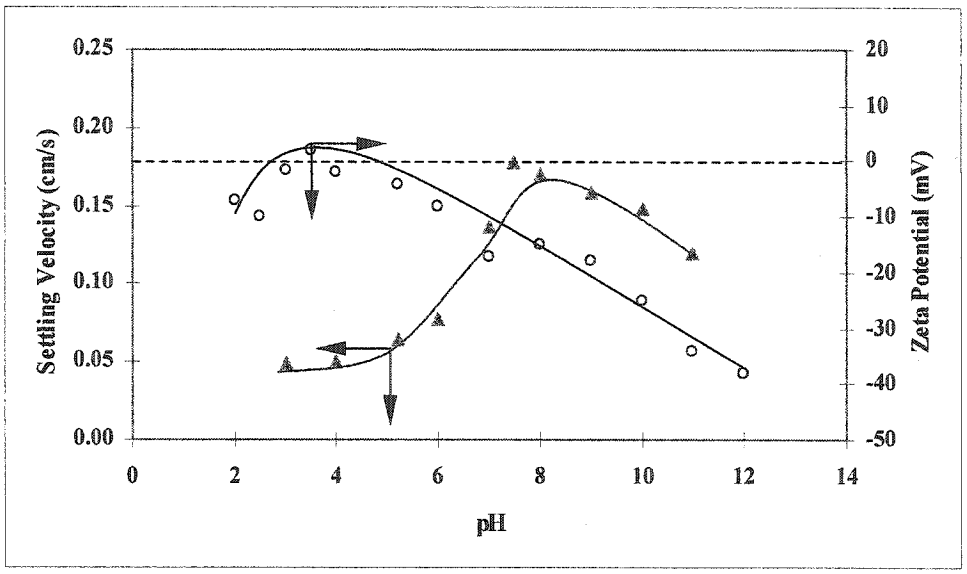

(c)

Figure 5.4: Zeta potential and settling velocity of three sphalerite samples. a) Ward's, b) Hudson Bay and c) Les mines Selbaie. Zeta potential measurements done after settling (a and b) indicated by ●.

5.5.2 ZnO, and test of hypothesis

Figure 5.5 shows the aggregation (settling rate) and zeta potential as a function of pH for zinc oxide. The maximum in aggregation occurred at a pH above the pH_{iep}, as found by Healy and Jellet (1967).

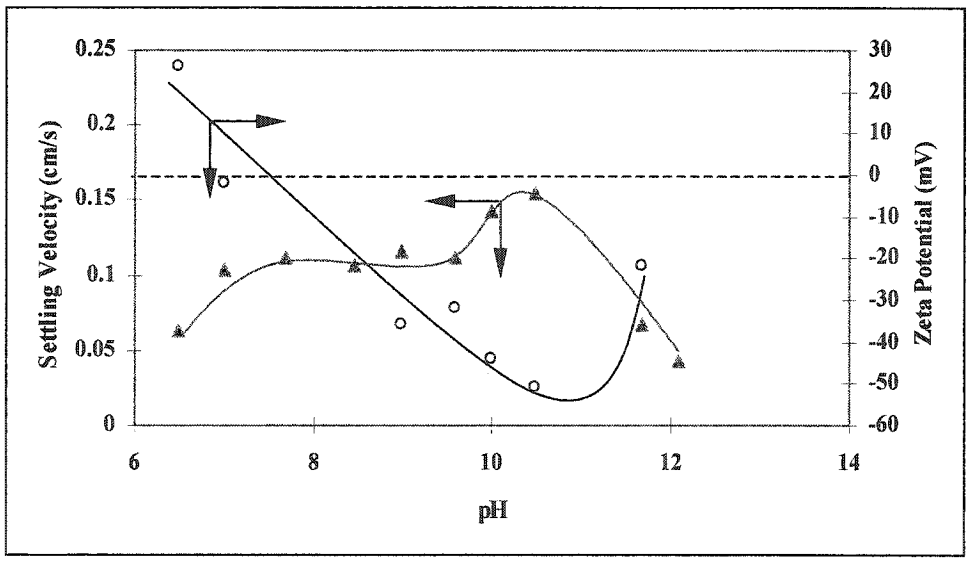

Figure 5.5: Settling velocity and zeta potential of ZnO as a function of pH (pH > 6 to avoid dissolution).

Their proposed hypothesis, that aggregation is related to release of zinc ions to form $Zn(OH)_2$ that causes flocculation, was tested using silica and chalcopyrite. Figure 5.6 shows the silica suspension in the absence of Zn^{2+} ions remained completely dispersed but as little as 10 ppm Zn caused aggregation, which reached a maximum around pH 9.

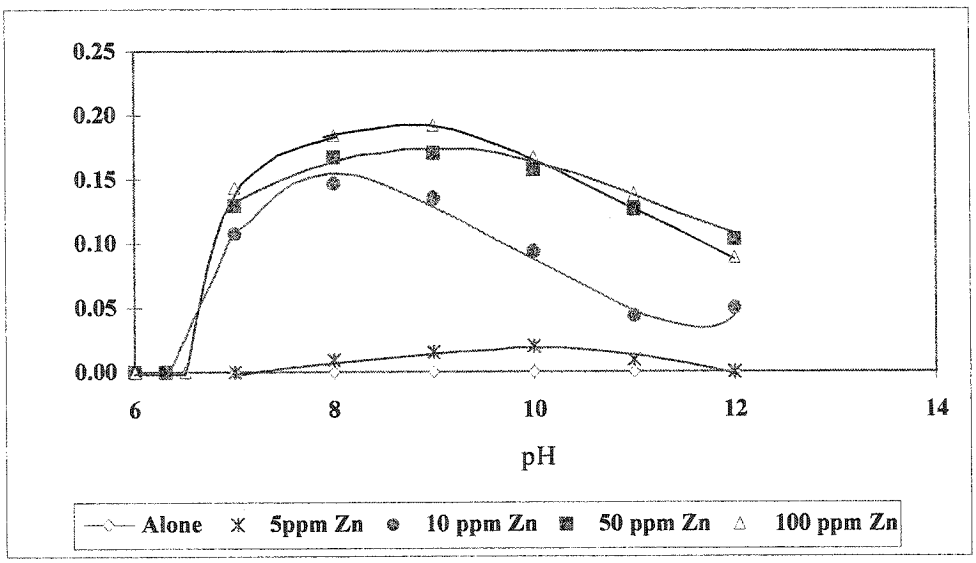

Figure 5.6: Aggregation behaviour of silica in the presence of Zn^{2+} ions.

Suspension analysis on chalcopyrite indicated that doping with 50 ppm Zn^{2+} ions induced aggregation and the maximum aggregation again occurred around pH 9 (Fig. 5.7).

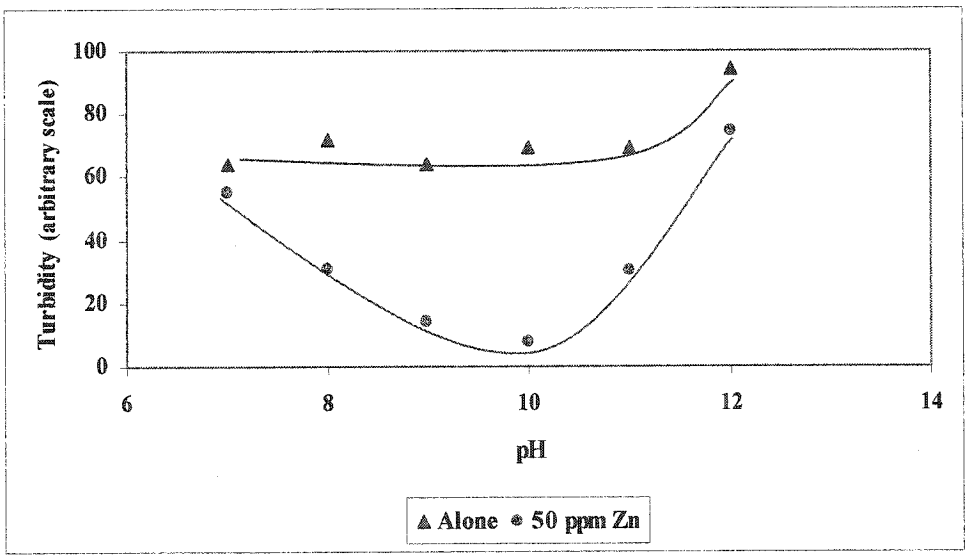

Figure 5.7: Aggregation behaviour of chalcopyrite in the presence of Zn^{2+} ions.

Comparing aggregation results with the species distribution diagram for 50ppm Zn^{2+} in solution it is evident that the maximum aggregation corresponds to the pH range where zinc is present in the hydroxide form (Fig. 5.8).

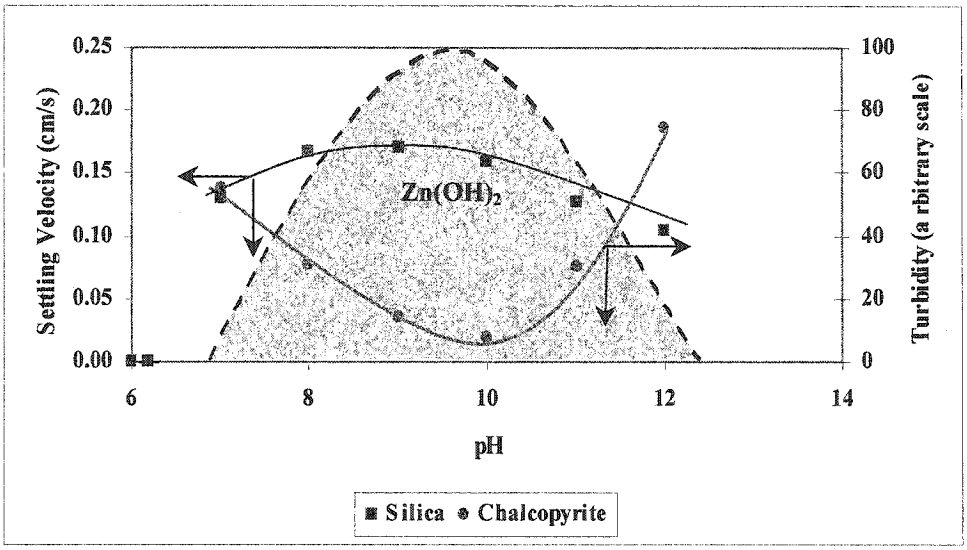

Figure 5.8: Comparison of the aggregation pH region for silica and chalcopyrite with region of $Zn(OH)_2$ formation for 50 ppm Zn^{2+}.

Solution analysis and EDTA extraction (surface analysis) (Table 5.3) on the Ward's sphalerite sample revealed that at pH 6 there is sufficient zinc ions (27 ppm) in solution to induce aggregation when the pH is raised to alkaline, by comparison with the results in Figures 5.6 and 5.7. At pH 9 the amount of Zn in solution decreased but there is a corresponding increase in surface Zn.

Table 5.3: Solution analysis and surface analysis (EDTA extraction) for Ward's sphalerite

pH	Zn^{2+} Concentration ppm	
	in Solution	EDTA Extracted
6	27	30
9	3	65

5.6 Discussion

The results for sphalerite over a range in composition indicate that maximum aggregation occurs in the pH range 7-9 and does not correspond to the pH_{iep}, which is in the range 2-6. The one example in the literature (Muster and Prestidge, 1995) showing the maximum in aggregation does occur at the pH_{iep} is the result of the pH_{iep} being high (ca. pH 7) suggesting an oxidized surface which is not the case here.

The result for sphalerite mirrors that for ZnO reported by Healy and Jellet (1967). A test of their hypothesis confirms that the aggregation corresponds to the formation of $Zn(OH)_2$. There appears to be sufficient Zn^{2+} released by sphalerite for this "autogenous" aggregation mechanism to be tenable. The role of Zn ions in aggregation is, therefore, central to our understanding.

Matijević et al (1962) applied a coagulation method to detect the hydrolysis of zinc ions. By measuring the concentration of zinc to coagulate negative silver bromide sol, they determined the species from pH 2-8.7. Their results indicated that the critical coagulation concentration at pH<6.7 corresponded to that of a simple doubly-charged ion, (hydrated) Zn^{2+}. At ca. pH 8 the critical coagulation concentration decreased to a value close to that expected for a simple triply charged ion. They concluded this could be accounted for if polynuclear complexes were assumed. Accepting that Zn:OH=1:1, they introduced $Zn_3(OH)_3^{3+}$ as the dominant species at ca. pH 8. They did not exclude the possibility of Zn_2OH^{3+} as long as the Zn:OH ratio was not known with certainty. These cations should exhibit a marked effect on the zeta potential, if they are present on the sphalerite surface in this region (pH 8-9). This does not seem to be the case, sphalerite remains strongly negatively charged at pH 8-9.

Dyer and Scrivner (1998) predicted the solubility of zinc hydroxide in water as a function of pH. They found that for zinc concentrations $<10^{-2}$ molal, polynuclear complexes had minimal effect on zinc solubility and could be neglected. Details on the hydrolysis of Zn^{2+} and its solubility products can be found in Baes and Mesmer (1976).

Aggregation of ZnO particles in the alkaline region was considered by Healy and Jellet (1967) to be due to flocculation by polymeric zero charged Zn(II) hydrolyzed species. They proposed that soluble zinc hydroxide, which forms above pH 7, had the necessary properties to explain both the electrophoretic mobility and aggregation data. The species is zero charged and since it is the precursor to precipitation of insoluble $Zn(OH)_2$, it can be expected to be in polymeric form. Such inorganic polymers are known to induce aggregation by a bridging mechanism. Considering the anionic nature of the sphalerite surface at alkaline pH, proton abstraction from adjacent $[Zn(OH)_2\ (H_2O)_2]^0_n$ species at the surface to form bridged dimer, trimer, etc., units is suggested.

The qualitative evidence of the adsorption-flocculation reaction of $[Zn(OH)_2\ (H_2O)_2]^0_n$ was examined quantitatively by Healy and Jellet following Grahame's (1947) treatment of the compact double layer. From mobility measurements, they concluded that the OH^- and Zn(II) anions must adsorb much more strongly than the Zn^{2+} ion at pH values around 8 to 9. Due to OH and Zn(II) anion adsorption, the $[Zn(OH)_2]_{sol}$ species is the dominant Zn(II) species at the interface, and to promote aggregation at that pH it must be in polymeric form.

The sphalerite appears to react the same as ZnO. Analysis indicates that sphalerite yields sufficient hydrolyzable zinc(II) ions in solution to promote aggregation. The zeta potential data suggest the presence of anionic species is dominant at moderately alkaline pH. Thus the same aggregation mechanism of ZnO can be proposed for sphalerite. Aggregation in sphalerite-water dispersions is considered to be due to flocculating action of the polymeric zero charged Zn(II) species, $[Zn(OH)_2\ (H_2O)_2]^0_n$. The value of n will not be large since the polymers are effective at around 10^{-5} M compared to organic flocculants (e.g., polyacrylamide), which are effective at around 10^{-7} (Healy and Jellet, 1967). Hence we do not need to invoke very long chains as bridges.

These arguments refer to ZnO and sphalerite. The aggregation tests on silica and chalcopyrite in the presence of Zn^{2+} ions was to show that the effect is related to Zn hydrolysis products. It is not intended that the bridging/flocculation mechanism involved for ZnO and sphalerite is universal whenever Zn^{2+} ions are involved. The silica/chalcopyrite/ Zn^{2+} ion systems would need additional investigation to try to decide that.

5.7 Conclusions

Similar aggregation behaviour was observed for sphalerite of a range in composition from a variety of sources: Aggregation was maximum around pH 7-9 and did not correlate to the iso–electric point (pH 2-6).

The Zn^{2+} ion has an aggregating effect over the pH range where hydroxide species form.

Aggregation of sphalerite is considered to be due to the flocculating action of polymeric zero-charged Zn(II) species, similar to that proposed for the aggregation of ZnO.

5.8 References

Adler, P. M., Hydrodynamic properties of fractal aggregates. *Faraday Disc. Chem. Soc.* **83**, pp. 145-152 (1987).

Baes, C.F. J., Mesmer, R.E., *The Hydrolysis of Cations*. John Wiley and Sons, Inc., New York (1976).

DiFeo, A., Finch, J.A., Xu, Z., Sphalerite – silica interactions: effect of pH and calcium ions. *Int. J. Miner. Process.*, **61**, pp. 57-71 (2001).

Ducker, W. A., Senden, T.J., Pashly, R.M., Measurement of forces in liquids using a force microscope. *Langmuir,* **8**, pp. 1831-1836 (1992).

Dyer, J.A. and Scrivner, N.C., A practical guide for determining the solubility of metal hydroxides and oxides in water. *Environmental Progress*, **17**, (1), pp. 1-8 (1998).

Gaudin, A.M. & Sun, S.C., Correlation between mineral behaviour in cataphoresis and in flotation. *Trans, AIME*, **169**, p. 347 (1946).

Graham, D.C., The electrical double layer and the theory of electrocapillarity. *Chemical Reviews*, **41**, pp. 441-501 (1947).

Gregory, J., The action of polymeric flocculants. In: B.M. Moudgil and P. Somasundaran (Eds.), *Flocculation, sedimentation and consolidation,* Engineering Foundation, New York, N.Y., pp. 125-138 (1986).

Healy, T.W. and Jellet V.R. Adsorption coagulation reactions of Zn(II) hydrolyzed species at the zinc oxide-water interface. *J. Colloid Interface Science*, **24**, pp. 41-46 (1967).

Healy, T.W. and Moignard, M.S., A review of electrokinetic studies of metal sulphides. In M.C. Fuerstenau (Ed.), *Flotation,* A.M. Gaudin Memorial Volume. AIME, NewYork, pp. 275-297 (1976).

Hiemenz, P. C. and Rajagopalan, R., *Principles of colloid and interface chemistry*, Marcel Dekker, Inc. N.Y., p. 588 (1997).

Israelachivili, J.N., Adhesion forces between surfaces in liquids and condensable vapours. *Surface Science Report, A review journal*, **14**, 3, pp. 109-159 (1992).

Lange, A.G., Skinner, W.M. & Smart, R. St. C., Fine: coarse particle interactions and aggregation in sphalerite flotation. *Minerals Engineering*, **10**, (7), pp. 681-693 (1997).

La Mer, V.K., Coagulation symposium introduction. *J. Colloid Science,* **19**, pp. 291-293 (1964).

Laskowski, J.S., Oil assisted fine particle processing, In Laskowski, J.S. and Ralston, J. *Colloid chemistry in mineral processing,* Developments in Mineral Processing Series, Vol. 12, Elsvier Science Publishers B. V., Netherlands, p. 387 (1992).

Leja, J., *Surface chemistry of froth flotation.* Plenum, New York, NY pp. 43-44 (1982).

Maroto, j. A., de, las Nieves, F. J. Influence of multiple light scattering on the estimate of homocoagulation and heterocoagulation rate constant by turbidity measurements, *Colloids and Surfaces A- Physicochemical & Engineering Aspects.* V 132 n 2-3 Jan 30, pp. 153-158 (1998).

Matijevic, E., Couch, J.P., Kerker, M., Detection of metal ion hydrolysis by coagulation. IV zinc. *J. Physical Chemistry*, **66**, pp. 111-114 (1962).

Muhle, K., Floc stability in laminar and turbulent flow. In Dobias B. (ed.), *Coagulation and flocculation,* Surfactant Science Series, Vol. 47, Marcel Dekker, New York, p. 356 (1993).

Muster, T.H. & Prestidge, C.A., Rheological investigations of sulphide mineral slurries. *Minerals Engineering*, **8** (9), pp. 1541-1555 (1995).

Muster, T.H., Toikka, G Hayes, R.A., Prestidge, C.A., Ralston, J., Interactions between zinc sulphide particles under flotation-related conditions. *Colloids and Surfaces*, **106**, pp. 203-211 (1995).

O'Melia, C.R., Polymeric inorganic flocculants. In: B.M. Moudgil and P. Somasundaran (Eds.), *Flocculation, sedimentation and consolidation*, Engineering Foundation, New York, N.Y., pp. 159-169 (1986).

Sillen, L.G., Quantitative studies of hydrolytic equilibria. *Quarterly Reviews*, **13**, pp. 146-168 (1959).

Somasundaran, P., Principles of flocculation, dispersion and selective flocculation. In: P. Somasundaran (Editor), *Fine Particles Processing.* SME, **2**, pp. 947-976 (1980).

Subrahmanyam, T.V. and Forssberg, K.S.E., Fine particles processing: shear flocculation and carrier flotation – a review. *Int. J. Mineral Processing.* **30**, pp. 265-288 (1990).

Sui, C., Grimmelt, J.C.A., Rashchi, F., Rao, R., Finch, J.A., Lead ions and sphalerite recovery in copper rougher flotation. In B.A. Hancock and M.R.L Pon. Proceedings of Copper 99 International Environment Conference, *Mineral Processing/Environment, Health and Safety,* The Minerals, Metals & Materials Society, Vol. 2, pp. 145-157 (1999).

Uribe-Salas, A., Gomez, C.O., Finch, J.A., A conductivity technique for gas and solids holdup determination in three-phase reactors. *Chemical Engineering Science*, **49** (1), pp. 1-10 (1994).

Uribe-Salas, A., Vermet, F., Finch, J.A., Apparatus and technique to measure settling velocity and holdup of solids in water slurries. *Chemical Engineering Science*, **48** (4), pp. 815-819 (1993).

Vergouw, J.M. Anson, J., Dahlke, R., Xu, Z., Gomez, C. O. & Finch, J.A., A new automated data acquisition technique for settling tests. *Minerals Engineering,* **10** (10), pp. 1095-1105 (1997).

Vergouw, J.M., DiFeo, A., Xu, Z., Finch, J.A., An agglomeration study of sulphide minerals using zeta potential and settling rate: Part II. sphalerite/pyrite and sphalerite/galena. *Minerals Engineering,* **11**, (7), pp. 605-614 (1998).

Zhang, Q., Xu, Z., Finch, J., A., Prediction of species distribution at sphalerite / water interface. *Minerals Engineering*, **8**, (9), pp. 999-1007 (1995).

CHAPTER 6

Aggregation by Magnesium Ions

6.1 Abstract

The presence of Mg^{2+} ions causes aggregation of sphalerite and silica above pH 10, i.e., corresponding to magnesium hydroxide precipitation. The mechanism is explored using settling velocity, zeta potential and scanning electron microscopy. The mechanism for sphalerite appears to be chemical bridging, different from silica, which appears to be electrostatic bridging.

6.2 Introduction

Magnesium species are among the most common encountered in process water in flotation. Iwasaki and co-workers in a series of studies revealed their impact on iron ore processing (Iwasaki, 1989). In comparison, their possible role in sulphide mineral flotation has received scant attention. This may be because the Mg^{2+} concentration ($[Mg^{2+}]$) in the pulp liquor is typically around 50 ppm compared to 500 ppm for Ca^{2+} (Lascelles et al., 2001), which in contrast, has received considerable attention (Fuerstenau et al.,1985).

One effect of magnesium ion described by Krishnan and Iwasaki (1986) was marked aggregation of quartz at pH>10, i.e., corresponding to precipitation of the hydroxide, $Mg(OH)_{2(s)}$ (Fig. 6.1). In a study on samples drawn from various streams in sulphide mineral flotation plants, El-Ammouri et al. (2002) likewise observed aggregation due to Mg^{2+} above pH 10.

Aggregation in the presence of magnesium ion is the subject of this chapter. Two minerals are studied, silica, essentially to repeat the work of Krishnan and Iwasaki (1986), and sphalerite, being the focus of the thesis. The main objective is to identify the aggregation mechanism.

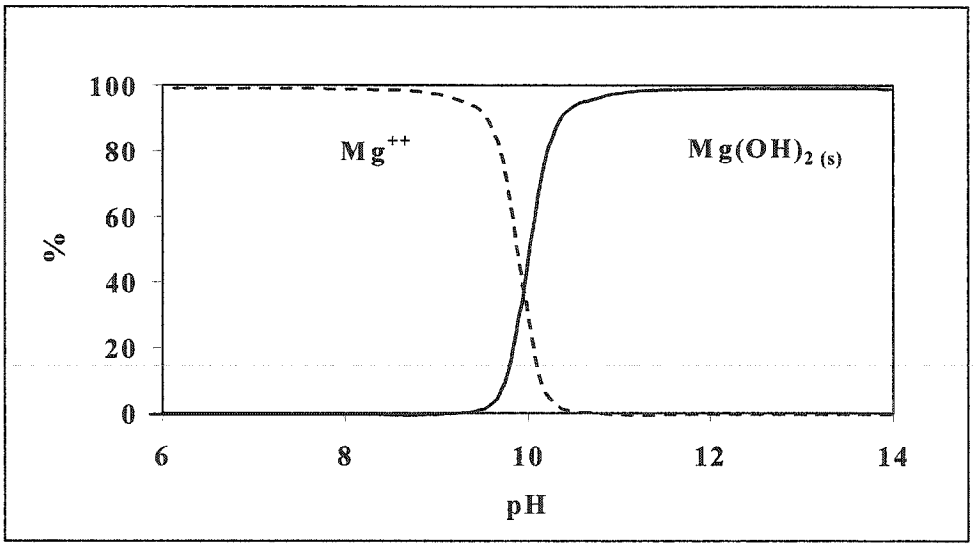

Figure 6.1: Magnesium species relative distribution diagram as a function of pH (note: $MgOH^+$ concentration is negligible).

6.3 Mechanisms

Most early attempts to explain the stability of a suspension considered only the surface charge on the particles. The existence of a charge was recognized as the primary cause of stability; thus neutralization of the charge would lead to aggregation (or coagulation). It is now evident that mechanisms other than charge neutralization can be involved. Matijević (1973) demonstrated that there are various processes such as ion exchange, condensation, coordination, and polymerization, which play a role in aggregation.

Polyvalent cations like Mg^{2+}, are known to promote aggregation, notably when present as hydrolysis products. For example, Mg^{2+} undergoes a series of hydrolysis reactions:

$$[Mg(H_2O)_4]^{++} + H_2O \longrightarrow [Mg(H_2O)_3(OH)]^{+} + H_3O^{+}$$
$$[Mg(H_2O)_3(OH)]^{+} + H_2O \longrightarrow [Mg(H_2O)_2(OH)_2] + H_3O^{+}$$

The reactions are sensitive to pH and the products ("complexes") influence aggregation via different mechanisms.

The aggregation effect of Mg^{2+} is associated with hydroxide precipitate formation (Krishnan and Iwasaki, 1986). Three mechanisms have been proposed to explain aggregation in this case: 1) Charge neutralization by adsorption of positively charged precipitates (the iso-electric point (iep) of $Mg(OH)_2$ is ca pH 13); 2) Sweep flocculation, due to aggregation (polymerization) of the hydroxide itself trapping other particles (Packham,1965); 3) Bridging through hydroxide species (Healy and Jellet, 1967; Krishnan and Iwasaki, 1986). By considering the characteristics of each, experiments can be designed to distinguish the mechanisms.

Charge neutralization has three main characteristics related to increasing "coagulant" addition: 1) Suspension de-stabilization, 2) A maximum in aggregation when zero charge (or point of charge reversal) is reached and 3) Re-stabilization with excess dosage (Dentel, 1988).

Sweep flocculation describes domains where abundant precipitation of hydrolyzable metal ion occurs that enmeshes the suspended particulates. In that case, the optimal conditions (pH, coagulant concentration) for aggregation are reported to be independent of the nature of suspended particles being those which maximize the aggregation of precipitates (Packham, 1965).

The bridging mechanism has two sub-categories: electrostatic (Krishnan and Iwasaki, 1986) and chemical (Healy and Jellet, 1967). In electrostatic bridging, also known as

"patch flocculation" (Dobiáš et al., 1999), positively charged hydroxide precipitates bridge between negatively charged particles (Fig. 6.2). If the particles become fully coated, the resultant positive charge causes dispersion. Electrostatic bridging can be distinguished from aggregation due to charge neutralization as the pH of maximum aggregation does not occur at the pH of charge reversal. The conditions causing re-dispersion are high pH and/or high salt concentration, which promote more complete coverage.

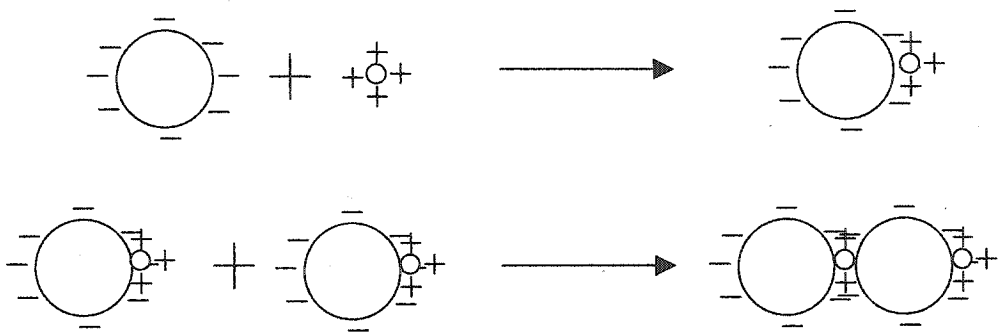

Figure 6.2: Electrostatic bridging: Positively charged hydroxide precipitate bridges two negatively charged particles. (Note: The opposite situation, negatively charged precipitates and positively charged particles could also promote electrostatic bridging but is a less likely scenario.)

In the case of chemical bridging one form is H-bonding via the hydration layers on the hydroxide species (Attia, 1992). In this mechanism surface charge does not play a significant role and increasing the amount of hydroxide either by raising the pH or by increasing the salt concentration should not cause re-dispersion unlike the case of electrostatic bridging.

To try to identify the Mg^{2+} aggregation mechanism the settling rate of sphalerite and silica suspensions (individually) was determined as a function of salt concentration, pH and suspension density (%v/v solids). Aggregation at pH >10 was found for both minerals corresponding to magnesium hydroxide but their response to the three variables

suggests the mechanism for each is different. The mechanism was further explored by complementary zeta potential and surface characterization studies.

6.4 Experimental

6.4.1 Materials

Sphalerite (Carthage, Tennessee, USA) was purchased from Ward's Natural Science Establishment. It was crushed, hand sorted, pulverized and wet sieved to obtain –38 μm fraction for the aggregation (settling rate) and zeta potential study and a 25-38 μm fraction for examination under a field emission scanning electron microscope (FE-SEM). Silica (–30 μm, 99.50% pure) was purchased from US Silica for the settling and zeta potential studies; for FE-SEM analysis a 25-30 μm fraction was isolated.

The reagents, all A.C.S. reagent grade from Fisher Scientific Co, were magnesium chloride, hydrochloric acid and sodium hydroxide.

6.4.2 Techniques

6.4.2.1 Settling rate

Settling rate is used as a relative measure of aggregation. A cylinder was modified to collect suspension settling data automatically by monitoring electrical conductivity (Uribe-Salas et al., 1993; Vergouw et al., 1997). The cylinder was made from Plexiglas (non-conductive) and was 3.8 cm in diameter and 29 cm high. The cylinder stands on a plastic base and the top is covered with a rubber stopper after filling with suspension. Two identical ring electrodes, separated L=8.3 cm, are mounted internally flush to the wall and connected to a conductivity meter (Taccusel model CD 810) interfaced with a computer (data acquisition board, DAS-8PGA). A computer program was developed in Visual BASIC to record the conductance as a function of time (every 0.5 s).

To start, the suspension (usually 2% v/v) was mixed by rhythmic end-over-end rotation of the cylinder. Data collection was initiated once the cylinder was stood vertically. The conductivity vs. time was plotted on the monitor to maintain a visual check on the

process. Two times were determined from the change in slope of the plot, namely: when the solid/liquid interface passes the first electrode then the second. Measuring this time to pass through the cell, T, gives the settling rate (or velocity), 8.3/T. The data were processed using Excel. The relative standard deviation on the settling rate from repeat experiments was ca. 1%.

6.4.2.2 Zeta potential

Electrophoretic mobility measurements were performed using the Zeta Plus (Brookhaven Instruments Corporation, USA). This instrument determines the mobility and converts to zeta potential using the model of Smoluchowski. The suspension was made by adding 0.1 g of mineral to 500 mL 10^{-3} M KCl supporting electrolyte and conditioned in the same way as for the aggregation tests.

6.4.3 Field Emission Scanning Electron Microscopy (FE-SEM)

Samples for imaging were prepared by adding known concentration of Mg^{2+} to silica and sphalerite samples. The conditioning regime was the same as in the aggregation tests with 2% v/v solids. Secondary electron images were taken up to 100 k times magnification on a Hitachi S-4700 FE-SEM.

6.5 Results

6.5.1 Aggregation

6.5.1.1 Sphalerite

Previous work on sphalerite has shown that the mineral self-aggregates at moderately alkaline pH, tending to re-disperse above ca. pH 10 (Mirnezami et al., 2002; DiFeo et al., 2001; Vergouw et al., 1998). This is re-confirmed here (Fig. 6.3a). Adding 50 ppm Mg^{2+} to the sphalerite dispersion, either 2% v/v or 3% v/v, did not have a significant effect up to pH 9. Above this, the presence of Mg^{2+} caused aggregation up to at least pH 12 (Fig. 6.3a). The tendency for the settling rate to drop between pH 10-11 in the presence of Mg^{2+} appears to be related to the decrease in settling rate which occurs for sphalerite alone; the net aggregation effect of $Mg^{2+}$is roughly constant above pH 10.

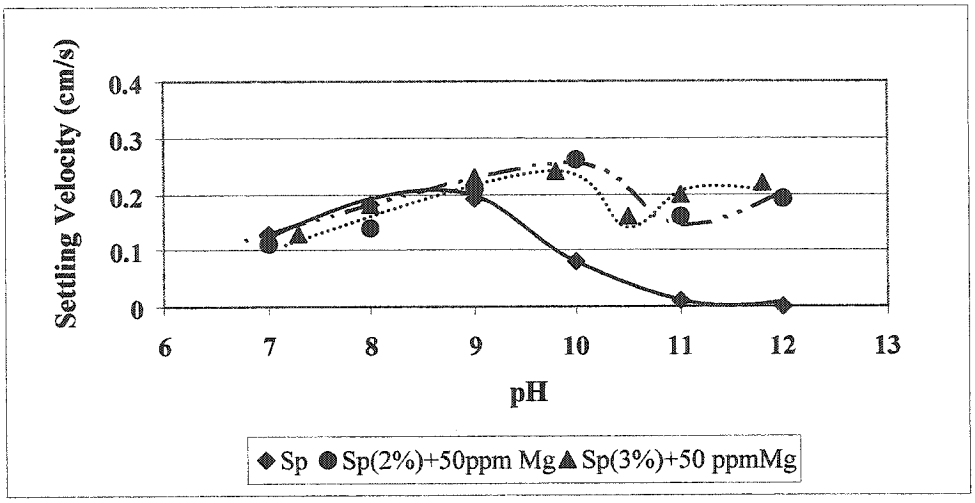

Figure 6.3a: Aggregation of sphalerite (2% and 3% v/v solids) as a function of pH with and without 50 ppm Mg^{2+}.

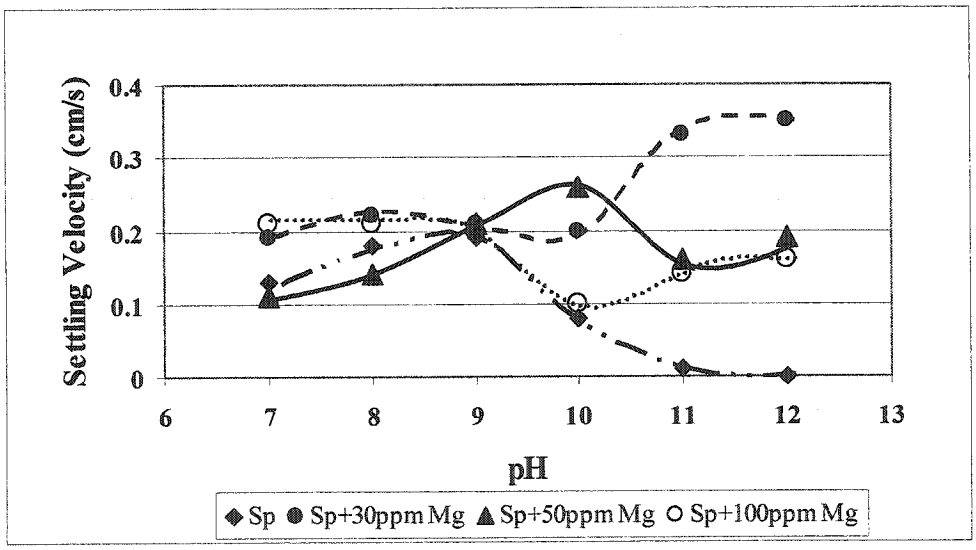

Figure 6.3b: Aggregation of sphalerite as a function of [Mg^{2+}].

Figure 6.3b shows the effect of [Mg^{2+}]. There is some effect on aggregation evident at pH< 9 and a notable concentration dependence at pH>9: the highest level of aggregation occurs at 30 ppm, the least at 100 ppm. In all cases, however, there was no maximum in the aggregation at a given pH (allowing for that of sphalerite alone).

6.5.1.2 Silica

Figure 6.4 shows the behaviour of silica (Sa) in the presence of Mg^{2+}. Above pH 9 with increasing pH the settling velocity increases to a maximum at a certain pH and then tends to decreases. This pH of maximum aggregation tends to decrease as $[Mg^{2+}]$ increases (Table 6.1). This pH effect is different from the sphalerite case; what is similar is that aggregation is highest at an intermediate $[Mg^{2+}]$.

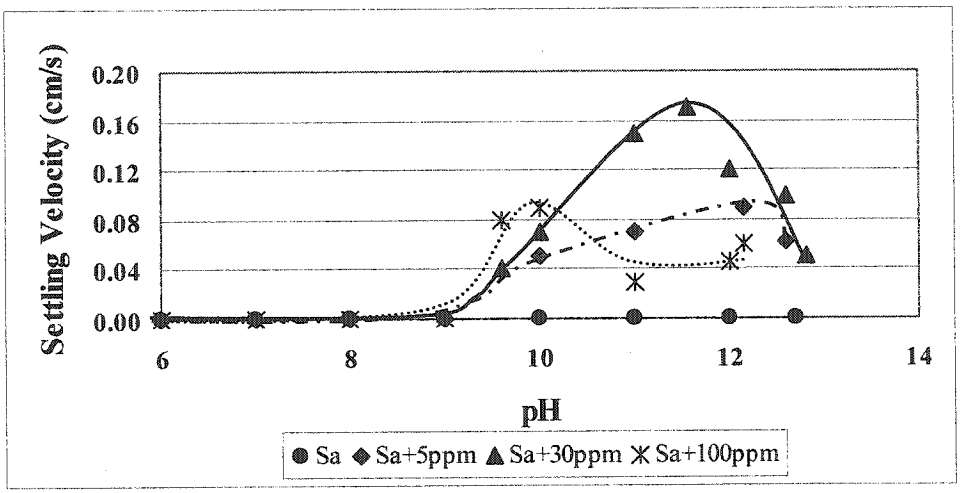

Figure 6.4: Aggregation of silica (Sa) as a function of pH and $[Mg^{2+}]$ (Note: suspension 2% v/v).

Table 6.1: Comparison of pH of maximum aggregation ($pH_{max,A}$) and the pH of point of charge reversal (pH_{pcr}) for silica

$[Mg^{2+}]$ ppm	$pH_{max.A}$	pH_{pcr}
0	dispersed	2.6*
5	12.2	10.9
10	12.1	10.8
30	11.6	10.6
50	11	10.1
100	10	9.6

*i.e., iso-electric point

Figure 6.5 shows the effect of solids concentration. In the case of sphalerite, increasing the solid concentration did not have any significant effect on the aggregation (Fig. 6.3a). For silica, however, Figure 6.5 shows that increasing the suspension concentration from 2 to 3% v/v solids increased the pH of maximum aggregation. (Within experimental error the maximum settling velocity achieved is the same for all the concentrations.)

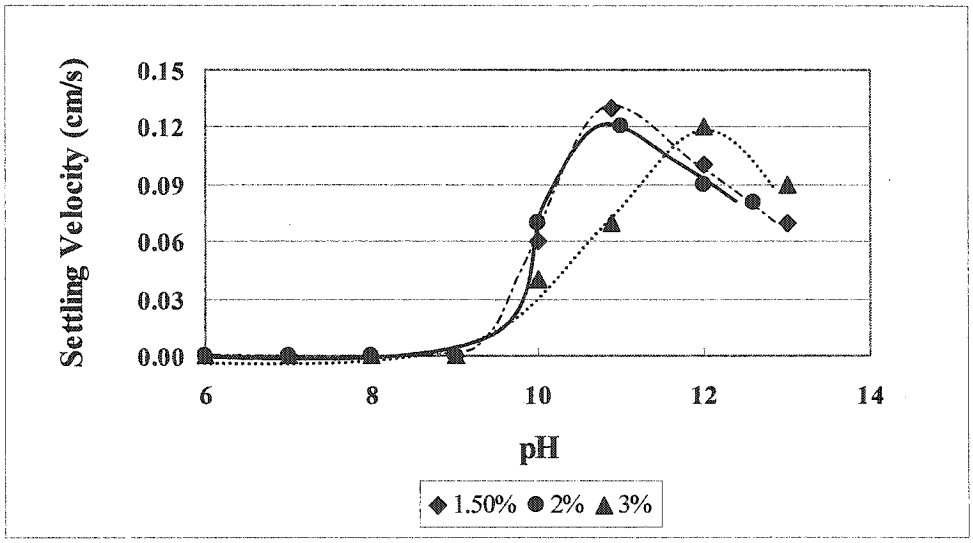

Figure 6.5: Effect of solids concentration (% v/v) on aggregation of silica.

6.5.2 Zeta Potential

6.5.2.1 Sphalerite

Zeta potential as a function of pH and [Mg^{2+}] for the sphalerite sample is given in Figure 6.6. There is evidence of Mg^{2+} uptake at pH < 8. The most notable change, however, occurred above pH 8 with charge reversal around pH 9. As the pH increased above the point of charge reversal (pcr), the zeta potential became progressively more positive reaching a zeta potential of ca. +50 mV at pH 12 with 50 ppm Mg^{2+} (compared to –50 mV in the absence of Mg^{2+}).

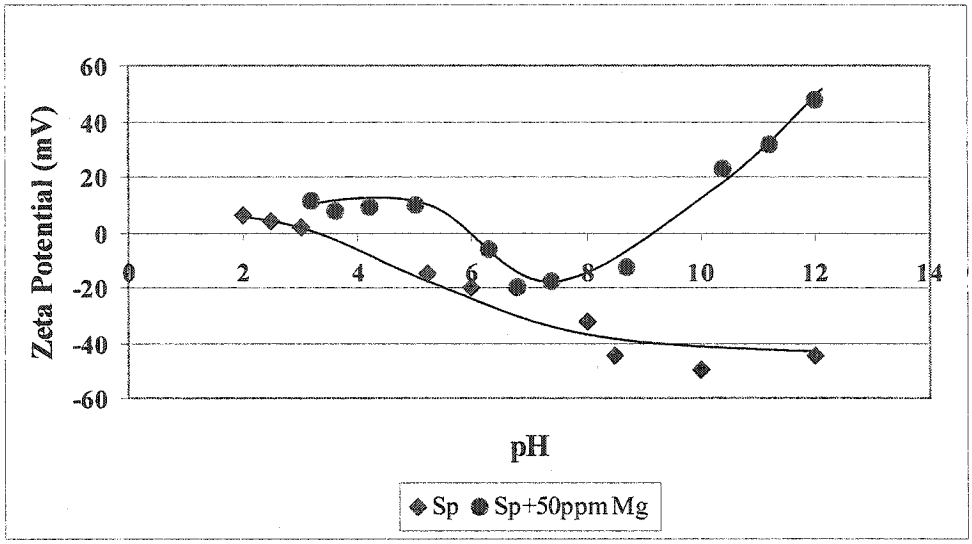

Figure 6.6: Zeta potential of sphalerite as a function of pH with and without Mg^{2+}.

6.5.2.2 Silica

The zeta potential of silica, corresponding to the conditions in Figure 6.4, is shown in Figure 6.7. The results indicate that in the presence of Mg^{2+} increasing the pH increased the charge, and the pH of charge reversal shifted to lower pH as [Mg^{2+}] was increased.

The point of charge reversal (pH_{pcr}) is included in Table 6.1. It is evident that the pH_{pcr} values do not coincide with the pH of maximum aggregation, especially at low [Mg^{2+}].

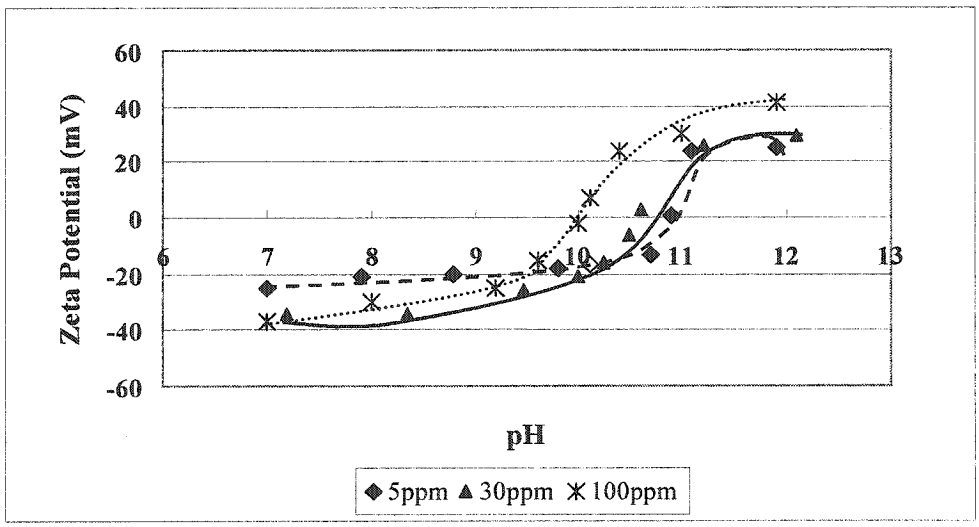

Figure 6.7: Zeta potential of silica as a function of pH and [Mg^{2+}].

6.5.3 FE-SEM

6.5.3.1 Sphalerite

The secondary electron images in Figure 6.8 (left side, low magnification, right side high magnification) show the difference in surface morphology of sphalerite treated with 50 ppm Mg^{2+} at pH 9, 10.2 and 12. At pH 9 (Fig. 6.8a) the surface shows morphology typical of broken grains but otherwise clean surfaces. At pH 10.2 (Fig. 6.8b) magnesium hydroxide precipitates are detected, the surface apparently being coated. Increasing the pH to 12 (Fig. 6.8c) does not change the interpretation, except the coating appears thicker when comparing the high magnification images, b and c.

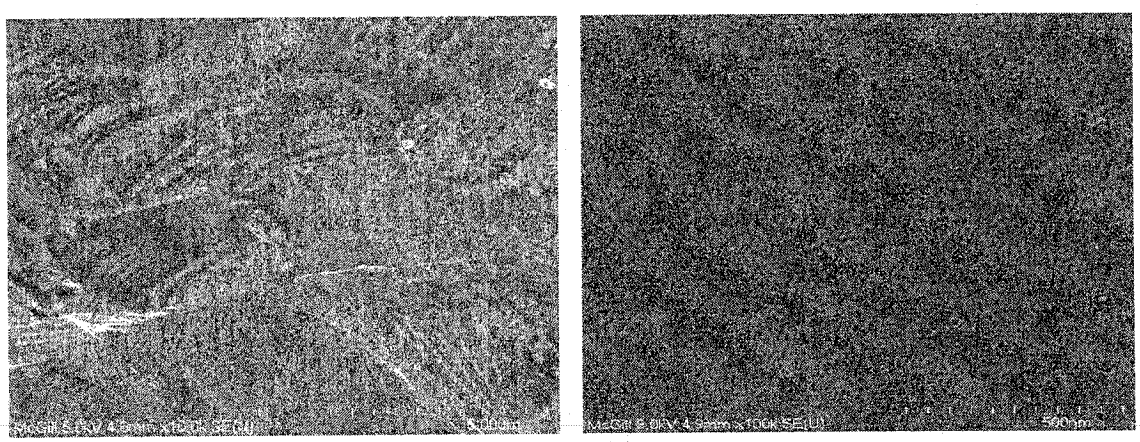

(a)

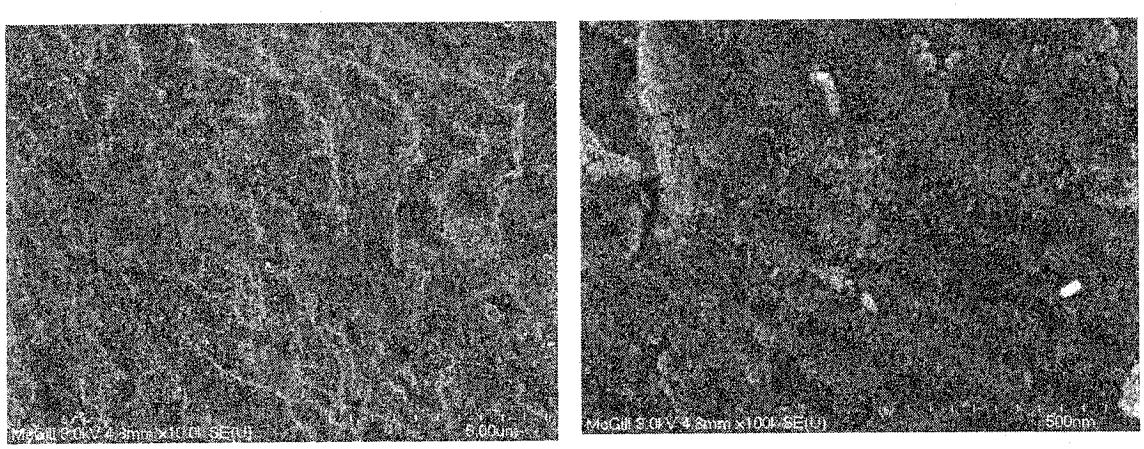

(b)

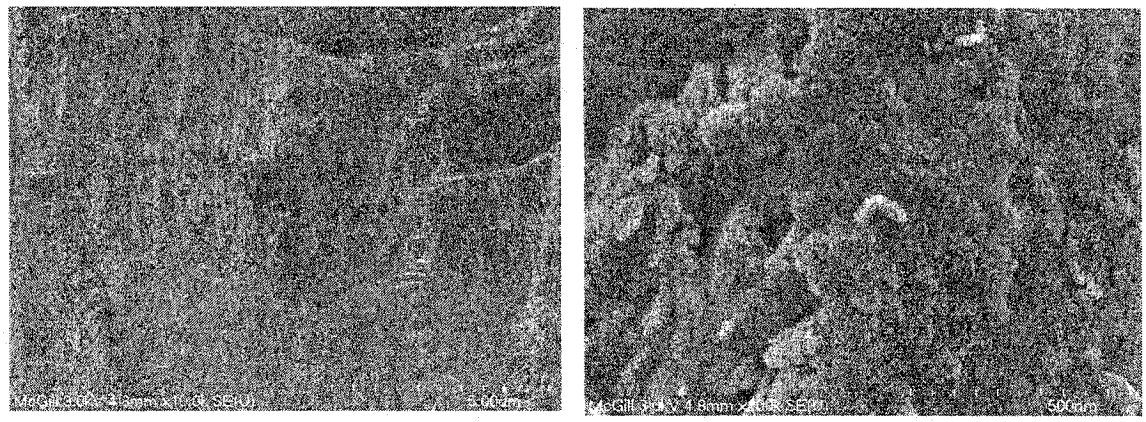

(c)

Figure 6.8: FE-SEM images of sphalerite conditioned with 50 ppm Mg^{2+} at (a) pH 9, (b) pH 10.2 and (c) pH 12. Note: Low magnification on left, high magnification on right.

6.5.3.2 Silica

The morphology (Fig. 6.9) as a function of pH in the presence of Mg^{2+} is different from the situation with silica. With 50 ppm Mg^{2+}, the surface remains clean at pH 9 (Fig. 6.9a) but at pH 10.3 (Fig. 6.9b) patches of $Mg(OH)_{2s}$ precipitates are apparent rather than the coating in the case of sphalerite. This is particular clear at low magnification (Fig. 6.9b, left), the high magnification image being of the patch itself (Fig. 6.9b, right). By pH 12 the morphology is indicative of a coating (Fig. 6.9c).

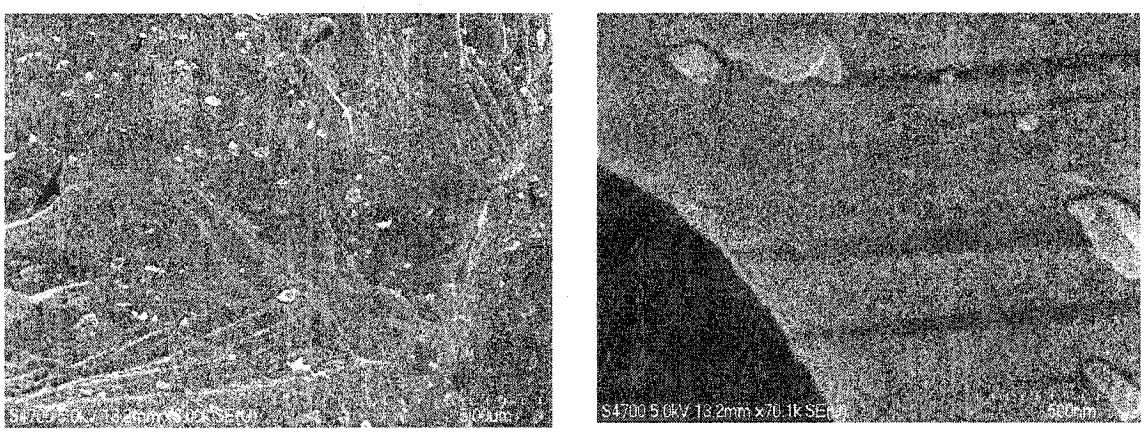

(a)

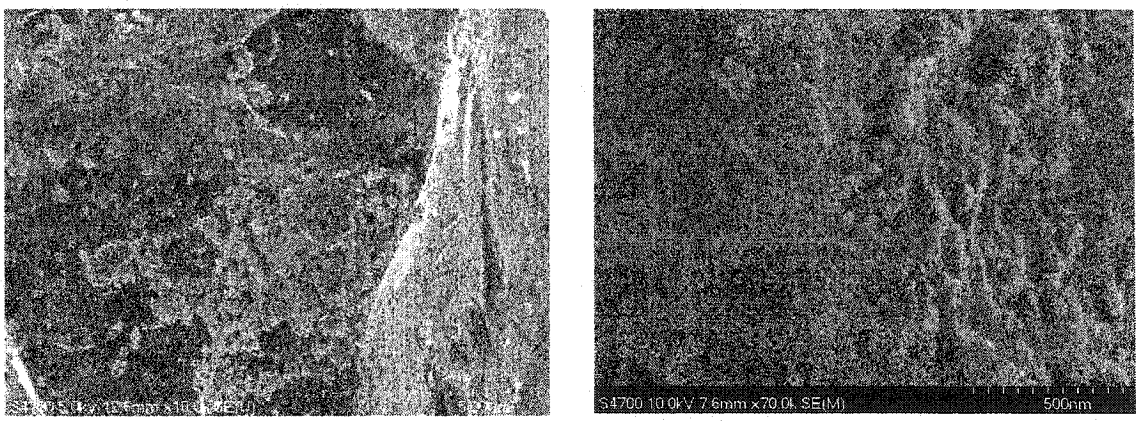

(b)

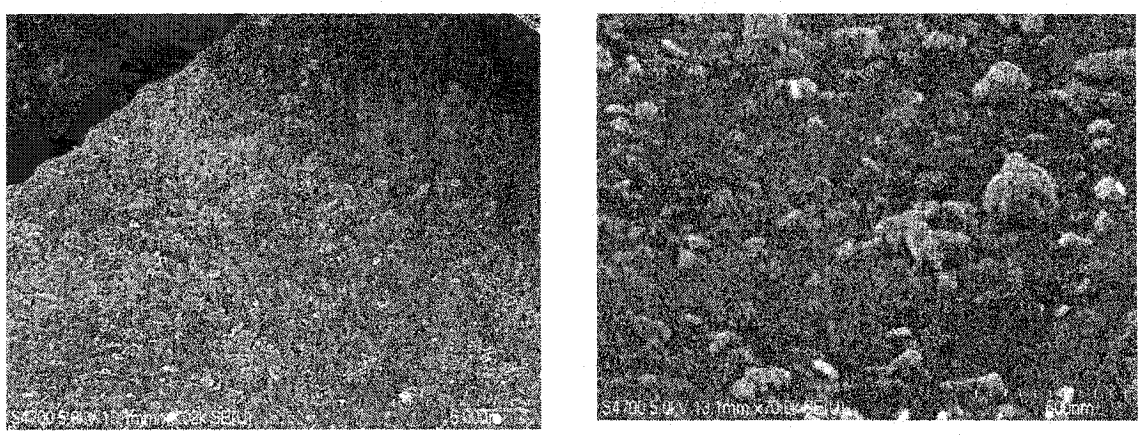

(c)

Figure 6.9: FE-SEM images of silica conditioned with 50 ppm Mg^{2+} at (a) pH 9, (b) pH 10.3 and (c) pH 12.

6.6 Discussion

6.6.1 Sphalerite

Previous work had shown that aggregation of sphalerite occurred at a pH greater than the iso-electric point, a finding confirmed here. Comparison of Figures 6.3 and 6.6 shows that the variation in aggregation in the presence of Mg^{2+} is also not related to the surface charge: The maximum aggregation does not occur at the pH of charge reversal and aggregation continues to pH 12, where the surface is strongly positive (i.e., a force of repulsion is expected).

Sweep flocculation implies that the level of aggregation (increase in settling rate) should either level out or possibly continue to increase with increasing Mg^{2+} concentration and solid content should have no effect. The results are supportive of the latter case (Fig. 6.5), but not in the former: rather than increasing with $[Mg^{2+}]$ aggregation passes through a maximum at an intermediate $[Mg^{2+}]$ (Fig. 6.3b). Also this mechanism implies that the settling rate of the aggregated hydroxides exceeds that of the particles (in order to enmesh and cause their sedimentation) which seems unlikely given the relatively large size of the particles used (–38 μm).

Electrostatic bridging is revealed by a maximum with both coagulant concentration and pH. While there is a maximum with $[Mg^{2+}]$ there is none with pH (after allowing for the self-aggregation of sphalerite). Further, surface morphology requires patches of the bridging material (magnesium hydroxide in this case) and the FE-SEM images showed no evidence of this.

The second category of bridging is through some chemical means. Transferring the mechanism proposed for $Zn(OH)_{2s}$ – H-bonding via hydration layers (Healy and Jellet, 1967) – then this mechanism is proposed for magnesium hydroxide. The maximum in aggregation at intermediate $[Mg^{2+}]$ is one piece of evidence against the chemical bridging mechanism. This maximum may reflect a balance between the increasing surface concentration of Mg^{2+} promoting the chemical bridges and at the same time promoting increased positive charge and repulsion. There may also be changes in the form of the aggregates; if the water content increases with $[Mg^{2+}]$ that would reduce the settling velocity.

Aggregation results for Mg^{2+} are broadly similar for those for Ca^{2+} /sphalerite. Vergouw et al. (1998) and DiFeo et al (2001) found that Ca^{2+} promoted aggregation above ca. pH 9. The cause of aggregation is likely $CaOH^{+}$, but certainly not the hydroxide based on known species distribution diagram (Fuerestenau et al, 1985).

In both these studies the zeta potential showed a positive shift but no charge reversal suggesting the aggregation mechanism is again not charge neutralization. The interaction of Ca^{2+} species with sphalerite is possibly similar to that accepted for quartz where surface-OH groups interact with $CaOH^+$ by a condensation (splitting out of water) reaction, but no study has been conducted.

6.6.2 Silica

Iwasaki et al. (1980) found that Ca^{2+} ion has a similar effect to Mg^{2+}, on the aggregation of quartz, but the species involved are different. For both ions the flocculation behaviour was strongly dependent on pH, particularly above pH 9. But Ca^{2+} adsorbs as $CaOH^+$, while for Mg^{2+} it is hetero-coagulation with $Mg(OH)_2$ precipitate. The aggregation mechanism is different: with Mg^{2+} the settling rate reached a maximum near pH 11 and then decreased, whereas for Ca^{2+} the settling rate approached a plateau suggesting chemical bridging.

The interpretation, for silica and Mg^{2+} follows that proposed by Krishnan and Iwasaki (1986). The pH, $[Mg^{2+}]$ and solid concentration effects are compatible with electrostatic bridging, as is the morphology. Hydroxide patches were also identified by Iwasaki et al. (1980) although, we suggest, the images here are more persuasive compared to those available on the prior-art instruments.

6.7 Conclusions

The aggregating effect of Mg^{2+} has been studied on sphalerite and silica. It was found that:

1- Mg^{2+} has a significant aggregating effect above pH10 which corresponds to precipitation of $Mg(OH)_2$.
2- The proposed mechanism of aggregation by $Mg(OH)_2$ for sphalerite is chemical bridging and for silica, electrostatic bridging.

6.8 References

Attia, Y. A., In *Colloid Chemistry in Mineral Processing*, (J.S. Laskowski, and J. Ralston, Eds.) Developments in Mineral Processing Series, Vol. 12, Elsvier Science Publishers B. V., Netherlands, 295 (1992).

Dentel, S.K. Application of the precipitation-charge neutralization model of coagulation. *Eviron. Sci. Technol.* **22**, pp 825-832 (1988).

Dobiáš, B., Qiu, X., and Rybinski, W. v. *Solid-liquid dispersion,* Surfactant Science Series, Vol. **81**, Marcel Dekker Inc. New York, p. 269(1999). .

El-Ammouri E., Mirnezami, M., Lascelles, D. and Finch, J.A. (2002). Aggregation index and a methodology to study the role of magnesium in aggregation of sulphide slurries *CIM Bulletin*, in press.

Fuerstenau, M.D., Miller, J.D., Kuhn, M.C., *Chemistry of flotation*, American Institute of Mining, Metallurgical and Petroleum Engineers, Inc., New York, pp. 5-7, 102 (1985).

Healy, T.W. and Jellet V.R. Adsorption coagulation reactions of Zn(II) hydrolyzed species at the zinc oxide-water interface. *J. Colloid Interface Science*, **24**, pp. 41-46 (1967).

Iwasaki, I. Bridging theory and practice in iron ore flotation. In *Advances in Coal and Mineral Processing Using Flotation,* (Chander, S. and Klimpel, R.R. Eds), pp. 177-190 (1989).

Iwasaki, I., Smith, K.A., Lipp, R.J., and Sato, H. Effect of calcium and magnesium ions on selective desliming and cationic flotation of quartz from iron ores. In *Fine particles processing*, Proceedings of the International Symposium on Fine Particles Processing, Las Vegas, Nevada, February 24-28, (P. Somasundaran, Ed.), **2**, pp. 1057-1082 (1980).

Krishnan, S.V. and Iwasaki, I. Heterocoagulation vs. surface precipitation in a quartz-$Mg(OH)_2$ system, *Environ. Sci. Technol.*, **20**, (12), pp1224-1229 (1986).

Lascelles, D., Finch, J.A., and Sui, C. Depressant action of Ca and Mg on flotation of Cu-activted sphalerite, In: *Interactions in Mineral Processing,* (Finch, J.A. Rao, S.A., and Huang, L.,Eds.), 4th UBC-McGill Symposium on Mineral Processing Fundamentals, Proceedings of the Conference of Metallurgists, Toronto, Canada, pp.125-140 (2001).

Matijević, E. Colloid stability and complex chemistry, *J. Colloid and Interface Science*, **43**, (2), pp. 217-245 (1973).

Mirnezami, M., L. Restrepo, L., Finch, J.A. (2002). Aggregation of sphalerite: role of zinc ions" accepted for publication by *Journal of Colloid and Interface Science.*

Packham, R.F. Some studies of the coagulation of dispersed clays with hydrolyzing salts. *J. Colloid Science.* **20**, pp 81- 92 (1965).

Uribe-Salas, A., Vermet, F., Finch, J.A., Apparatus and technique to measure settling velocity and holdup of solids in water slurries. *Chemical Engineering Science*, **48** (4), pp. 815-819 (1993).

Vergouw, J.M. Anson, J., Dahlke, R., Xu, Z., Gomez, C. O. & Finch, J.A., A new automated data acquisition technique for settling tests. *Minerals Engineering,* **10** (10), pp. 1095-1105 (1997).

Vergouw, J.M., DiFeo, A., Finch, J., A., "An agglomeration study of sulphide minerals using zeta-potential and settling rate. Part II: Sphalerite/Pyrite and sphalerite/galena", *Minerals Engineering,*

CHAPTER 7

Conclusions, Contributions, and Future Work

7.1 Conclusions

7.1.1 Measurement of Conductivity of Particles Dispersed in Water

- The conductivity-settling technique has been adapted to measure the conductivity of sulphide particles dispersed in water by locating the iso-conductivity point.

- The effect of surface modification was detected: xanthate adsorption on chalcopyrite reduced the conductivity and Cu^{2+} activation of sphalerite increased the conductivity but not lead activation.

- The conductivity measured appears to be associated with the solid-water interface and is much lower than the bulk value.

- The trend in conductivity correlated with the (electrochemical) rest potential, as expected.

7.1.2 Aggregation of sphalerite: role of zinc ions

- Similar aggregation behaviour was observed for sphalerites of a range in composition from a variety of sources: Aggregation was maximum around pH 7-9 and did not correlate to the iso–electric point (pH 2-6).

- The Zn^{2+} ion has an aggregating effect over the pH range where hydroxide species form.

7.1.3 Mechanisms of Aggregation by Magnesium Ions

- Mg^{2+} has a significant aggregating effect especially about pH 10.

- The aggregating effect corresponds to precipitation of $Mg(OH)_2$.

- The mechanism of aggregation for sphalerite is different from silica: for sphalerite it appears to be chemical bridging and for silica, electrostatic bridging.

7.2 Contributions to knowledge

- Surface conductivity of some sulphide minerals were measured and correlated with rest potential values from literature.

- Mechanism of aggregation of sphalerite self-induced by zinc ions produced by superficial oxidation/hydrolysis was established through electrokinetic, settling rate, turbidity and optical microscopy measurements.

- From zeta potential, settling rate and FE-SEM data, it was proposed that the mechanism of aggregation of sphalerite with Mg^{2+} ion was chemical bridging in contrast to electrostatic bridging as established for silica.

7.3 Recommendation for future work

- For settling experiments, utilizing the conductivity method, it is recommended to use a background electrolyte to avoid possible complications regarding the conductivity of the mineral.

- Effect of aggregate morphology on the settling rate should be considered in future.

- To correlate settling results with electrophoretic measurements, it is suggested to use the concentrations on a surface area basis (g/m^2).

- Since Ca^{2+} ion is probably the most common and abundant ion in flotation systems the effect of calcium ions on the aggregation of sulphide minerals and the mechanism of aggregation is advised. The data in the literature on this topic is too perfunctory to reveal the mechanism.

- The dual action of Mg^{2+} and Ca^{2+} is worthy of consideration.

APPENDIX A

Aggregation Index (AI) and a Methodology to Study the Role of Magnesium in Aggregation of Sulphide Slurries

A.1 Abstract

Aggregation, i.e., the tendency of particles to cluster, can be expected to influence flotation selectivity. In this paper, a method of measuring aggregation is introduced and used to conduct plant surveys.

Aggregation is measured using settling rate and turbidity converted to an aggregation index (AI) where 0 corresponds to most dispersed and 1 to most aggregated over the range of conditions tested, normally pH. Surveys of Cu and Zn flotation stages at four concentrators showed the AI increased significantly above pH 9. The metal ions identified in the process waters, principally Ca and Mg, were tested to determine which

might be responsible. The presence of Mg was found to be the most important. In doping tests, Mg was shown to cause significant variation in AI over the pH range 9 – 12.

The impact of Mg was restricted to pH > 9. Over this pH range Mg forms a range of hydroxy species, including $Mg(OH)_2$ precipitates. An aggregation mechanism associated with these precipitates, electrostatic bridging, is suggested. Possible problems and opportunities in flotation practice arising from the findings are discussed.

A.2 Introduction

Process waters in flotation circuits contain a variety of metal ions that may introduce unwanted effects. Two common metal ions are calcium and magnesium. Typical concentrations are in the range 50 ppm for magnesium ion and 500 ppm for calcium ion (Marticorena et al., 1994, Negeri et al., 1997, Nesset et al., 1998).

Compared to Ca ion, there is much less literature on the possible role of Mg ion in flotation systems. In a comparison with Ca^{2+}, Iwasaki (1989) showed that Mg^{2+} had a much greater impact on quartz flotation (with amine), causing depression above ca. pH 10. This was related to precipitation of the hydroxide, which for Mg^{2+} commences at ca. pH 9 while is delayed to ca. pH 12.5 for Ca^{2+} (Fig. A.1, Sui and Huang (1998)).

Recently, Lascelles et al. (2001) repeated this comparison for Cu-activated sphalerite. In the presence of 50 ppm Mg, above ca. pH 10.5, the depressant effect was significantly greater than with 500 ppm Ca^{2+} even above pH 12 (Figure A.2, Lascelles et al. (2001)).

Krishnan and Iwasaki (1986) reported that Mg^{2+} above ca. pH 10 also caused aggregation (i.e., clustering) of quartz particles. Aggregation and depression, therefore, appear to be two phenomena related to precipitation of $Mg(OH)_2$.

Aggregation may be a factor in reduced flotation selectivity. Particles of one type may be entrapped in clusters (aggregates) of another and report to the wrong product. This

possibility has long been speculated (Gaudin and Sun, 1946) but its significance in plant practice is largely unknown. Slime coating is a variety of aggregation that is known to reduce selectivity (Kitchener, 1992, Fuerstenau et al., 1985). The possible role of magnesium ion in aggregation of sulphide mineral slurries is investigated here.

To investigate aggregation, suspension settling rate and turbidity are used. The data from plant process streams tends to vary due to changes in pulp characteristics (% solids, particle size). To try to minimize these variations, the data are converted to a dimensionless aggregation index, AI, with a scale ranging from 0 to 1 where 0 refers to most dispersed and 1 to most aggregated over the range of conditions tested, typically pH. The procedure is described.

Surveys were undertaken at four Cu/Zn concentrators: Hudson Bay Mining and Smelting (HBM&S), Boliden Westmin (Westmin), Les Mines Selbaie (Selbaie) and Mine Louvicourt (Louvicourt). At the same time, basic studies on chalcopyrite/sphalerite mixtures were used to isolate process water and metal ion effects.

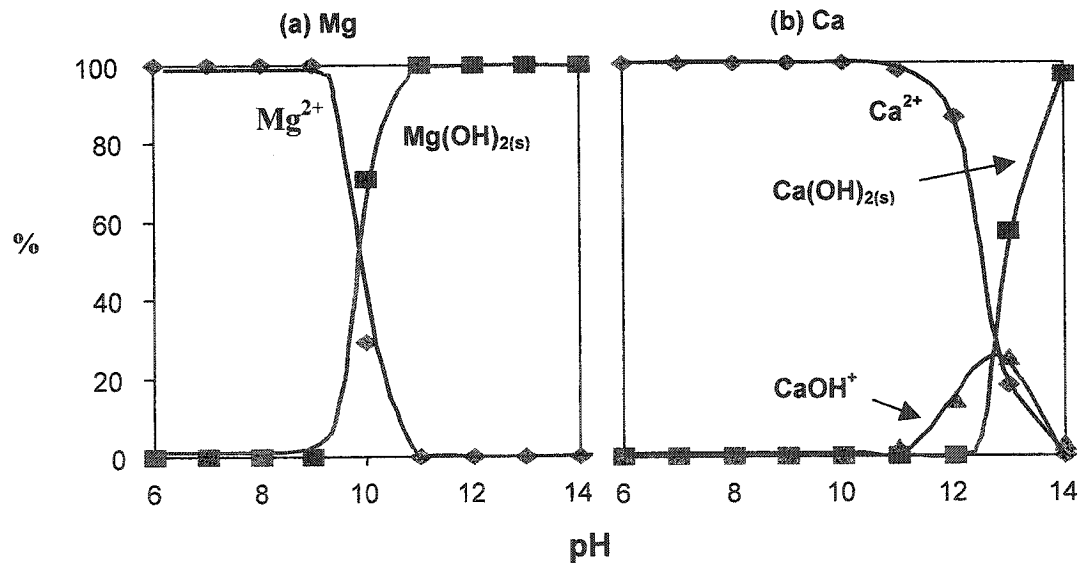

Figure A.1: Solution species distribution diagram for 50 ppm Mg^{2+} (a) and 500 ppm Ca^{2+} (b) as a function of pH (Sui and Huang, 1998).

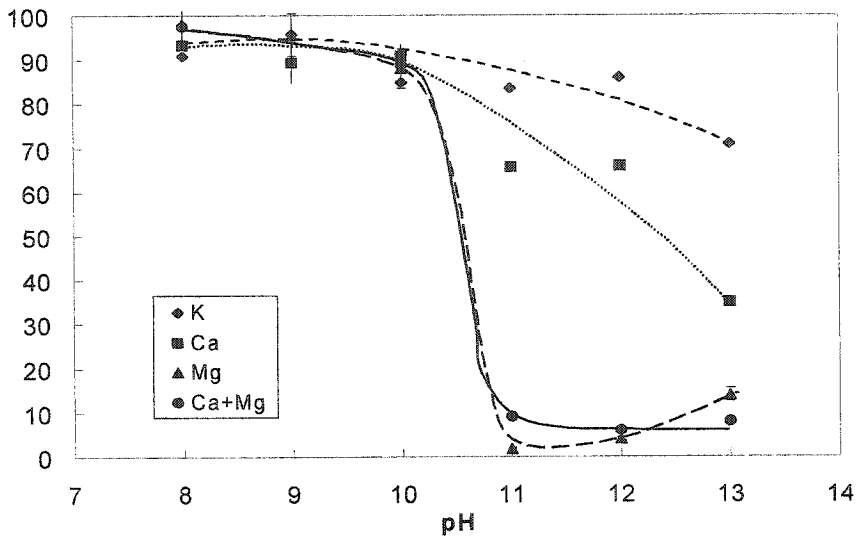

Figure A.2: Flotation recovery of Cu-activated sphalerite as a function of pH and solution composition: 500 ppm K, 500 ppm Ca, 50 ppm Mg, 500 ppm Ca^{2+} + 50 ppm Mg^{2+} (microflotation tests, Lascelles et al., 2001).

A.3 Aggregation index

A.3.1 From settling experiments

A typical settling rate vs pH curve is shown in Figure A.3. Over the pH range tested (or in general any variable that alters the rate), a dimensionless aggregation index (AI) can be defined as:

AI= (Rp - Rd) / (Ra - Rd)

Where:

Rd = settling rate for most dispersed condition (i.e., lowest settling rate).

Ra = settling rate for most aggregated condition (i.e., highest settling rate).

Rp = any settling rate in between.

The AI curve in Figure A.3 has preserved the settling rate trend but with a scale 0 to 1.

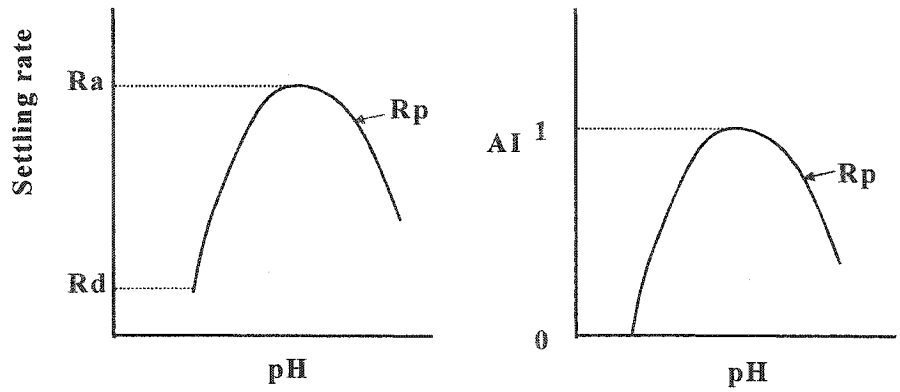

Figure A.3: Aggregation index (AI) from settling rate measurements.

When AI = 0 the system is most dispersed (over the range investigated) and when AI = 1 it is most aggregated.

Reference to the AI scale tends to eliminate variations in the settling velocity of a given stream due to differences in slurry characteristics (i.e., pulp density, particle size, etc..). To illustrate, Figure A.4 a) shows settling rate vs pH for the Westmin Cu rougher feed measured on two occasions (1999 and 2001). The rate in 2001 reached a higher maximum than in 1999 (0.045 vs 0.035 cm/s); however, Figure A.4 b) shows that after normalization to the AI scale the curves become one.

A.3.2 From turbidity measurements

The approach is essentially the same. Since the shape of a turbidity-pH curve is (usually) the inverse of the settling rate-pH response (high turbidity corresponds to low settling rate) then the conversion to AI is:

AI= (Td -Tp) / (Td - Ta)

Where:

Td = turbidity for most dispersed condition

Ta = turbidity for most aggregated condition

Tp = any turbidity point in between

Turbidity here is measured as mass of suspended solids at a given depth in a given sampled volume.

Conversion to the AI scale can be done for each data set (curve) individually where all the curves go from 0 to 1 as in Figure A.4 b), or by treating the data globally when trying to reveal the effect of some chemical change (e.g., addition of magnesium. Whether data are treated "individually" or "globally" will be indicated in each Figure caption.

The AI is a relative scale, i.e., the same value of AI for two streams treated individually does not mean the same absolute level of aggregation. In principle, streams can be compared if the data are treated individually (provided particle size and % solids are similar).

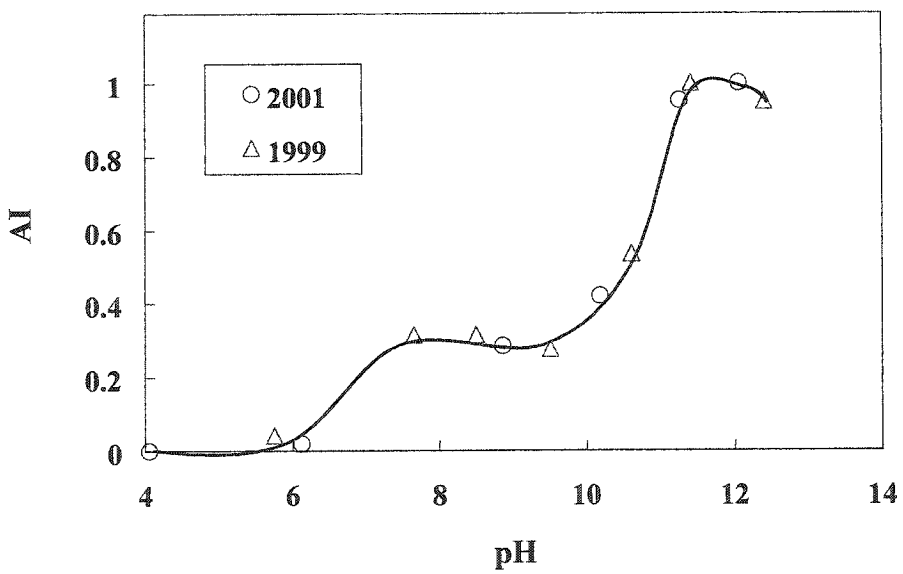

Figure A.4a): Settling rate vs pH for feed to Cu rougher at Westmin (11/3/1999 and 5/6/2001).

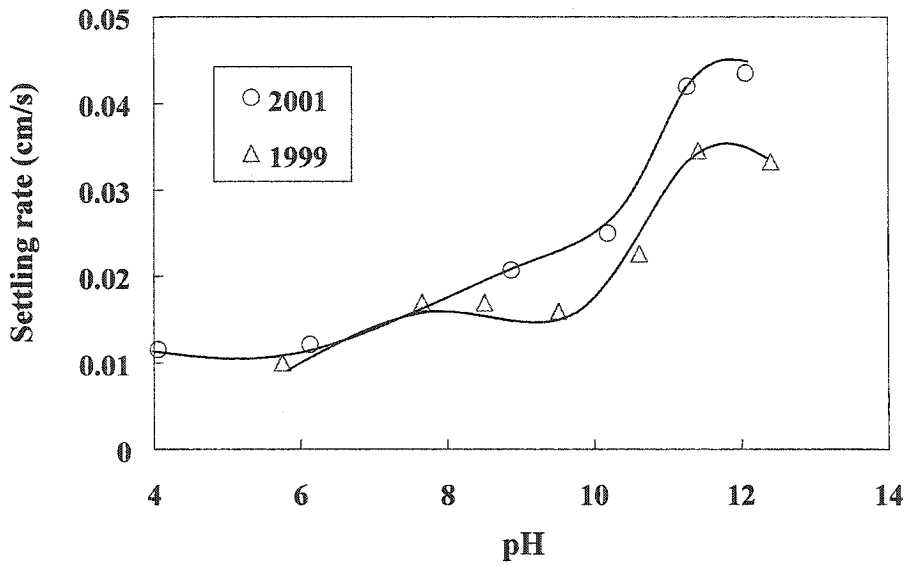

Figure A.4b): As a, but each data set converted to AI (i.e., data treated individually).

A.4 Materials

For the basic study, sphalerite (Carthage, Tennessee) and chalcopyrite (Durango, Mexico) specimens were purchased from Ward's Natural Science Establishment. They were crushed in a jaw crusher, hand sorted, pulverized and wet sieved. The final size fraction for sphalerite was 25-38 μm and –8 μm for chalcopyrite.

For the plant work, slurries were collected from the Cu and Zn circuits (rougher and cleaner feeds). Any dilution used recycle water.

The following reagents used were A.C.S. reagent grade: Magnesium chloride ($MgCl_2$, $6H_2O$) from Mallinckdrodt, Calcium chloride ($CaCl_2$, $2H_2O$), hydrochloric acid (HCl), sulphuric acid (H_2SO_4) and sodium hydroxide (NaOH) all from Fisher Scientific.

A.5 Procedures

A.5.1 Settling tests

These were performed on the plant slurry samples using the conductivity-settling set-up shown in Figure A.5. A 350 mL cylinder (transparent Plexiglas) was modified to include a conductivity cell by mounting two ring electrodes flush to the inner wall at a distance H = 10 cm apart. The electrodes are connected to a conductivity meter interfaced with a computer. The cylinder, 3.8 cm in diameter and 34 cm high, stands on a plastic base and the open top is covered with a stopper after filling with slurry. Mixing is achieved by end-over-end rotation for approximately one minute. After agitation, the cell is placed vertically on the counter and data collection is initiated immediately and recorded as a conductivity-time response curve. The descent of the solid/liquid interface past the top then bottom electrodes is detected by a change in slope of the conductivity-time curve (points A and B respectively) and recorded as time T (s). The settling velocity is then H/T (cm/s). The technique is explained in detail elsewhere (Uribe-Salas et al., 1993, 1994, Vergouw et al., 1997, Vergouw et al., 1998(a and b)).

Measurements were at ca. 25 ^{o}C using the initial slurry or by diluting from 1-5 times with plant recycle water. The standard technique adopted at this time is to measure the settling rate as a function of pH adjusted with sodium hydroxide (NaOH) and sulphuric acid (H_2SO_4). For pH measurements, an electrode is inserted from the top.

A.5.2 Turbidity

Turbidity was used only in the basic study on the sphalerite-chalcopyrite mixture. A 2 v/v % slurry was prepared in a beaker and conditioned for 20 minutes then transferred to a tube (volume = 50 mL, length = 35 cm) and allowed to settle for 2 minutes. One mL of suspension was taken from a specific height (16 cm from top), filtered, air dried and weighed. The mass of solid determined is the measure of turbidity.

Measurements were made in distilled water, distilled water doped with metal ions and in process water isolated from the plant samples. The process water was obtained by acidifying a slurry sample (with HCl) to pH 6 to re-dissolve adsorbed hydroxy species, followed by filtering.

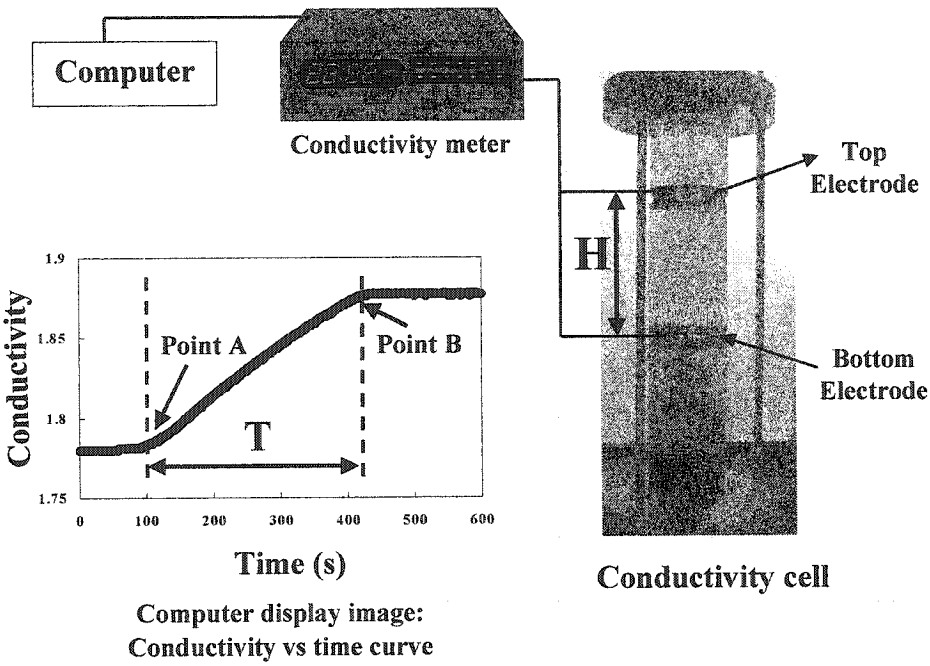

Figure A.5: Conductivity-settling set-up.

A.6 Results

A.6.1 Basic study

The initial tests involved distilled water treated with, independently, 50 ppm Mg^{2+} and 500 ppm Ca^{2+}, taken as typical values. The result (Fig. A.6) shows the chalcopyrite/sphalerite system becomes progressively more aggregated in the presence of Mg^{2+} as the pH is raised to 12. In contrast, in the presence of Ca^{2+}, significant – but still less than with Mg^{2+} – aggregation occurred only around pH 12 (the un-doped system was actually most dispersed at pH 12).

As a case study, the results for the Louvicourt Cu rougher and cleaner feed process waters are considered. The process water composition is given in Table 1. The AI vs pH results (Fig. A.7) show the process waters from both stages give the same trend as obtained for Mg-treated distilled water (included for reference).

A similar AI vs pH trend was found for Selbaie and Westmin process waters that had similar Ca and Mg ions levels to Louvicourt. The situation at HBM&S was less clear which could be related to the lower Mg^{2+} level (and maybe high Fe levels in the Cu rougher) (Table A.1).

Table A.1: Composition of process water* for the four plants.

Plant (Date of sampling)	**Feed to:**	**Fe**	**Zn**	**Cu**	**Pb**	**Mg**	**Ca**
Louvicourt	Cu rougher	23.0	0.09	< 0.01	<0.05	55.0	1245
(9/11/2000)	Cu cleaner	35.0	0.50	<0.01	<0.05	33.0	945
Selbaie	Cu rougher	45.6	19.4	0.28	< 0.01	94.7	565
(9/11/2000)	Cu cleaner	0.25	9.9	< 0.01	< 0.01	23.8	945
HBM&S	Cu rougher	214	0.6	< 0.01	< 0.02	28.8	661
(5/6/2001)	Cu cleaner	16.6	3.2	< 0.01	< 0.02	13.5	205
Westmin (5/6/2001)	Cu rougher	0.0	15.0	0.1	0.3	70.0	615

- Note: process water is the filtrate after acidifying (with HCl) to pH 6 for 30 minutes then filtering.

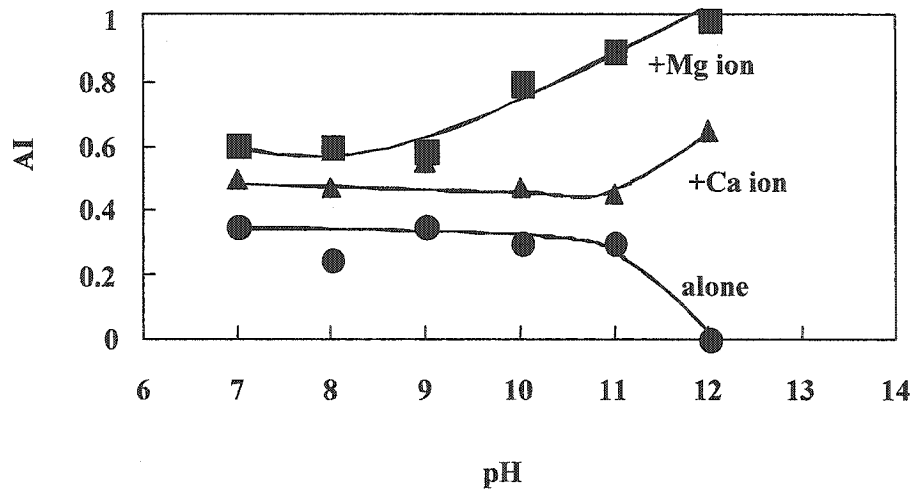

Figure A.6: AI as a function of pH for sphalerite/chalcopyrite system in distilled water (alone), and in the presence of 50 ppm Mg^{2+} (+Mg) and 500 ppm Ca^{2+} (+Ca). Data treated globally.

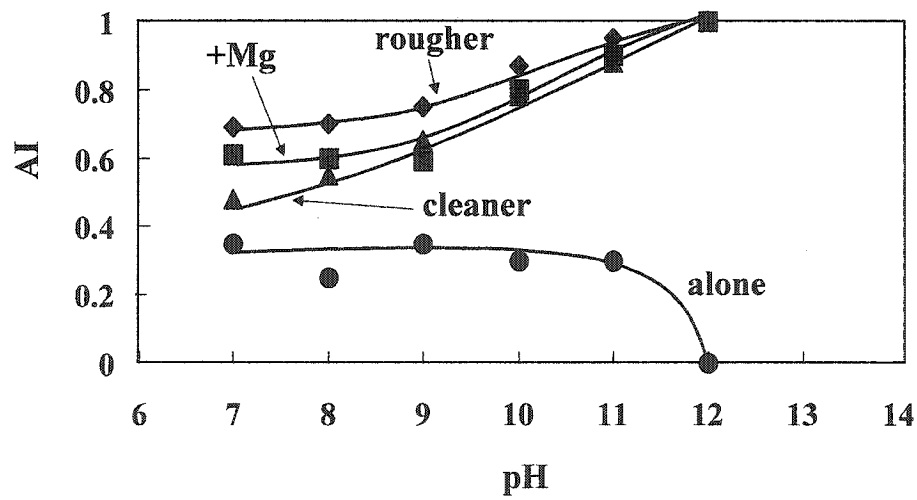

Figure A.7: AI as a function of pH for sphalerite/chalcopyrite system using Louvicourt Cu rougher and cleaner process waters. Included from Figure 3: sphalerite/chalcopyrite system in distilled water (alone), and in the presence of 50 ppm Mg^{2+} (+Mg). Data treated globally.

A.6.2 Plant surveys

Figure A.8 summarizes the AI vs pH for Cu rougher feed slurries for all four concentrators. The trends are similar: an increase in AI with pH, and generally an operating pH that corresponds to at least a partially aggregated state. Figure A.9 shows that the AI data are repeatable using Louvicourt and Westmin as examples (even the plateaux between pH 7-10 appear to be reproduced). Figure A.10 shows this was not the situation at HBM&S. From the basic study result, one reason could be variation in Mg^{2+} concentration in the process water. (Variation in Mg ion content in the ore does occur at this operation.) Treating with 50 ppm Mg^{2+} clearly increased the aggregation index for both the Zn rougher (Fig. A.11) and cleaner (Fig. A.12) samples over the pH range 9 to 11. Figure A.13 shows a more detailed test of magnesium ion addition to the Cu rougher feed at Louvicourt. In this case, the AI increased with Mg^{2+} concentration up to 100 ppm, but at 250 ppm Mg^{2+} the AI above pH 10 decreased to a level similar to no Mg^{2+} ion addition. The tendency for AI to also decrease above a certain pH is evident in Figures A.8-A.12.

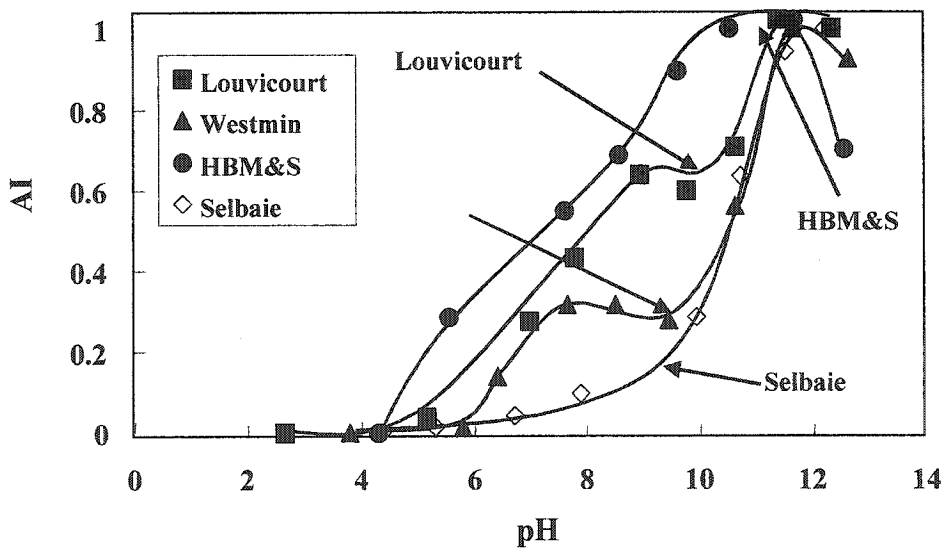

Figure A.8: AI as a function of pH for Cu rougher feed slurry at the four concentrators.

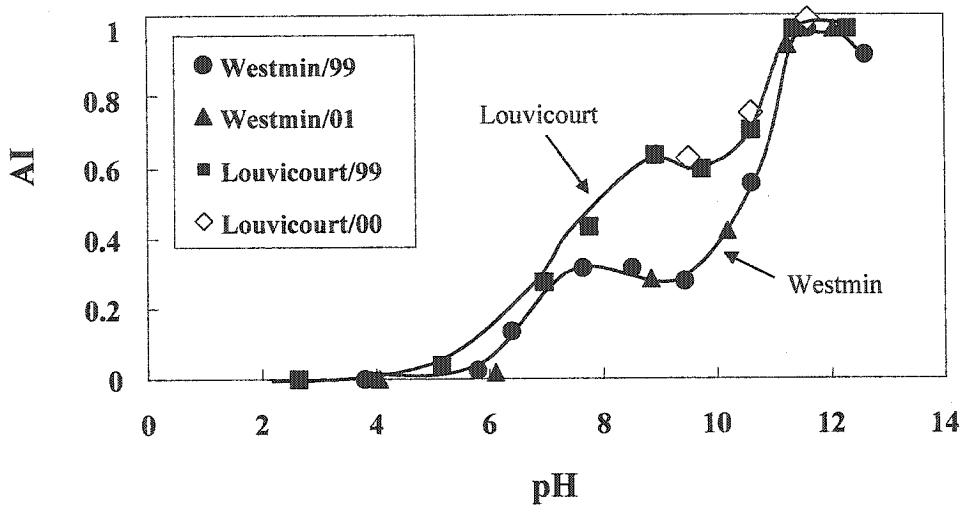

Figure A.9: AI as a function of pH for Cu rougher feed slurry at Louvicourt (on 5/26/1999 and 9/11/2000) and Westmin (11/5/1999 and 5/6/2001). Data treated individually.

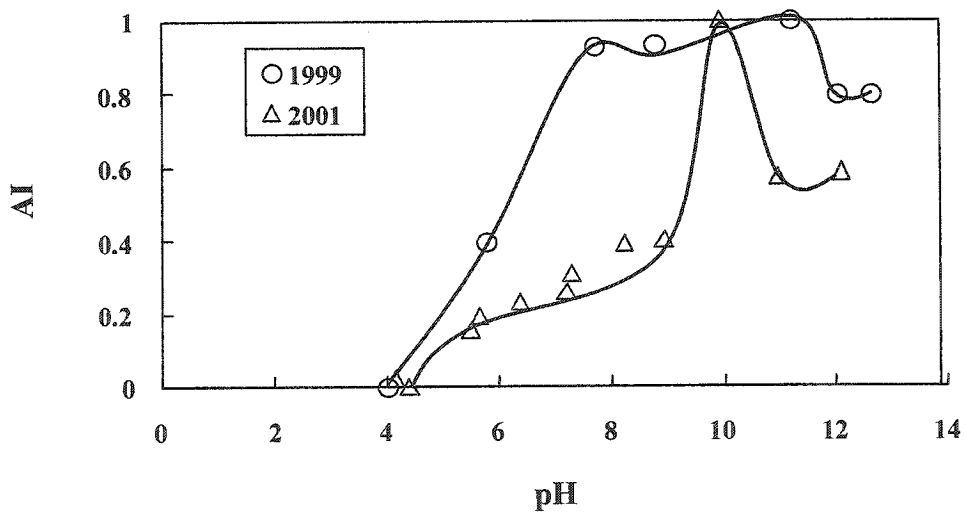

Figure A.10: AI as a function of pH for Zn rougher feed slurry at HBM&S, on 11/8/1999 and 5/11/2001. Data treated individually.

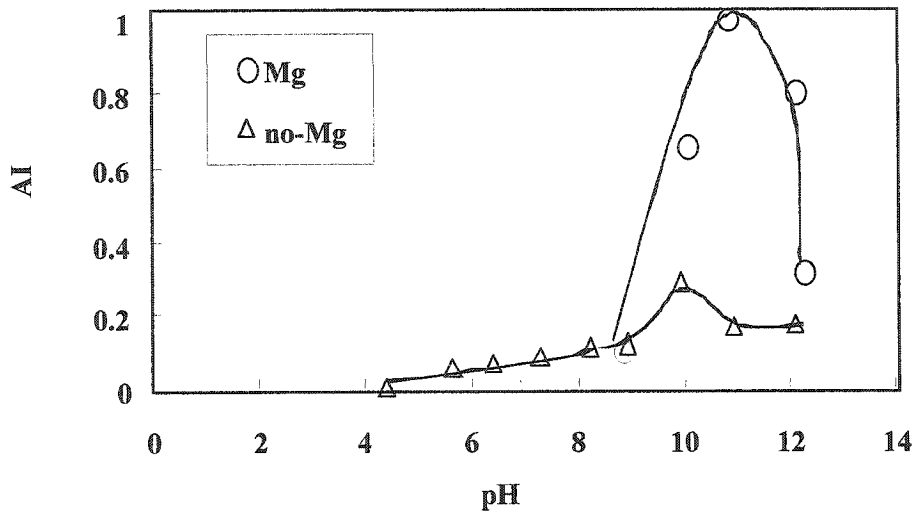

Figure A.11: AI as a function of pH for Zn rougher feed slurry at HBM&S (2001 sample) from Figure A.10 (no-Mg) and after the addition of 50 ppm Mg^{2+} (Mg). Data treated globally.

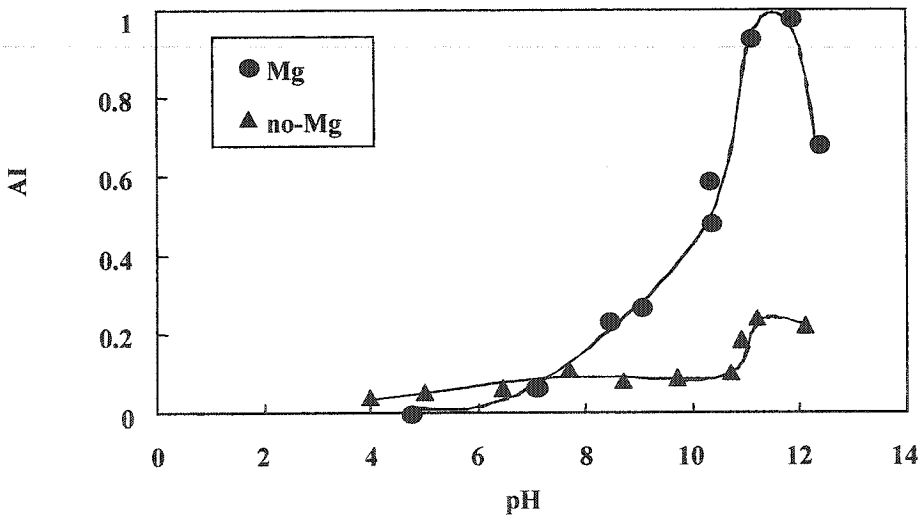

Figure A.12: Same as Figure A.8, but for Zn cleaner feed slurry. Data treated globally.

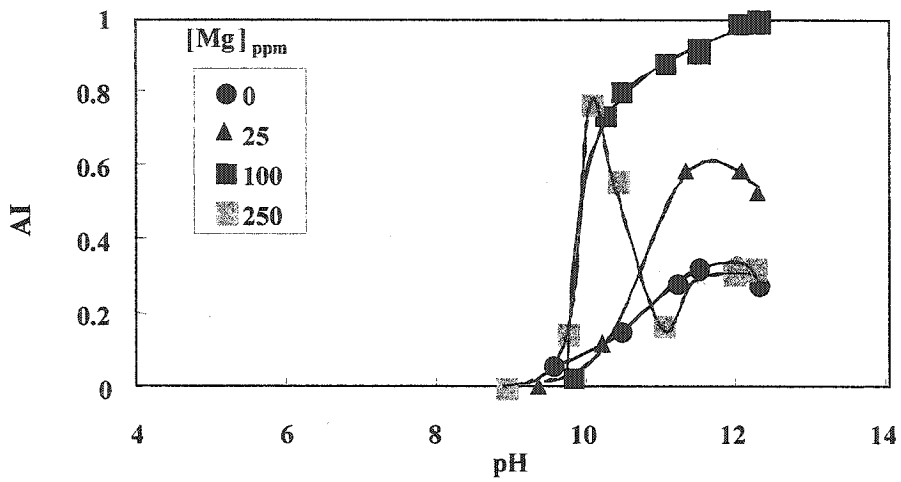

Figure A.13: Effect of Mg^{2+} addition on Louvicourt Cu-rougher feed (on 1/10/2002). Data treated globally.

A.7 Discussion

Procedures based on readily performed settling and turbidity tests have provided insight into the aggregation/dispersion behaviour of sulphide mineral flotation slurries. The tests can be readily performed on-site. The conversion of the data, however obtained, to an aggregation index scale reduces the impact of variations in pulp density and particle size between sampling campaigns. It is however necessary to decide whether to treat data sets individually or globally: to identify chemical effects, as here, the data sets are best treated globally.

The AI vs pH data have provided direct evidence that Mg^{2+} causes aggregation in sulphide mineral slurries, principally over the pH range 9-12. As noted, Krishnan and Iwasaki (1986) had likewise found Mg ion aggregated quartz. Their results, converted to AI, are given in Figure A.14. The similarity, especially with Figures A.11 and A.12, is striking and suggests a common mechanism.

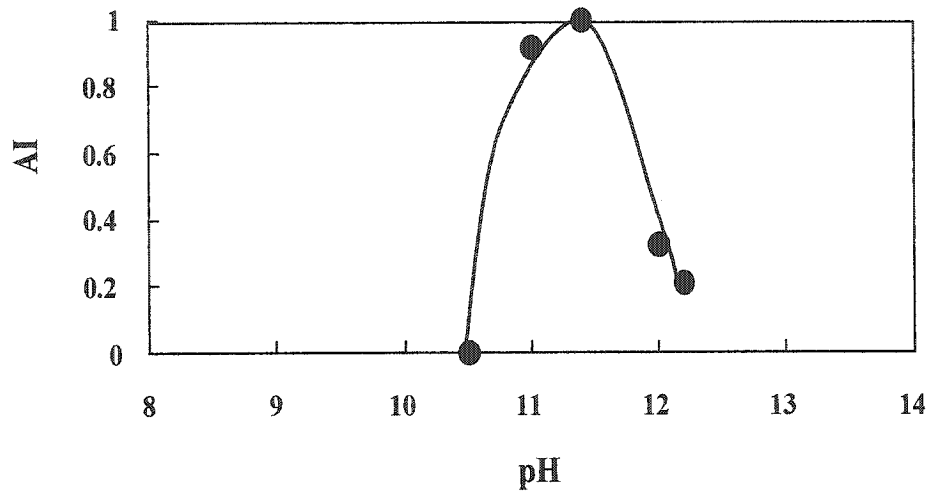

Figure A.14: AI as a function of pH for quartz in the presence of 10^{-4} M magnesium chloride (modified from the original by Krishnan and Iwasaki, 1986).

The mechanism proposed by Krishnan and Iwasaki, illustrated in Figure 15, is uptake (or abstraction) of $Mg(OH)_2$ precipitates on the mineral surface followed by aggregation of partially coated particles. The uptake is through electrostatic interaction: $Mg(OH)_{2(S)}$ is positively charged up to ca. pH 12.5 (its iso-electric point) while many minerals, certainly quartz and most sulphides, are negatively charged. This process is known as hetero-aggregation (or hetero-coagulation). Abstraction may also involve nucleation and growth of the hydroxide on the surface.

The subsequent aggregation of the coated particles was attributed to electrostatic bridging: patches of positively charged $Mg(OH)_2$ on one mineral interacting with precipitate-free negatively charged parts of a second mineral. (Hence the reference to "partially coated" particles above.) When particles become fully coated, through a combination of pH and Mg^{2+} concentration, the charge becomes positive, repulsion occurs and AI decreases. This is evident in the results: at high concentration of Mg^{2+} in Figure A.13 the AI decreased, compatible with the particles being fully coated; in other cases, above a certain pH the AI decreased which again may suggest fully coated

particles as Mg precipitation as hydroxide becomes more complete. At pH > iep of $Mg(OH)_2$ (≈ pH 12.5) all interacting surfaces become negatively charged and mutual repulsion will also inhibit aggregation.

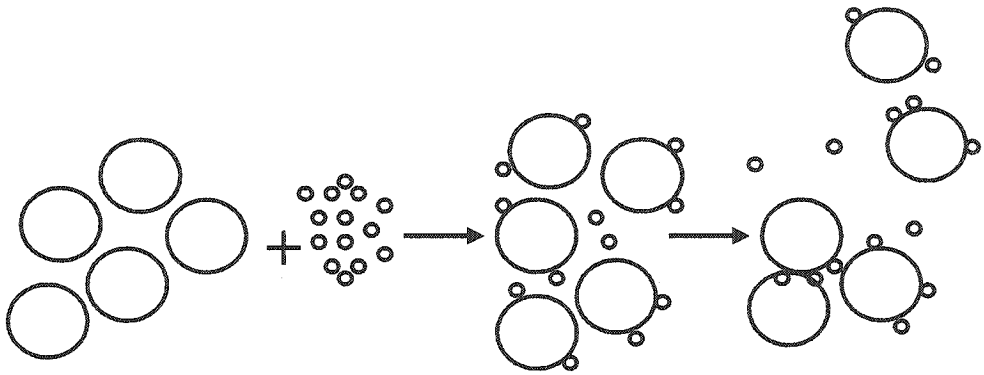

Figure A.15: Schematic representation of aggregate formation in the presence of $Mg(OH)_2$ precipitates by electrostatic bridging (after Krishnan and Iwasaki, 1986).

At this stage there seems no reason to speculate on other mechanisms but it is appreciated that Mg speciation can involve mono and polynuclear complexes such as $Mg(OH)^+$and $Mg_4(OH)_4^{4+}$ which may also have an influence (Baes et al., 1986). To leave open, the abstracted particles in Figure A.15 may be considered as "magnesium hydroxy species".

Aggregation and the role of Mg ion over a pH range frequently used in flotation have been revealed but any link to flotation performance is speculative at this juncture. We can suspect that unselective aggregation (there is no evidence here that it is selective) is counter to selectivity. Aggregation, by increasing (apparent) particle size, may, however, give increased flotation rates. Some combination of enhanced flotation rate and reduced selectivity may be acceptable in roughing but less so in cleaning. Control over the level of aggregation may contribute to the pH selected by an operation. Future work will explore links between AI and flotation performance. This will need to consider that

$Mg(OH)_2$ not only causes aggregation but being hydrophilic also causes depression, as indicated in Figure A.2. Whether Mg^{2+} levels can be exploited to promote selective aggregation and/or depression is an intriguing possibility.

Control of aggregation in the four concentrators would seem to be related to Mg ion concentration in the process water. It is pertinent to enquire where the Mg^{2+} originates. The ore is the most likely source but Mg^{2+} is a contaminant in most commercial lime supplies. The Mg^{2+} could be controlled through chemical additions – e.g., metal complexing agents like ethylenediaminetetraacetate (EDTA) and polyphosphate - or by mechanical means, - e.g., removal of hydroxides by attrition. Agitation in mechanical cells may already counter aggregation to some extent.

A.8 Conclusions

A measurement of aggregation suited to plant studies has been introduced. The effect of magnesium in the process water on aggregation of sulphide mineral slurries above ca. pH 10 in the Cu and Zn stages at four concentrators is shown, similar to the observation of Krishnan and Iwasaki (1986) in the case of quartz. Aggregation is related to the presence of $Mg(OH)_2$ precipitates and the magnesium concentration and pH effects are compatible with an electrostatic bridging mechanism. Aggregation and depression are two phenomena related to the properties of $Mg(OH)_2$ precipitates.

A.9 Acknowledgement

The authors acknowledge the financial support of the Canadian Mining Industry Research Organisation – Metallurgical Processing Division, CAMIRO–MPD (representing Rio Algom, Hudson Bay Mining and Smelting, Les Mines Selbaie, Louvicourt Mine, Noranda, Boliden-Westmin, Breakwater Resources Ltd. and Agnico-Eagle) and the Natural Sciences and Engineering Research Council of Canada (NSERC) under the Collaborative Research and Development program.

A.10 References

Baes, C.F. and Mesmer, R.E., *The Hydrolysis of Cations*, R.E. Kreiger Publishing Company, Inc., Florida, 1986.

Fuerstenau, M.C., Miller, J.D. and Khun, M.C., *Chemistry of Flotation*, AIME, New York, pp. 150-153, 1985.

Gaudin, A.M. and Sun, S.C., "Correlation between mineral behaviour in cataphoresis and in flotation" *Trans American Institute of Mining, Metallurgical and Petroleum Engineers* (AIME), 169, p. 347, 1946.

Iwasaki, I, "Bridging theory and practice in iron ore flotation," In: *Advances in Coal and Mineral Processing Using Flotation,* Chander, S. and Klimpel, R.R., eds., AIME, Colorado, USA, pp. 177-190, 1989.

Kitchener, J.A., In: *Developments in Mineral Processing Series, Vol. 12, "Colloid Chemistry in Mineral Processing",* eds., Laskowski, J.S. and Ralston, J., Elsvier Science, B. V., Netherlands, p. 34, 1992.

Krishnan, S.V. and Iwasaki, I., "Heterocoagulation vs. surface precipitation in a quartz-$Mg(OH)_2$ system", *Environmental Science and Technology*, Vol 20, No 12, pp. 1224-1229, 1986.

Lascelles, D., Finch, J.A. and Sui, C., "Depressant action of Ca and Mg in flotation of Cu-activated sphalerite", In: *Interactions in Mineral Processing*, Finch, J.A., Rao, S.R., and Huang, L., eds., Metallurgical Society of CIM, Montreal, Canada, pp. 125-140, 2001.

Marticorena, M. A., Hill, G., Kerr, A. N., Liechti, D. and Pelland, D. A., "Inco develops new pyrrhotite depressant," In: *Innovations in Mineral Processing*, Yalçin, T., ed., ACME Printers, Sudbury, Ontario, pp. 15-33, 1994.

Negeri, T., Wilson, J. and Chevalier, G., "Investigation of Les Mines Selbaie sphalerite flotation characteristics by surface and solution analysis techniques," In: *Proceedings – 29th Annual CMP Meeting*, CIM, Ottawa, Ontario, pp. 118-145, 1997.

Nesset, J.E., Sui, C., Kim, J.Y., Cooper, M., Li, M., and Chryssoulis, S.L., "The effect of soda ash and lime as pH modifiers in sphalerite flotation," In: *Proceedings – 30th Annual CMP Meeting*, CIM, Ottawa, Ontario, pp. 460-481, 1998.

Sui, C. and Huang, J., EQUILCOM, "A software for chemical thermodynamics analysis," McGill University, 1998.

Uribe-Salas, A., Gomez, C.O. and Finch, J.A., "A conductivity technique for gas and solids holdup determination in three-phase reactors", *Chemical Engineering Science*, 49 (1), pp. 1-10, 1994.

Uribe-Salas, Vermet, A. and Finch, J.A., "Apparatus and technique to measure settling velocity and holdup of solids in water slurries", *Chemical Engineering Science*, **48** (4), pp. 815-819, 1993.

Vergouw, J.M., Anson, J., Dalhke, R., Xu, Z., Gomez, C., and Finch, J., A., "An automated data acquisition technique for settling tests"; *Minerals Engineering*, **10**, 10, pp.1095-1105, 1997.

a. Vergouw, J.M., DiFeo, A., Finch, J., A., "An agglomeration study of sulphide minerals using zeta-potential and settling rate. Part I: Pyrite and galena", *Minerals Engineering*, **11**, 2, pp.159-169, 1998.

b. Vergouw, J.M., DiFeo, A., Finch, J., A., "An agglomeration study of sulphide minerals using zeta-potential and settling rate. Part II: Sphalerite/Pyrite and

sphalerite/galena", *Minerals Engineering,* Part I: Pyrite and galena", *Minerals Engineering*, **11**, 7, pp. 605-614, 1998.

APPENDIX B

Aggregation Effect of Zn^{2+} and Mg^{2+} ions in Sulphide Mineral Pulps Slurries

B.1 Abstract

Settling rate studies on slurries from Cu/Zn flotation plants occasionally revealed two aggregation maxima at pH 8-10 and 10-12. From measurements on sphalerite and silica suspensions the double maxima were replicated by Zn^{2+} ions (pH 8-10) and Mg^{2+} ions (pH 10-12) corresponding to the presence of zinc hydroxide and magnesium hydroxide, respectively. A combination of chemical and electrostatic bridging by the hydroxides is considered to be the aggregation mechanism.

B.2 Introduction

Separation by flotation involves a continual search for incremental improvements aided by research into the underlying causes of mineral misplacement. One mechanism by which minerals may misreport is through aggregation and recovery by entrapment. Aggregation is generally counter productive for all physical separations (Rushton et al, 1996), unless selective aggregation can be achieved. Aggregation as a possible cause of misplacement of minerals in flotation has long been suspected (Gaudin and Sun, 1946).

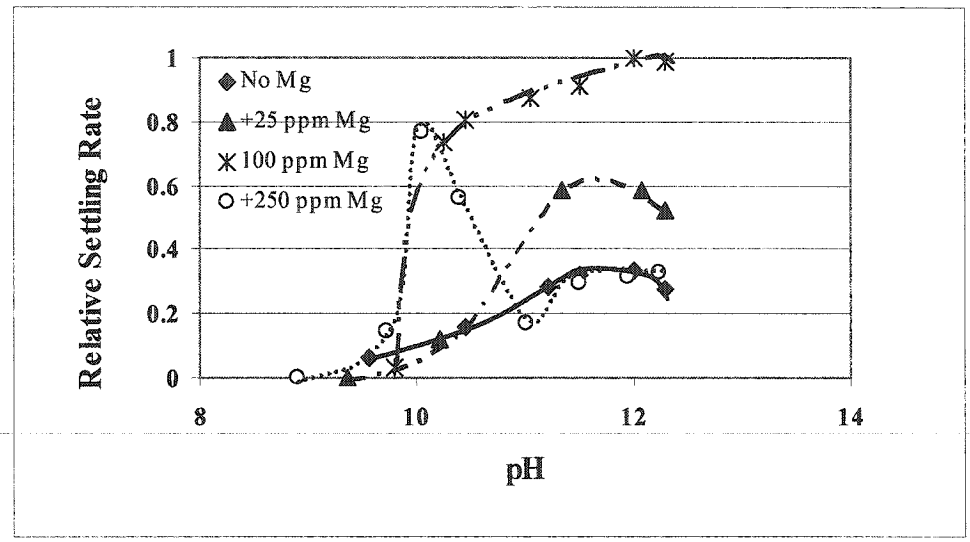

Figure B.1: Effect of added [Mg^{2+}] on settling rate of Louvicourt Cu-rougher feed. (Adapted from El-Ammouri et al., (2002). Note, they used the term "aggregation index" for relative settling rate.)

Magnesium and zinc species have recently been shown to impact sulphide mineral aggregation. El-Ammouri et al. (2002), following work by Krishnan and Iwasaki (1986) on quartz, showed aggregation by Mg^{2+} on Cu/Zn sulphide pulps at pH>10 (Fig. B.1), where the dominant species is the hydroxide, $Mg(OH)_2$, (Fig. B.2). In the case of zinc ions, the clue was in the anomalous behaviour of sphalerite, which tends to aggregate over the pH range 8-10, well above the iso-electric point (DiFeo et al., 2002; Vergouw et al., 1998). Mirnezami et al. (2002), based on the work of Healy and Jellet (1966), who likewise observed that ZnO aggregated over the same pH range which did not correspond

to its iso-electric point, suggested the cause was Zn^{2+} ions released by the sphalerite that appear to have aggregating effect. The hypothesis was confirmed with tests on silica and chalcopyrite; the tendency to aggregate is associated with $Zn(OH)_2$ as the dominant phase (Fig. B.3).

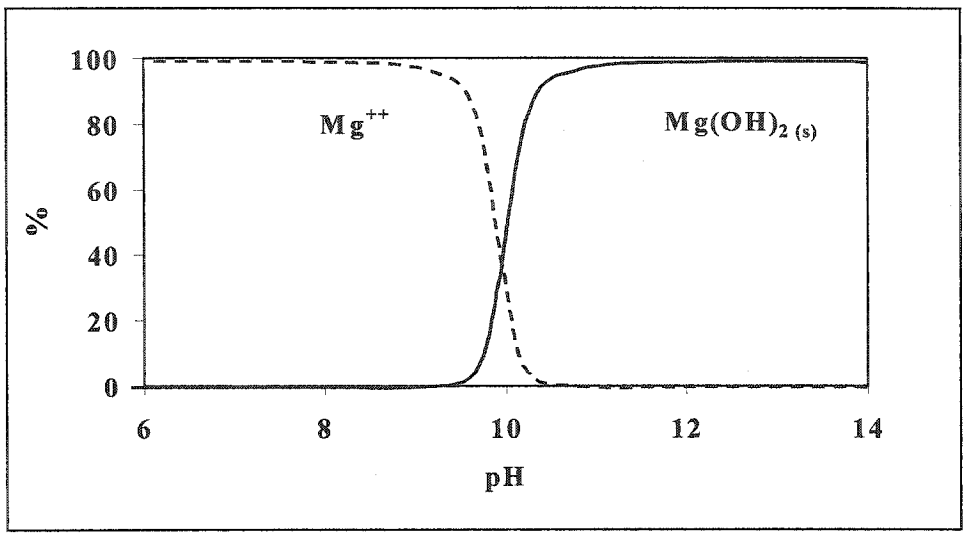

Figure B.2: Ma^{2+} species relative distribution diagram as a function of pH (note: $MgOH^+$ concentration is negligible).

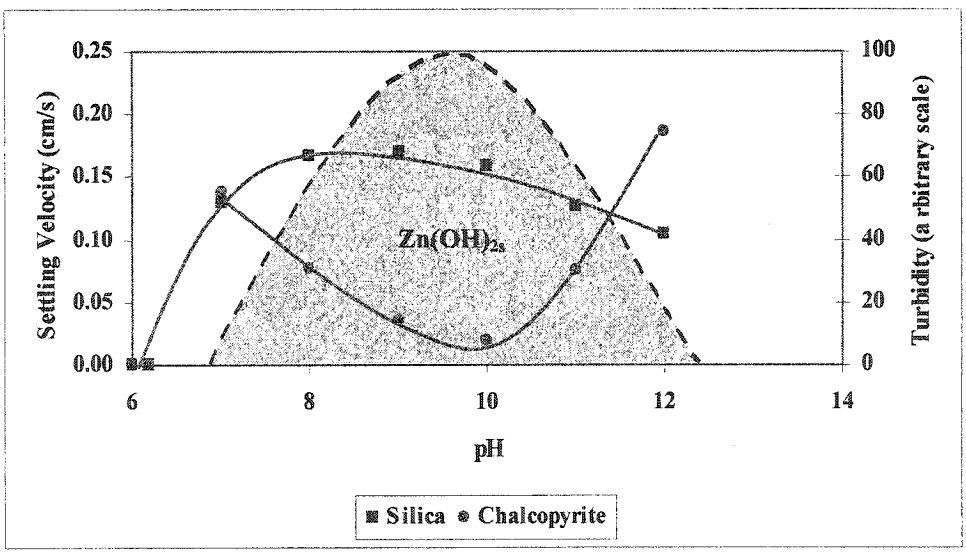

Figure B.3: Comparison of the aggregation pH region for silica and chalcopyrite with region of $Zn(OH)_2$ formation (dashed line) for 50 ppm Zn^{2+} (After Mirnezami et al., 2002).

The observation of aggregation maxima at pH 10-12 with Mg^{2+} and pH 8-10 with Zn^{2+} prompted a return to the data of El-Ammouri et al (2002). At some locations they observed two aggregation maxima at pH regions reminiscent of those due to Zn^{2+} and Mg^{2+} (Fig.B.4). Solution analysis (after acidification to pH 6 to solubilize hydroxides) showed Zn^{2+} up to 15ppm and Mg^{2+} up to 70ppm. These observations initiated the present study – to determine if Zn/Mg combinations under controlled conditions could replicate the double maxima.

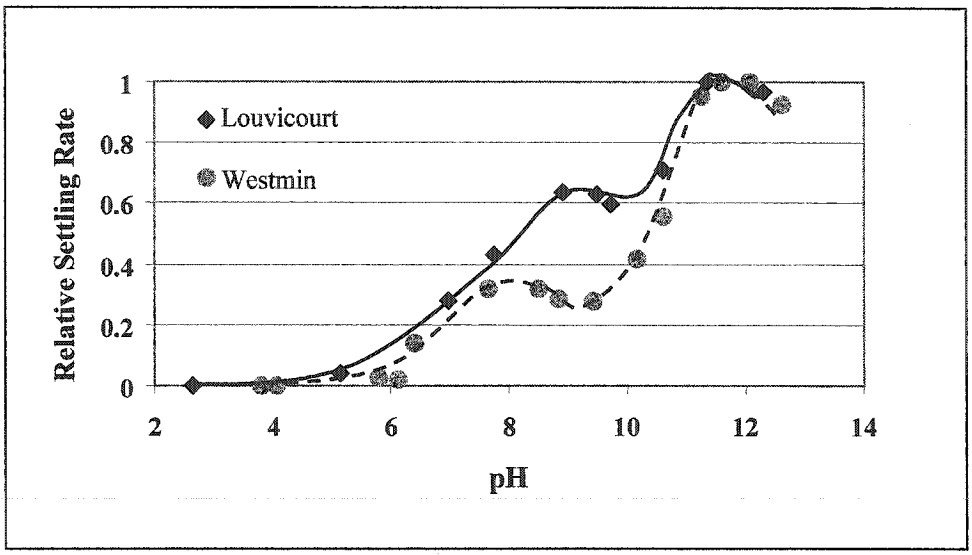

Figure B.4: Relative settling rate as a function of pH for Cu rougher feed slurry at Louvicourt ◆ and Westmin ● (Adapted from El Ammouri et al., 2002).

The feature in common for both Zn^{2+} and Mg^{2+} is that aggregation corresponds to hydroxide formation. Three mechanisms have been proposed to account for aggregation due to hydroxides. Assuming a negatively charged mineral (the usual case at alkaline, i.e., flotation, pH) the mechanisms are: 1) Charge neutralization by adsorption of positively charged precipitates; 2) Sweep flocculation, due to aggregation (polymerization) of the hydroxide itself trapping other particles (Packham, 1965); and 3) Bridging. The bridging mechanism has two sub-categories: electrostatic (Krishnan and Iwasaki, 1986) and chemical (Healy and Jellet, 1967). In electrostatic bridging, positively charged hydroxide precipitates bridge between negatively charged particles. (Another

term is "patch flocculation" (Dobiáš et al., 1999).) In the case of chemical bridging one form is H-bonding via the hydration layers on the hydroxide species (Attia, 1992).

In this communication we investigate combinations of Zn^{2+} and Mg^{2+} ions on the aggregation of silica and sphalerite as model systems and discuss the possible aggregation mechanisms.

B.3 Methodology

B.3.1 Materials and reagents

Sphalerite (Carthage, Tennessee, USA) was purchased from Ward's Natural Science Establishment. It was crushed, hand sorted, pulverized and wet sieved to obtain -38 μm. Silica (-30 μm, 99.50% pure) was purchased from US Silica.

The reagents, all A.C.S. reagent grade from Fisher Scientific Co, were magnesium chloride, zinc chloride, hydrochloric acid and sodium hydroxide.

B.3.2 Experimental procedure

For the settling tests, suspensions were prepared by adding the required mass of mineral to the relevant solution in a conditioning vessel to give 2% (v/v). The slurry was continuously stirred by a magnetic stirrer and conditioned for 15 minutes at a given pH to allow equilibrium (established by reaching a stable pH) then settling tests were performed.

To study the effect of Zn^{2+} + Mg^{2+} two series of experiments were conducted using silica. In one the ions were added together and in the second the Zn^{2+} was added first then the Mg^{2+}. With Zn^{2+} present settling tests were performed as a function of pH up to pH 10 when Mg^{2+} was added, the suspension conditioned for 15 minutes and settling tests performed as a function of pH up to pH 12.

B.3.3 Technique

B.3.3.1 Settling Rate

Settling rate is used as a relative measure of aggregation. A cylinder was modified to collect suspension settling data automatically by monitoring electrical conductivity (Uribe-Salas et al., 1993; Vergouw et al., 1997). The cylinder was made from Plexiglas (non-conductive) and was 3.8 cm in diameter and 29 cm high. The cylinder stands on a plastic base and the top is covered with a rubber stopper after filling the cell with suspension. Two identical ring electrodes, separated L=8.3 cm, are mounted internally flush to the wall and connected to a conductivity meter (Taccusel model CD 810) interfaced with a computer (data acquisition board, DAS-8PGA). A computer program was developed in Visual BASIC to record the conductance as a function of time (every 0.5 s).

To start, the suspension (usually 2% v/v) was mixed by rhythmic end-over-end rotation of the cylinder. Data collection was initiated once the cylinder was stood vertically. Conductivity vs. time was plotted on the monitor to give a visual check on the process. Two times were determined from the change in slope of the plot: when the solid/liquid interface passes the first electrode then the second. Measuring this time to pass through the cell, T(s), gives the settling rate (or velocity), 8.3/T (cm/s). The data were processed using Excel. The relative standard deviation on the settling rate from repeat experiments was ca. 1%.

B.4 Results

B.4.1 Silica + Mg^{2+}

Alone, silica is dispersed over the pH range 6-13 (Fig. B.5), reflecting high negative charge and strong hydrophilicity. In the presence of Mg^{2+}, above pH 9 the settling velocity increases to a maximum at a certain pH and then decreases. This pH of maximum aggregation tends to decrease as $[Mg^{2+}]$ increases and shows maximum value at intermediate $[Mg^{2+}]$ (30ppm in this case).

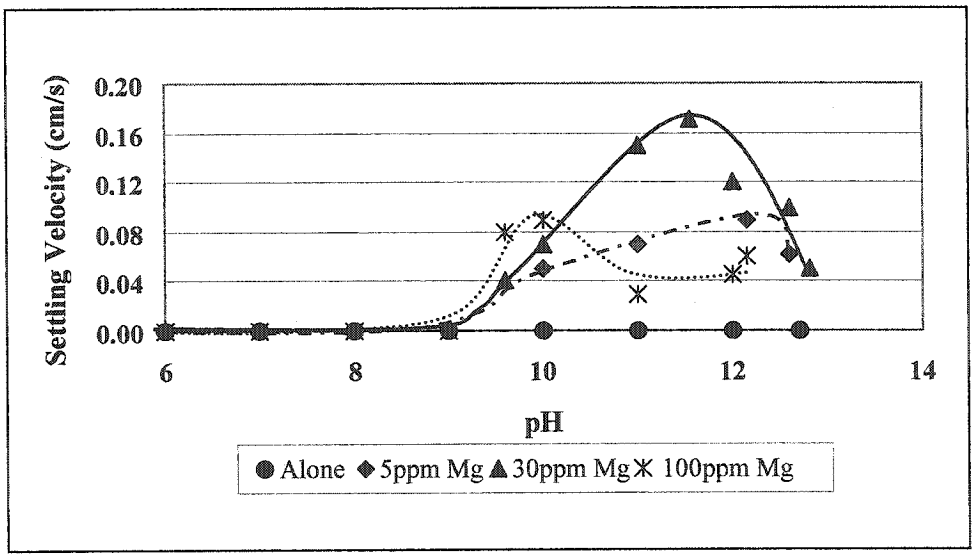

Figure B.5: Aggregation of silica as a function of pH and [Mg^{2+}].

B.4.2 Sphalerite + Mg^{2+}

Previous work on sphalerite has shown that the mineral self-aggregates at moderately alkaline pH, tending to re-disperse above ca. pH 10 (Mirnezami et al., 2002; DiFeo et al., 2001; and Vergouw et al., 1998). This is re-confirmed here (Fig. B.6). Introducing Mg^{2+} did not have a significant effect up to pH 9; above this, the Mg^{2+} caused aggregation up to at least pH 12. Aggregation increased with concentration and, the focus of the work, the two maxima are evident.

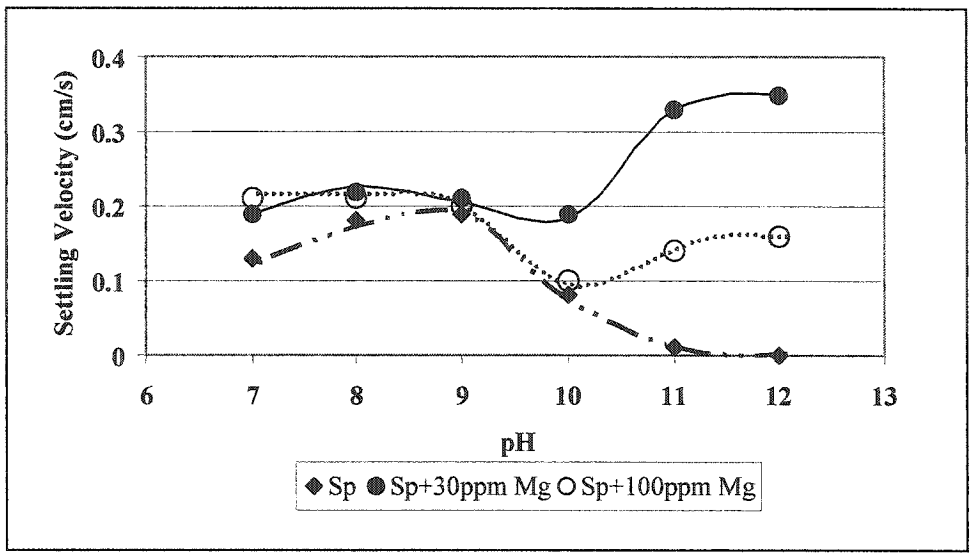

Figure B.6: Aggregation of sphalerite as a function of pH and [Mg^{2+}].

B.4.3 Silica + Zn^{2+}, Silica + Zn^{2+} & Mg^{2+}

Figure B.7 shows silica is aggregated by Zn^{2+} ions over the pH range 7-11(cf. Fig. 3). Unlike the case with Mg^{2+} ions, aggregation increased with concentration and the pH of maximum aggregation remained constant at ca. pH 9.

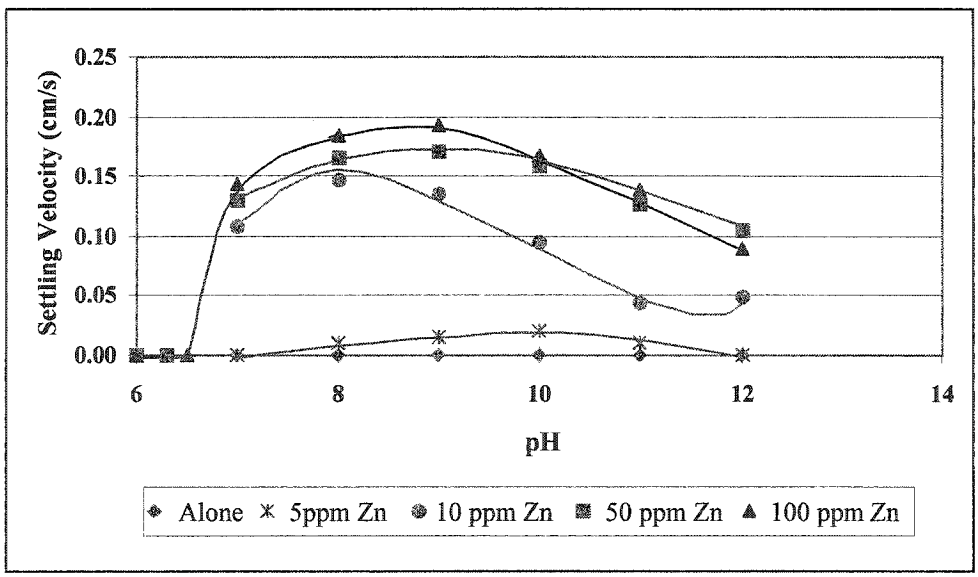

Figure B.7: Aggregation of silica as a function of pH and [Zn^{2+}].

The treatment with the two ions was done with them together and in sequence: in either case the double maxima are evident, Figures B.8 and B.9, respectively. The position (pH) of the maxima is similar to Figure B.4: the response of silica to Zn^{2+} and Mg^{2+} appears to replicate the response of sulphide ores seen in Figure B.4.

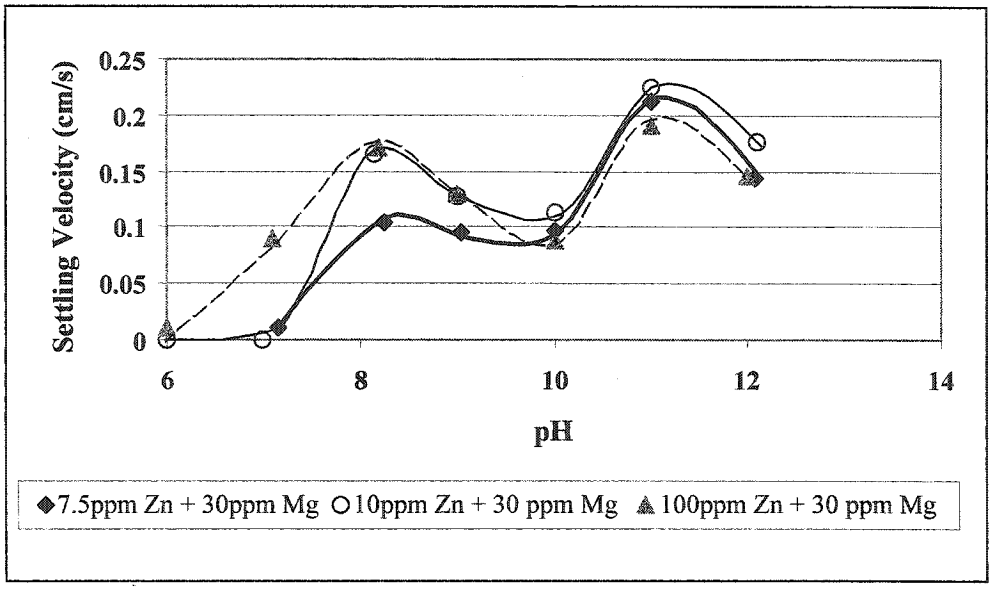

Figure B.8: Aggregation of silica treated with combinations of Zn^{2+} and Mg^{2+} added simultaneously.

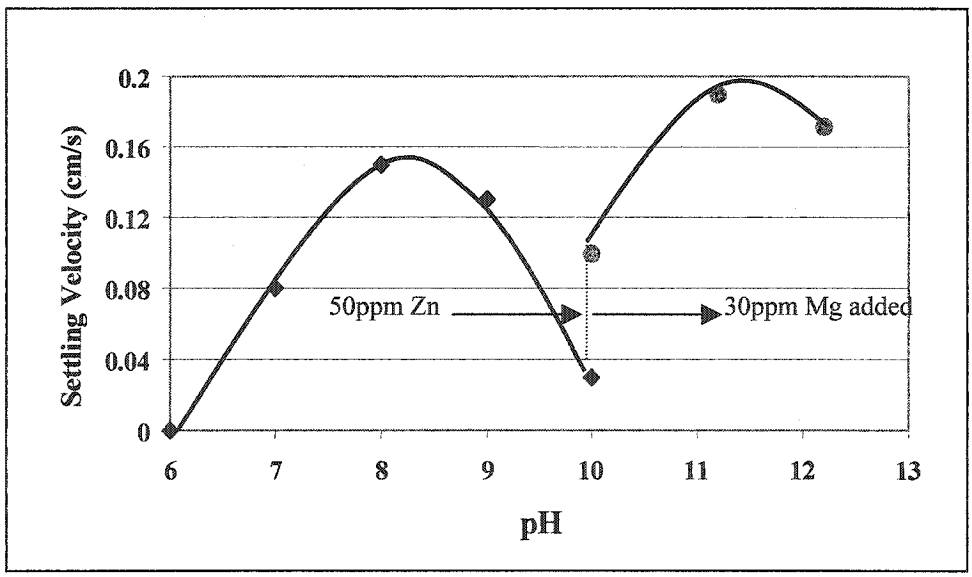

Figure B.9: Aggregation of silica treated with Zn^{2+} and Mg^{2+} added sequentially.

B.5 Discussion

The circumstantial evidence is that the double maxima in the aggregation behaviour of some Cu/Zn slurries (Fig. B.4) result from the presence of Zn^{2+} and Mg^{2+} ions. They appear to act independently, Zn^{2+} promoting aggregation at pH 7-10 and Mg^{2+} above pH 10. These pH regions correspond to the presence of the respective hydroxide as the stable species. Some work on the mechanism of each individually has been done (Mirnezami et al., 2002; El-Ammouri et al., 2002), which is extended here to the mixture of ions.

Hydroxides promote aggregation via one of three mechanisms, charge neutralization, sweep flocculation, and bridging. Sweep aggregation involves a settling network of polymerizing hydroxide enmeshing particles as it descends. However, particles of the size here (-30 μm) would likely settle faster than this network (i.e., the mechanism applies to particles more colloidal in size). One of the remaining two mechanisms, therefore, seems to be at play in the present case.

Charge neutralization implies aggregation when the zeta potential is close to zero (ca. -15 mV to + 15 mV). Self-aggregation of sphalerite, however, occurs when the zeta potential is –20 to –40 mV indicating charge neutralization is not the cause. As noted, chemical bridging via the surface $Zn(OH)_2$ was proposed (Mirnezami et al., 2002). In the second system for which the mechanism has been investigated, silica/Mg^{2+}, charge neutralization was also not indicated, and electrostatic bridging was suggested (Krishnan and Iwasaki, 1986). The evidence for this mechanism is seen here: aggregation does not maximize at the point of charge reversal (ca. pH 10.5 (Krishnan and Iwasaki, 1986)) (i.e, it is not aggregation by charge neutralization) and aggregation as a function of $[Mg^{2+}]$ (at a given pH) passes through a maximum (Fig. B.5), which can be explained by particles becoming coated with $Mg(OH)_2$ and developing a net positive charge that induces mutual repulsion. El-Ammouri et al. (2002) showed the same response to $[Mg^{2+}]$ occurred with Cu/Zn sulphide pulps.

The aggregation mechanism appears to be one of bridging. With this in mind the other systems tested here (silica + Zn^{2+} and sphalerite + Mg^{2+}) were considered. The evidence is more limited (no corresponding zeta potential data, for example) but in both these systems aggregation did not pass through a maximum with cation concentration (Figs. B.6 & B.7). This suggests that hydroxide-coated particles remain in an aggregated state and thus chemical bridging is the likely mechanism.

The two ions appear to act independently (Figs. B.7, B.8 & B.9) via a combination of electrostatic and chemical bridging mechanisms. For sulphides chemical bridging seems to dominate for both Zn^{2+} and Mg^{2+} while the indications are that both types of bridging apply to non-sulphides (silica being the "model"), Mg^{2+} being electrostatic and Zn^{2+} chemical. In the Cu/Zn sulphide rougher feed pulps the response to $[Mg^{2+}]$, aggregation passed through a maximum (El-Ammouri et al., 2002), indicates electrostatic bridging, which can be attributed to the large component of non-sulphides.

For sulphides the proposal is that both zinc- and magnesium-hydroxides promote aggregation through a chemical bridging mechanism.

B.6 Conclusions

From this study of the aggregating effect of Zn^{2+} and Mg^{2+} ions, the following has been found:

1- Zn^{2+} and Mg^{2+} have a significant aggregating effect corresponding to the pH of hydroxide formation.

2- The mechanism of aggregation for sulphide minerals is attributed to chemical bridging and for non-sulphide pulps to electrostatic bridging.

3- Flotation pulps can exhibit aggregation corresponding to the effect of Zn^{2+} and Mg^{2+} ions.

B.7 Acknowledgements

The authors acknowledge the financial support of the Canadian Mining Industry Research Organization–Metallurgical Processing Division, CAMIRO-MPD (representing Noranda, Boliden-Westmin, Hudson Bay Mining and Smelting, Les mines Selbaie, Louvicourt, Breakwater Resources and Agnico-Eagle) and the Natural Sciences and Engineering Research Council of Canada (NSERC) under the NSERC Collaborative Research and Development Program.

B.8 References

Attia, Y. A., (1992). In *Colloid Chemistry in Mineral Processing*, (J.S. Laskowski, and J. Ralston, Eds.) Developments in Mineral Processing Series, Vol. 12, Elsvier Science Publishers B. V., Netherlands, 295.

DiFeo, A., Finch, J.A., and Xu, Z. (2001). Sphalerite – silica interactions: effect of pH and calcium ions. *Int. J. Miner. Process.*, **61**, pp. 57-71.

Dobiáš, B., Qiu, X., and Rybinski, W. v. (1999). *Solid-liquid dispersion,* Surfactant Science Series, Vol. **81**, Marcel Dekker Inc. New York, p. 269.

El-Ammouri E., Mirnezami, M., Lascelles, D. and Finch, J.A. (2002). Aggregation index and a methodology to study the role of magnesium in aggregation of sulphide slurries., accepted for publication in *CIM Bulletin.*

Gaudin, A.M. & Sun, S.C., (1946). Correlation between mineral behaviour in cataphoresis and in flotation. *Trans, AIME*, **169**, p. 347.

Healy, T.W. and Jellet V.R. (1967). Adsorption coagulation reactions of Zn(II) hydrolyzed species at the zinc oxide-water interface. *Journal of Colloid Interface Science*, **24**, pp. 41-46.

Krishnan, S.V. and Iwasaki, I. (1986). I. Heterocoagulation vs. surface precipitation in a quartz- $Mg(OH)_2$ system, *Environ. Sci. Technol.*, **20**, (12), pp. 1224-1229.

Mirnezami, M., L. Restrepo, L., Finch, J.A. (2002). Aggregation of Sphalerite: Role of Zinc Ions" accepted for publication by *Journal of Colloid and Interface Science.*

Packham, R.F. (1965). Some studies of the coagulation of dispersed clays with hydrolyzing salts. *J. Colloid Sci.* **20**, pp 81- 92.

Rushton, A., Ward, A.S., Holdich, R.G., Solid-liquid filtration and separation technology, VCH, Weinheim, pp. 1-31 and 221-226 (1996).

Uribe-Salas, A., Vermet, F., Finch, J.A. (1993). Apparatus and technique to measure settling velocity and holdup of solids in water slurries. *Chemical Engineering Science*, **48** (4), pp. 815-819.

Vergouw, J.M. Anson, J., Dahlke, R., Xu, Z., Gomez, C. O. & Finch, J.A. (1997). A new automated data acquisition technique for settling tests. *Minerals Engineering,* **10** (10), pp. 1095-1105.

Vergouw, J.M., DiFeo, A., Xu, Z., Finch, J.A. (1998). An agglomeration study of sulphide minerals using zeta potential and settling rate: Part II. Sphalerite/Pyrite and sphalerite/galena. *Minerals Engineering,* **11**, (7), pp. 605-614.